TECHNISCHE UNIVERSITÄT WIEN

DIPLOMARBEIT

# Finite Elemente Methoden für Nicht-Abelsche Eichfeldtheorien

zur Erlangung des akademischen Grades

**Diplom-Ingenieur**

im Rahmen des Studiums

**Technische Mathematik**

eingereicht von

**DI Srinath Bulusu**

Matrikelnummer: 01303708

ausgeführt am

Institut für
Analysis und Scientific Computing
der Fakultät für Mathematik der Technischen Universität Wien

Betreuung

**Prof. Dr. Joachim Schöberl**

Mitwirkung

**Privatdoz. Dr. Andreas Ipp**
**Dr. David Müller**



Wien, 14.02.2024

Unterschrift Verfasser

Unterschrift Betreuer

## Kurzfassung

Die starke Kernkraft, eine der uns derzeit bekannten vier fundamentalen physikalischen Wechselwirkungen, wird durch eine sogenannte nicht-Abelsche Eichfeldtheorie beschrieben. Gittereichtheorien (auch bekannt unter dem Begriff Lattice Gauge Theories - LGT) basieren auf Finite Differenzen und sind derzeit die Go-to-Methoden, um Simulationen in diesem Kontext durchzuführen. Andererseits hat sich die Finite Elemente Methode (FEM) im Bereich des Elektromagnetismus - einer Abelschen Eichtheorie - als beliebte Simulationstechnik etabliert. In dieser Arbeit erforschen und kombinieren wir beide Methoden mit dem Ziel eine eichsymmetrische und Ladungs-erhaltende numerische Diskretisierung für nicht-Abelsche Eichfeldtheorien zu konstruieren.

## Abstract

The strong nuclear force, one of the four fundamental physical interactions presently known, is modeled by a so-called non-Abelian gauge theory. Lattice Gauge Theory (LGT), a finite difference discretization, represents the current state-of-the-art method towards numerical simulations in this context. The more general and flexible Finite Element Method (FEM), on the other hand, has proven to be effective for electromagnetism - an Abelian gauge theory. In this thesis we explore these fields with the aim to construct a gauge symmetric and charge conserving numerical discretization for non-Abelian gauge theories that combines LGT with FEM.

## Acknowledgements

This work was supported by funds provided by the Austrian Science Fund (FWF) in part 10 of the project SFB 65 “Taming the Complexity of Partial Differential Equations - Automated Discretization in Multiphysics”. I would like to take this opportunity to express my gratitude to my advisor Prof. Joachim Schöberl whose ongoing support and never ending curiosity towards new research ideas made this work possible. I would like to extend this sentiment towards our collaborators Prof. Andreas Ipp and Dr. David Müller whose insights during our discussions have repeatedly proven to deliver valuable contributions in this project. Furthermore, I would like to thank our research group as a whole, in particular Michael Neunteufel, Edoardo Bonetti, Xaver Mooslechner, Michael Leumüller, Markus Wess and Valentin Hanser, whose resourceful advice and expertise have continually helped me grow and actively drive this project forward. Finally I want to offer my special thanks to my partner Clara, my parents as well as all friends and colleagues who have demonstrated their continuing support towards assisting me in my endeavours.

# Contents

# 1 Introduction

Gauge theories have become an important backbone in modern physics. Already in Maxwell's equations for electrodynamics it is noticeable that there does not exist a unique solution, but infinitely many of them [32]. Later it was realized that this freedom can be linked to the symmetry of quantities, in particular to the phase-invariance in quantum mechanics. This degree of freedom has been dubbed "gauge freedom" [10]. Extending this idea by demanding more symmetries led to the development of Quantum ChromoDynamics (QCD) - a theory describing the strong nuclear interaction in particle physics [26]. A key ingredient for this purpose is the concept of a symmetry group: a (continuous) set of transformations acting on objects that leave physics invariant [54] [42]. The twist in QCD as opposed to electrodynamics, is that the former carries a non-Abelian symmetry group. QCD is therefore referred to as a non-Abelian gauge theory. Further research revealed that the mathematical foundations of said theories can be understood using differential geometry, in particular, connections, curvatures, Lie groups and bundles [52].

The complex nature of non-Abelian gauge theories has paved the way for numerical simulations to be an essential tool for research. Lattice gauge theory (LGT) [22], the current state of the art method, has helped to simulate, understand and predict phenomena in QCD such as the confinement of particles [25] [33], the quark-gluon plasma [28] [37], properties of composite particles [21] [18] and heavy-ion collisions [40] [31] [46]. However, it remains a computationally expensive method because of the large number of degrees of freedom involved and the limitations of finite difference methods.

On the other hand, the Finite Element Method (FEM) has proven to be an effective method for numerical simulations in structural mechanics [56], fluid mechanics [36] and electromagnetism [43] [29]. Backed up by a rich and solid theory of functional analysis, it offers higher order methods and flexible meshes with possible refinement while being able to deliver rigorous accuracy predictions and guarantees [53] [30]. A breakthrough in a research topic of current interest is provided by Finite Element Exterior Calculus (FEEC) - a FEM framework for discretizing continuous spaces while preserving the structure present in the continuum [3] [2] [4]. This has enabled simulations in electromagnetism that preserve exact gauge symmetry and charge conservation. Discrete differential geometry is a rapidly developing field in FEM research because of its potential for applications in mechanics, general relativity and gauge theories [24] [23] [17] [38] [47] [14] [8].

The goal of this thesis is to explore the use of FEM for non-Abelian gauge theories to obtain constraint and symmetry preserving numerical discretizations for simulating the strong nuclear interaction.

In the first part we will lay the basic theoretic foundation for FEM as described in FEEC, which includes exterior calculus as well as simplicial complexes. We will then proceed to cover gauge theories by starting with electromagnetism, the notion of gauge symmetry and finally move towards non-Abelian gauge theories. After a quick introduction to the concept of parallel transport we introduce LGT and mention Regge calculus. Both are differential geometric frameworks tailored towards discretizing gauge theories and general relativity respectively.

In the second part we will apply a standard FEM method for electromagnetism to non-Abelian gauge theories and investigate the behaviour of real-time simulations, especially in terms of gauge invariance and charge conservation.

The third part will be dedicated towards a FEM discretization which holds the potential to be gauge symmetric and fulfill a discrete notion of charge conservation. We will motivate this by using LGT [22], Regge calculus [47] and research in this direction [14] [27]. We formulate building blocks for a future time stepping simulation for heavy-ion-collisions and conclude by summarizing open questions and points for future endeavors.

## Notation

This work will take use of the (Einstein) index notation and sum convention, meaning that indices which occurr twice are summed over by default as in

$$v^\mu e_\mu := \sum_\mu v^\mu e_\mu$$

unless stated otherwise. We reserve greek letters for space-time indices and differentiate between lower $v_\mu$ and upper positions $v^\mu$ for co- and contra- variant indices respectively. Sums over such indices may only be performed in pairs with different positions, meaning that one must be lowered and the other one raised. The space-time metric $g$ is chosen to be the Minkwoski metric with the following signature

$$g_{\mu\nu} = \begin{pmatrix} -1 & 0 & 0 & 0 \\ 0 & 1 & 0 & 0 \\ 0 & 0 & 1 & 0 \\ 0 & 0 & 0 & 1 \end{pmatrix}_{\mu\nu} .$$

We will also apply the pair sum convention for other types of indices $v_a$ (such as color and counting indices) but the raised $v^a$ and lowered positions $v_a$ will be chosen by mere convenience for the sake of legibility. Standard derivatives in coordinate directions will be denoted with the partial sign $\partial_\mu$ and indices $\mu = 0, 1, 2, 3$ or equivalent coordinate symbols $\mu = t, x, y, z$. The nabla symbol $\nabla_\mu$ will be reserved for the gauge-covariant derivative. We will try to distinguish between Lie algebra-valued and other functions by using calligraphic and regular roman symbols, such as $\mathcal{F}$ and $F$. If the context is clear, we will suppress space-time indices of differential forms.

# 2 Theory

## 2.1 Exterior Calculus

In this section we will be assuming a pseudo-Riemannian manifold $(M, g)$ with dimension $\dim(M) = n \in \mathbb{N}$ and a non-degenerate metric $g$ of signature similar to the Minkowski metric.

**Definition 1.** *The Exterior Algebra of differential forms $\Lambda(M) = \bigcup_{k\in\mathbb{N}} \Lambda^k(M)$ consists of tensors $\omega$ of rank $(0, k)$ (purely covariant) that are fully antisymmetric in each argument.*

$$\omega : \begin{cases} \otimes_{l=1}^{k} TM & \to & \mathbb{R} \\ (v_l)_{l=1,\dots,k} & \mapsto & \omega(v_1, \dots, v_k) \end{cases}$$

*In other words, given any permutation of arguments $\sigma \in \Pi(k)$, there holds*

$$\omega(v_{\sigma(1)}, \dots, v_{\sigma(k)}) = (-1)^{\mathrm{sgn}(\sigma)} \omega(v_1, \dots, v_k).$$

*The wedge product $\wedge$ is defined as*

$$\wedge : \begin{cases} \Lambda^k(M) \times \Lambda^l(M) & \to & \Lambda^{k+l}(M) \\ (\omega, \phi) & \mapsto & \omega \wedge \phi \end{cases}$$

$$(\omega \wedge \phi)(v_1, \dots, v_{k+l}) := \frac{(k+l)!}{k!l!} \sum_{\sigma \in \prod_{k+l}} sgn(\sigma) \omega(v_{\sigma(1)}, \dots, v_{\sigma(k)}) \phi(v_{\sigma(k+1)}, \dots, v_{\sigma(k+l)}) \tag{2.1}$$

*and satisfies graded commutativity $\omega \wedge \phi = (-1)^{kl} \phi \wedge \omega$ as well as associativity $(\omega \wedge \phi) \wedge \psi = \omega \wedge (\phi \wedge \psi)$. A differential $k$-form with rank $k$ equal to the dimension of the manifold $k = \dim M$ is called a top-form.*

The antisymmetry of the maps implies that there exist no $k$-forms with rank $k > \dim M$ greater than the dimension of the manifold $M$ (except for the 0-map), hence the definition of a top-form.

Given a local basis of the exterior algebra, for instance, in terms of differentials of coordinate functions $(\mathrm{d}x^\mu)_{\mu=1,\dots,\dim(M)} \in \Lambda^1(M) = TM^*$, a differential $k$-form $\omega \in \Lambda^k(M)$ may be represented by local function components $\omega_{\mu_1 \dots \mu_k} \in C^\infty$ with antisymmetric $k$-index blocks with $(\mu_l)_{l=1,\dots,k}$.

$$\omega = \frac{1}{k!} \omega_{\mu_1 \dots \mu_k} \mathrm{d}x^{\mu_1} \wedge \dots \wedge \mathrm{d}x^{\mu_k}$$

$$\omega_{\mu_1 \dots \mu_l \dots \mu_m \dots \mu_k} = (-1)^{m-l} \omega_{\mu_1 \dots \mu_m \dots \mu_l \dots \mu_k}$$

The antisymmetry of these components implies that there are $n!/(k!(n-k)!)$ independent components in $\omega_{\mu_1 \dots \mu_k}$, while the remaining ones are fixed via permuations or vanish. We will refer to the functionals $(\mathrm{d}x^\mu)_{\mu=1,\dots,\dim(M)} \in \Lambda^1(M) = TM^*$ as the generators of the exterior algebra. Using them, operations on differential forms will be translated into index notation in section 6.1 of the appendix.

In order to provide a well defined notion of integration on manifolds, any such prescription must be well behaved under coordinate transformations and be independent of the charts chosen. It turns out that differential forms correspond to integrable objects.

**Definition 2.** *The integral of an $n$-form $\omega \in \Lambda^n(M)$ over $M$ is defined via an atlas of charts $\left\{ \left( O_{(k)}, x^\alpha_{(k)} \right)_{(k)\in\mathcal{I}} : O_\alpha \to \mathbb{R}^n \right\}$ with a matching a partition of unity $\left\{ \left( O_{(k)}, \psi_{(k)} \right)_{(k)\in\mathcal{I}} : M \to \mathbb{R}^+ \right\}$*

$$\sum_{(k)\in\mathcal{I}} \psi_{(k)} = 1$$

$$\int_M \omega := \sum_{(k)\in\mathcal{I}} \int_{O_{(k)}} \psi_{(k)}\omega_{1\dots n}\mathrm{d}^n x$$

*where $\omega_{12\dots n}$ are the components of $\omega$ with respect to the exterior algebra generators in a specific chart $\psi_{(k)}$.*

This enables the integration of $k$-forms over $k$-dimensional submanifolds $N \subset M$. In addition the integral over a function $f$ can be defined using a so-called volume form.

**Definition 3.** *A volume form* Vol *is a nowhere vanishing top form.*

**Example 2.1.1** (Volume Form induced by a Pseudo-Riemannian Metric)**.** *On a pseudo-Riemannian manifold $(M, g)$ it is possible to construct a volume form using the metric $g$.*

$$\mathrm{Vol} := \frac{1}{\sqrt{|g|}}\mathrm{d}x^{\mu_1} \wedge \ldots \wedge \mathrm{d}x^{\mu_n}$$

**Definition 4.** *The integral of a function $f \in C^\infty(M, \mathbb{R})$ with respect to a volume form $\mathrm{Vol} \in \Lambda^n(M)$ is defined as the integral of the top form $f \wedge \mathrm{Vol} = f\mathrm{Vol} \in \Lambda^n(M)$.*

From now on integrals will be formed using the volume form induced by the pseudo-Riemannian metric.

**Definition 5** (Inner Product)**.** *Given a non-degenerate metric $g \in (TM^*)^2$ the inner product of two $k$-forms $\omega \in \Lambda^k(M)$ and $\phi \in \Lambda^k(M)$ is defined as*

$$\langle\omega, \phi\rangle_{\Lambda^k(M)} : \begin{cases} \Lambda^k(M) \times \Lambda^k(M) & \to & \mathbb{R} \\ (\omega, \phi) & \mapsto & \int_M \sum_{\alpha_1=1}^d \cdots \sum_{\alpha_k=1}^d \omega(E_{(\alpha_1)}, \ldots, E^\mu_{(\alpha_k)})\phi(E_{(\alpha_1)}, \ldots, E(\alpha_k)) \end{cases}$$

*where $(E_{(\alpha)})_{\alpha=1,\ldots,d}$ is a $g$-orthonormal basis*

$$g(E_{(\alpha)}, E_{(\beta)}) = \delta_{(\alpha)(\beta)}.$$

The antisymmetry of differential forms allows identification of those of different rank.

**Definition 6** (Hodge Star Operator)**.** *Let $M$ be an $n$-dimensional manifold with a volume form $\mathrm{Vol} \in \Lambda^n$ and an inner product $\langle\cdot,\cdot\rangle$ between $k$-forms. The Hodge star operator*

$$\omega : \begin{cases} \Lambda^k(M) & \to & \Lambda^{n-k}(M) \\ \omega & \mapsto & \star\omega \end{cases}$$

*is defined as the unique map that satisfies*

$$\int_M \langle\star\omega, \phi\rangle = \int_M \omega \wedge \phi \quad \forall\phi \in \Lambda^{n-k}(M)$$

*and is an involution $\star\star\,\omega = (-1)^{k(n-k)}\omega$ where $k$ is the rank of the starting differential form.*

Sometimes an index $k$ is added $\star_k : \Lambda^k(M) \to \Lambda^{n-k}(M)$ to avoid ambiguity of maps.

**Definition 7** (Exterior Derivative)**.** *The exterior derivative is defined as*

$$\mathrm{d} : \begin{cases} \Lambda^k(M) & \to & \Lambda^{k+1}(M) \\ \omega & \mapsto & \mathrm{d}\omega \end{cases}$$

$$\mathrm{d}\omega\left(v_0, \ldots, v_k\right) = \sum_i (-1)^i \mathrm{d}_{v_i}\left(\omega\left(v_0, \ldots, \widehat{v_i}, \ldots, v_k\right)\right) + \sum_{i<j} (-1)^{i+j}\omega\left(\left[v_i, v_j\right], v_0, \ldots, \widehat{v_i}, \ldots, \widehat{v_j}, \ldots, v_k\right)$$

*where $\mathrm{d}_v f$ stands for the directional derivative of a function $f$ in the direction of the tangent vector $v$ and $[v, w]$ represents the differential geometric Lie Bracket of tangent vectors $v, w \in TM$ on the manifold $M$. It satisfies the graded product rule*

$$\mathrm{d}\left(\omega \wedge \phi\right) = \mathrm{d}\omega \wedge \phi + (-1)^k \omega \wedge \mathrm{d}\phi$$

*for $k$-forms $\omega \in \Lambda^k(M)$ and $l$-forms $\phi \in \Lambda^l(M)$ and vanishes when applied twice $d \circ d = 0$.*

Sometimes an index $k$ is added to the differential operator $\mathrm{d}_k : \Lambda^k(M) \to \Lambda^{k+1}(M)$ to avoid ambiguity of maps. The corresponding expression in coordinates is more straightforward to read

$$\mathrm{d}\omega := \frac{1}{(k+1)!}\delta^{\mu_1\mu_2\dots\mu_{k+1}}_{\nu_1\dots\nu_{k+1}}\partial_{\mu_1}\omega_{\mu_2\dots\mu_{k+1}}\mathrm{d}x^{\nu_1}\wedge\dots\wedge\mathrm{d}x^{\nu_{k+1}}$$

where $\partial_\mu$ stands for the partial derivative of functions in coordinates and $\delta^{\mu_1\mu_2\dots\mu_{k+1}}_{\nu_1\dots\nu_{k+1}}$ stands for the generalized Kronecker delta in 6.1.

The action of the exterior derivative is often visualized in a chain.

$$\Lambda^0(M) \overset{\mathrm{d}_0}{\to} \Lambda^1(M) \overset{\mathrm{d}_1}{\to} \dots \overset{\mathrm{d}_{n-1}}{\to} \Lambda^n(M)$$

This can be extended on both ends: on the left using the embedding $\mathrm{d}_{-1} : \mathbb{R} \to \Lambda^0(M)$ in the form of constant functions and on the right with the fact that there exist no differential forms with rank $k$ greater than the dimension of the manifold $k > n$.

**Definition 8** (de-Rham Complex)**.** *The de-Rham complex is defined as the chain of spaces $\Lambda^k(M)$ linked by the exterior derivative* d

$$\mathbb{R} \longrightarrow \Lambda^0(M) \xrightarrow{\mathrm{d}_0} \dots \xrightarrow{\mathrm{d}_{k-1}} \Lambda^k(M) \overset{\overset{\mathrm{d}_{k+1}\circ\mathrm{d}_k=0}{\frown}}{\xrightarrow{\mathrm{d}_k}} \Lambda^{k+1}(M) \xrightarrow{\mathrm{d}_{k+1}} \Lambda^{k+2}(M) \xrightarrow{\mathrm{d}_{k+2}} \dots \xrightarrow{\mathrm{d}_{n-1}} \Lambda^n(M) \xrightarrow{\mathrm{d}_n} 0$$

*where there holds* $\mathrm{ran}(\mathrm{d}_k) = \ker(\mathrm{d}_{k+1})$.

**Example 2.1.2.** *On three dimensional manifolds the exterior derivative can be recast into the form of gradient, curl and divergence operators with the help of the Hodge star.*

$$\mathrm{grad} : \left\{ \begin{array}{ccc} \Lambda^0(M) & \to & \Lambda^1(M) \\ f & \mapsto & \mathrm{d}_0 f \end{array} \right.$$

$$\Lambda^0(M) \overset{\mathrm{grad}}{\longrightarrow} \Lambda^1(M) \qquad \Lambda^2(M) \qquad \Lambda^3(M) \qquad 0$$

$$\mathrm{curl} : \left\{ \begin{array}{ccc} \Lambda^1(M) & \to & \Lambda^1(M) \\ \omega & \mapsto & \star_2\mathrm{d}_1\omega \end{array} \right.$$

$$\Lambda^0(M) \qquad \overset{\overset{\mathrm{curl}}{\frown}}{\Lambda^1(M)} \xrightarrow{\mathrm{d}_1} \Lambda^2(M) \qquad \Lambda^3(M) \qquad 0$$

$$\mathrm{div} : \left\{ \begin{array}{ccc} \Lambda^1(M) & \to & \Lambda^0(M) \\ \omega & \mapsto & \star_3\mathrm{d}_2\star_1\omega \end{array} \right.$$

$$\Lambda^0(M) \overset{\overset{\mathrm{div}}{\frown}}{\longleftarrow} \Lambda^1(M) \qquad \Lambda^2(M) \xrightarrow{\mathrm{d}_2} \Lambda^3(M) \xrightarrow{\mathrm{d}_3} 0$$

$\star_1$ between $\Lambda^1(M)$ and $\Lambda^2(M)$; $\star_3$ between $\Lambda^0(M)$ and $\Lambda^3(M)$

*The de-Rham sequence property* $\mathrm{d}_{k+1}\circ\mathrm{d}_k \equiv 0$ *reflects itself in the fact that* $\mathrm{curl}\circ\mathrm{grad} \equiv 0$ *and* $\mathrm{div}\circ\mathrm{curl} \equiv 0$.

**Remark 2.1.3.** *These operations can also act on vector- or contra-valued fields $v \in TM$ with the help of a musical isomorphism involving a non-degenerate Riemannian metric $g$.*

$$\flat : \left\{ \begin{array}{ccc} TM & \to & TM^* \\ v & \mapsto & g(v,\cdot) \end{array} \right.$$

An important result in exterior calculus is the generalization of Greens, Stokes' and Gauss theorem in vector analysis.

**Theorem 2.1.4** (Stokes' theorem for differential forms)**.** *Let $M$ be a smooth manifold, $\partial M$ its respective boundary and $\omega$ be a differential $k$-form with $k+1 = \dim M$. There holds Stokes' theorem*

$$\int_M \mathrm{d}\omega = \int_{\partial M} \omega.$$

## 2.2 Simplicial Complexes and Triangulations

We start discretizing manifolds $M$ by developing the concept of triangulations.

**Definition 9** (Simplex)**.** *A $k$-simplex $(p_0 \dots p_k)$ spanned by an affinely linearly independent set of points $(p_l)_{l=0,\dots,k}$ represents the $\mathbb{R}^n$-subset spanned by the convex hull of points $k+1$ points $(p_i)_{i=0\dots k} \in \mathbb{R}^n$.*

$$(p_0 \dots p_k) := \mathrm{co}\{(p_i)_{i=0\dots k}\} = \{x \in \mathbb{R}^n | x = \sum_{i=0}^{k} \lambda_i p_i, \quad \sum_{i=0}^{k} \lambda_i = 1, \lambda_i \geq 0\}$$

*An oriented $k$-simplex $\langle p_{i_0} \dots p_{i_k} \rangle \in \Sigma_k$ is a simplex with a particular ordering $(i_1, \dots, i_k) \in \Pi(k+1)$ of points. Orderings differing by an even permutation are identified. However, two simplices $C$ and $D$ that differ by an uneven permutation are formally related by a relative sign $C = -D$*

$$\langle p_{\sigma(0)} p_{\sigma(1)} \cdot \dots \cdot p_{\sigma(k-1)} p_{\sigma(k)} \rangle = (-1)^{\mathrm{sgn}(\sigma)} \langle p_0 p_1 \cdot \dots \cdot p_{k-1} p_k \rangle.$$

*A codimension-$k$-simplex refers to an $n-k$-simplex with $n$ standing for the dimension of $\mathbb{R}^n$. The set of all simplices is denoted as $\bigcup_{k=1}^{n} \Sigma_k = \Sigma$.*

**Example 2.2.1.** *For instance, the so-called standard $k-1$-simplex $\sigma_k$ can be spanned with the help of canonical coordinate vectors in $\mathbb{R}^n$*

$$T_k := \mathrm{co}\{(e_{i_l})_{l=0\dots k}, \quad (e_i)^j = \delta_i^j\}.$$

*Note that this does not contain the origin of the coordinate system.*

**Example 2.2.2.** *The $n$-simplex spanned by the origin and canonical coordinate vectors $\{0, (e_l)_{l=1,\dots,n}\} \subset \mathbb{R}^n$ is called the reference $n$-simplex, which is widely used in the context of Finite Element Methods. In 1,2 and 3 dimensions these are called the reference line, triangle and tetrahedron, respectively.*

**Definition 10** ($l$-Face)**.** *The lower dimensional $l$-simplex $F = \langle p_{i_0} \dots p_{i_l} \rangle \in \Sigma_l$ generated by a subset of points $(p_{i_m})_{m=0\dots l} \subseteq (p_i)_{i=0\dots k} \in \mathbb{R}^n$ belonging to a $k$-simplex $T = \langle p_0 \dots p_k \rangle \in \Sigma_k$ is called an $l$-face of $T$. $l$-faces with $l = 0, 1, 2$ are also referred to as vertices, edges and faces of $T$, respectively.*

**Definition 11** ($k$-Chains $C_k$)**.** *The vector space of $k$-chains $C_k$ is defined as the set of formal $\mathbb{Z}$-linear combination of oriented $k$-simplices $\Sigma_k$*

$$C_k(M) := \{\sum_{i=1}^{N} a_i T_i, a_i \in \mathbb{Z}, T_i \in \Sigma_k\}.$$

**Definition 12** (Boundary Operator)**.** *The boundary operator is defined as the linear homomorphism $\partial : C_k \to C_{k-1}$ that satisfies*

$$\partial \langle p_0 \dots p_k \rangle = \sum_{i=1}^{k} (-1)^i \langle p_0 \dots \widehat{p}_i \dots p_k \rangle \quad \forall \langle p_0 \dots p_k \rangle \in \Sigma_k$$

*where the hat in $\widehat{p}_i$ indicates that this element is left out of the $k-1$-simplex.*

**Example 2.2.3.** *For simplices in 3 dimensions one can check that the boundary operator generates the oriented boundary of objects which one can visualize geometrically in* $\mathbb{R}^3$.

$$\partial\langle p_0p_1\rangle = \langle p_1\rangle - \langle p_0\rangle$$
$$\partial\langle p_0p_1p_2\rangle = \langle p_1p_2\rangle - \langle p_0p_2\rangle + \langle p_0p_1\rangle$$
$$\partial\langle p_0p_1p_2p_3\rangle = \langle p_1p_2p_3\rangle - \langle p_0p_2p_3\rangle + \langle p_0p_1p_3\rangle - \langle p_0p_1p_2\rangle$$

Sometimes an index $k$ is added to the boundary operator $\partial_k : C_k \to C_{k-1}$ to avoid ambiguity of maps. Also reminiscent of the exterior derivative is the fact that there is no boundary of a boundary $\partial \circ \partial$.

**Lemma 2.2.4.** *The boundary operator composed twice vanishes:* $\partial \circ \partial \equiv 0$.

*Sketch of proof.* The boundary operator $\partial_k$ involves removing items $p_i$ from an ordered permutation $\langle p_1 \dots p_k\rangle \to (-1)^i\langle p_1 \dots \widehat{p}_i \dots p_k\rangle$ and multiplication with a prefactor $(-1)^i$ based on their respective previous positions. Doing this twice for different items $p_i$ and $p_j$ where $i < j$ (without loss of generality) one notices, that while order of operation does not influence the final permutation

$$\langle p_1 \dots p_k\rangle \xrightarrow{\widehat{p}_i} (-1)^i\langle p_1 \dots \widehat{p}_i \dots p_k\rangle \xrightarrow{\widehat{p}_j} (-1)^i(-1)^{j-1}\langle p_1 \dots \widehat{p}_i \dots \widehat{p}_j \dots p_k\rangle$$
$$\langle p_1 \dots p_k\rangle \xrightarrow{\widehat{p}_j} (-1)^j\langle p_1 \dots \widehat{p}_j \dots p_k\rangle \xrightarrow{\widehat{p}_i} (-1)^j(-1)^{i}\langle p_1 \dots \widehat{p}_i \dots \widehat{p}_j \dots p_k\rangle$$

it does affect the sign. Summing over all possible variations as they occur in the boundary operator, one can pair all terms, each pair being virtually identical, but bearing a different sign. Therefore $\partial_{k-1} \circ \partial_k \equiv 0$ holds as an operator. □

Similar to the case of the exterior derivative d we have a chain

$$C_n \xrightarrow{\partial_n} \dots \xrightarrow{\partial_{k+1}} C_k \xrightarrow{\partial_k} C_{k-1} \xrightarrow{\partial_{k-1}} C_{k-2} \xrightarrow{\partial_{k-2}} \dots \xrightarrow{\partial_1} C_0.$$

The idea of triangulations calls for a definition for a collection of simplices that are connected and related to one another in some manner.

**Definition 13** (Simplicial Complex)**.** *A simplicial k-complex* $\mathcal{S} \subseteq \Sigma$ *consists of a set of simplices where*

- *Every l-face f of any k-simplex* $T \in \mathcal{S}$ *is also inside* $f \in \mathcal{S}$.
- *The intersection of two k-simplices* $T_1, T_2 \in \mathcal{S}$ *is either an l-face of both or empty.*

*The space of k-chains associated to the simplicial complex* $\mathcal{S}$ *is denoted as* $C_k(\mathcal{S})$.

**Remark 2.2.5.** *If the setting admits it, we will be using the term simplicial complex a bit more flexibly in the sense that the spatial building blocks in our simplicial complex may not only be simplices, but also squares, cubes, and so on. These may not be simplices in the sense of definition 9 but still fit into the picture of definition 13 which intuitively represents a mesh where elementary geometric shapes are "glued together".*

**Definition 14** (Triangulation of a Smooth Manifold)**.** *A triangulation of a smooth manifold M with dimension n is given by a smooth surjective map* $\mathcal{T} : \mathcal{S} \to M$ *where* $\mathcal{S}$ *comes equipped with the standard subset topology of* $\mathbb{R}^n$*, whose restriction* $\mathcal{T}|_{T_k} : T_k \to \mathcal{T}(T_k)$ *on any k-simplex* $T_k$ *is a diffeomorphism.*

**Remark 2.2.6.** *To sketch the recipe for constructing such a map, we use charts* $(U \subseteq M, \phi : U \to \mathbb{R}^n)$. *We take, for instance, a standard simplex* $\sigma_k$ *near the origin, translate, rotate and or scale it with a map* $T : \mathbb{R}^n \to \mathbb{R}^n$ *in such a way that* $T\sigma_k$ *falls into the chart image* $T\sigma_k \subset \phi(U)$. *We then apply the inverse chart* $\phi^{-1}(T\sigma_k) =: S_k \subseteq M$ *to obtain a simplex mapped onto the manifold M. The thus defined* $S_k$ *is also sometimes called a singular simplex. We proceed by accumulating and gluing such singular simplices together using multiple charts to generate a triangulation. We mention without proof, that any smooth manifold possesses a triangulation.*

**Remark 2.2.7.** *The notions of the exterior algebra together with those of simplicial complexes provide the basic definitions and building blocks for proving Stokes' theorem. $\partial M$ refers to the boundary operator $\partial$ acting on $M$ by identification using a triangulation with a simplicial complex.*

As with any vector space $C_k(\mathcal{S})$, we may look at its dual space.

**Definition 15** ($k$-Cochains $C^k(\mathcal{S})$)**.** *The dual space of $C_k(\mathcal{S})$ is called the space of $k$-cochains $C^k(\mathcal{S})$.*

It can be intuitively understood that $k$-cochains $\phi \in C^k(\mathcal{S})$ assign to each $k$-simplex $T_k \in \mathcal{S}_k \subset C_k(\mathcal{S})$ a real number $\phi(T_k) = \phi_{T_k} \in \mathbb{R}$. Linearity implies that any formal linear combination of oriented simplices $\lambda_k T_k$ is mapped to a virtually identical linear combination of said individual real numbers $\phi_{\lambda_k T_k} = \lambda_k \phi_{T_k}$. Thinking in terms of simplices $(T_k)_{k\in\mathcal{I}}$ that span the basis of $\mathcal{S}_k$ we can alternatively interpret a $k$-cochain as a collection of real numbers $(\phi_{T_k})_{k\in\mathcal{I}}$.

**Definition 16** (Coboundary Operator $\delta$)**.** *The coboundary operator $\delta : C^k(\mathcal{S}) \to C^{k+1}(\mathcal{S})$ is defined as the conjugate map $\partial^*$ of the boundary operator $\partial : C_{k+1}(\mathcal{S}) \to C_k(\mathcal{S})$. It satisfies $\delta \circ \delta = 0$.*

$$\ldots \xrightarrow{\delta_{k-1}} C^k(\mathcal{S}) \xrightarrow{\delta_k} C^{k+1}(\mathcal{S}) \xrightarrow{\delta_{k+1}} C^{k+2}(\mathcal{S})(\mathcal{S}) \xrightarrow{\delta_{k+2}} \ldots \quad \overset{\delta_{k+1}\circ\delta_k=0}{\frown}$$

To make the coboundary operator more tangible we explicitly write down its action in terms of simplices. Let $\phi \in C^k(\mathcal{S})$ be a $k$-cochain which maps to each $k$-simplex $T_k \in \mathcal{S}_k$ a number $\phi(T_k) = \phi_{T_k}$. The conjugate of any map between vector spaces involves its composition with appropriate functionals, which in this case translates to $\partial^*_{k+1}(\phi) = \phi \circ \partial_{k+1}$. This means that $\delta(\phi) \in C^{k+1}$ acts on $k+1$-simplices $T_{k+1} \in \mathcal{S}_{k+1}$ as in

$$\delta(\phi) : T_{k+1} \mapsto \partial T_{k+1} \mapsto \phi_{\partial T_{k+1}}$$

and is therefore represented by the collection of numbers

$$((\delta(\phi))_{T_{k+1}})_{k\in\mathcal{I}} = (\phi_{\partial T_{k+1}})_{T_{k+1}\in\mathcal{S}_{k+1}}.$$

**Remark 2.2.8.** *In the practical setting of numerical simulations on a triangulated domain, one would like to formulate discrete function spaces (i.e. for differential forms) whose degrees of freedom are attached to geometric simplices. This is why the language of cochains is beneficial for this case and one, in particular, seeks a correspondence between cochains and differential forms.*

## 2.3 Dual Lattices

Given a triangulation, or in other words a lattice, it may be necessary in certain scenarios to approach it from a different perspective. The idea of a dual lattice, for which there exist different definitions (sometimes related, sometimes unrelated), provides a useful notion in this context. Here we want to mention two of them, one of which will become relevant for our simulations.

**Definition 17** (Voronoi Dual Lattice)**.** *Given a metric space $(M, \mathrm{d})$ and a simplical complex $\mathcal{S} = \cup_{k=1,\ldots,n}\mathcal{S}_k$ representing a triangulation with vertices $V_k \in \mathcal{S}_0$, the Voronoi cells $\tilde{T}_k$ associated to each vertex $V_k \in \mathcal{S}_0$ are each defined as the set of points which are closest to $V_k$ when compared to all other $V_{l\neq k} \in \mathcal{S}_0$.*

$$\tilde{T}_k := \{x \in |\mathcal{S}| \,|\, \mathrm{d}(x, V_k) \leq \mathrm{d}(x, V_l) \;\; \forall l \neq k\}$$

*The lattice spanned by Voronoi cells is called the Voronoi dual lattice.*

This, intuitively speaking, assigns to each $k$-simplex in $\mathcal{S}$ a $n-k$-dimensional counterpart in the Voronoi dual lattice. For instance in three dimensions $n = 3$, each vertex $V \in \mathcal{S}_0$ is assigned a three dimensional dual cell, and vice versa, each tetrahedron $T \in \mathcal{S}_3$ gets assigned a dual point. We mention one interesting property regarding the application of this dualization procedure.

**Definition 18** (Delauney Triangulation)**.** *A triangulation $\mathcal{S} = \cup_{k=1,\dots,n}\mathcal{S}_k$ is called Delauney, if the circumhemisphere of any $n$-simplex $T \in \mathcal{S}_n$ does not contain any points $V \in \mathcal{S}_0$ of the simplicial complex.*

**Lemma 2.3.1.** *Starting with a Delauney lattice the application of two successive Voronoi lattice dualizations yields the starting lattice.*

For practical purposes we note, that the mesh generator of the ngsolve library [49] is not guaranteed to generate Delauney meshes. In this case it may even occur that the points in the Voronoi lattice associated to $n$-simplices, do not lie inside, as can be seen in figure 2.2.

A different dual lattice of practical importance is given by barycentric dual lattice as defined below.

**Definition 19** (Barycentric Dual Lattice)**.** *The barycentric refinement of a $n$-simplex $T = \langle p_0 \dots p_n \rangle$ is defined as follows. Connect the barycenter $c = 1/n \sum_{k=0}^{n} p_k$ with the barycenters of each one of the $l$ $n-1$-faces $c_{n-1}^{(l)} = 1/(n-1) \sum_{k\neq l}^{n} p_n$ to obtain dual edges. Perform this procedure for each $n-1$-face as well as respective $n-2$-faces. Iteratively continue this process for each of the faces until reaching single points. All barycenters and constructed edges obtained in this way define the barycentric refinement of the $n$-simplex $T$. The barycentric lattice consists of barycentric refinements of all $n$-simplices.*

In three dimensions the barycentric refinement amounts to constructing and connecting barycenters of tetrahedrons as well as respective faces and edges. In contrast to the Voronoi dual lattice, the edges connecting tetrahedron barycenters will in general undergo a kink when crossing the connecting interface. Examples of both dual lattices in the case of a two-dimensional vertex patch lattice are depicted in figures 2.1a and 2.1b.

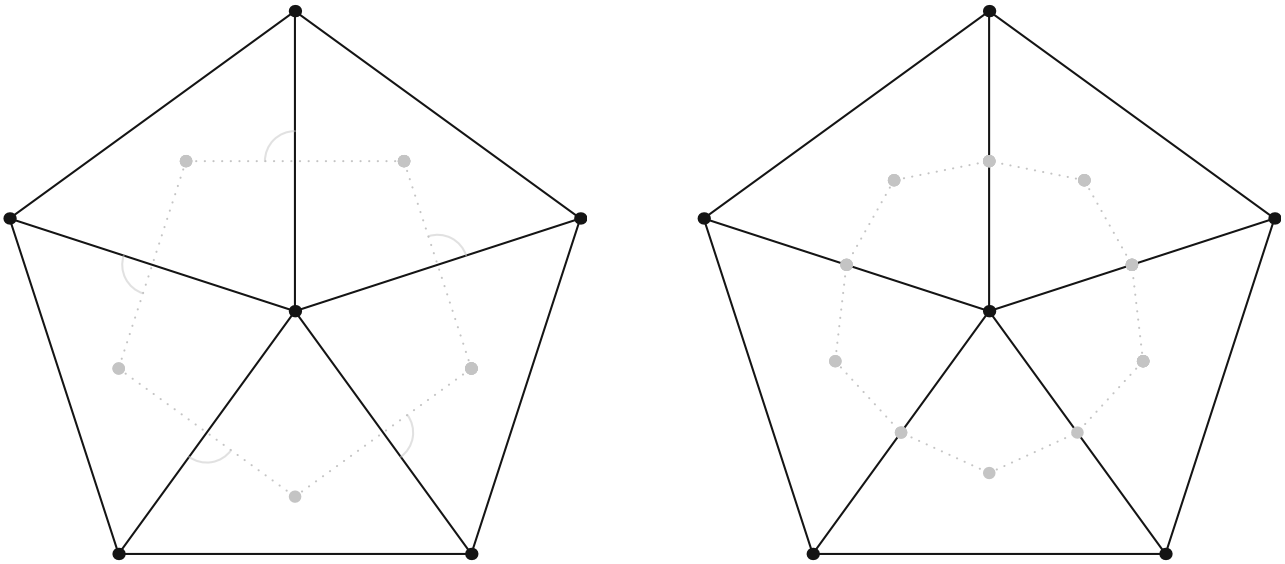

(a) The Voronoi dual lattice of a 2D vertex patch.

(b) The barycentric dual lattice of a 2D vertex patch.

Figure 2.1: Dual lattices of a 2D vertex patch.

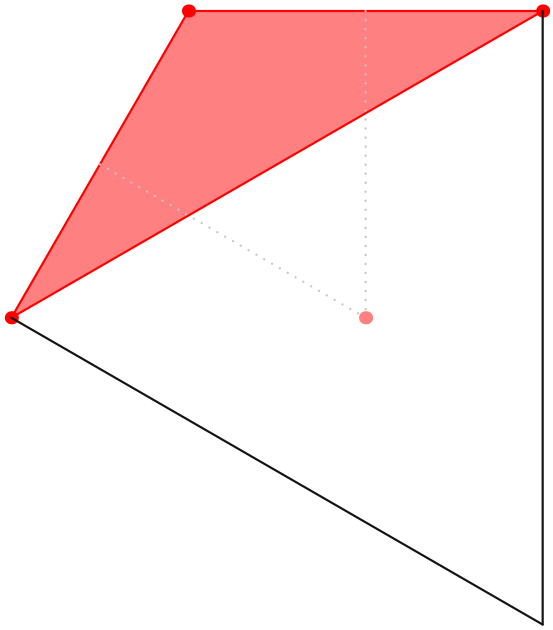

Figure 2.2: If triangles in the lattice are obtuse (such as the red one), it may happen that respective Voronoi dual points are located outside.

## 2.4 Finite Element Exterior Calculus

Differential Forms $\omega \in \Lambda^k(M)$ on a manifold $M$ intuitively carry a geometric character: they can be interpreted as integrable densities over $k$-dimensional sub-domains. For computational purposes it is required to approximate the infinite dimensional space $\Lambda^k(M)$ with a numerically implementable discrete finite counterpart. Furthermore, the space of smooth differential forms that are generated via $C^\infty$ functions is not complete. The framework of Finite Element Exterior Calculus (FEEC) works with the completion of these spaces in order to leverage the theory developed by functional analysis. It also provides a discretization for numerical purposes which fits well with the idea of triangulations and is able to preserve geometrical nuances of the continuum. For a more detailed background we refer to [4] [2] [3].

**Definition 20** (Sobolev Spaces Of Differential Forms)**.** *The space $H\Lambda^k(M)$ is defined as the completion of the space of smooth $k$-forms $\Lambda^k(M)$ with respect to the norm*

$$\|\cdot\|_{H\Lambda^k(M)} : \begin{cases} \Lambda^k(M) & \to & \mathbb{R} \\ \omega & \mapsto & \|\omega\|_{H\Lambda^k(M)} := \sqrt{\langle \omega, \omega \rangle_{\Lambda^k(M)} + \langle \mathrm{d}\omega, \mathrm{d}\omega \rangle_{\Lambda^{k+1}(M)}} \end{cases}$$

*together with the continuous extension of the exterior derivative $\mathrm{d}_{H\Lambda^k(M)} : H\Lambda^k(M) \to H\Lambda^{k+1}(M)$.*

**Example 2.4.1** ($H^1$ functions)**.** *For 0-forms $H\Lambda^0(M)$ the exterior derivative $\mathrm{d}_1 : H\Lambda^0(M) \to H\Lambda^1(M)$ can be interpreted as the gradient in the Sobolev space $H\Lambda^1(M) = H^1(M)$ with norm $\|f\|^2_{H\Lambda^0(M)} = \|f\|^2_{L^2(M)} + \|\mathrm{d}f\|^2_{L^2(M)}$.*

Some of the operations and properties associated with smooth differential forms $\Lambda^k(M)$ are inherited by its completion $H\Lambda^k(M)$ by means of extension and continuity arguments. This, for example, includes the evaluation of $k$-forms on $k$-dimensional sub-manifolds, also known as continuous trace operators. With this in mind, forms in $H\Lambda^k(M)$ can be in this regard still integrated over $k$-dimensional sub-manifolds $N \subset M$ where Stokes' theorem also holds.

We now seek discrete finite dimensional spaces of differential forms $H_h\Lambda^k(M) \subset H\Lambda^k(M)$ that are associated to the triangulation of the domain $M$. In other words, the discrete spaces' degrees of freedom should be attached to simplices $T \in \mathcal{S}$ forming the lattice. In this spirit we let the integrals of $k$-forms over $k$-simplices in the simplicial complex represent our discrete degrees of freedom. This insinuates a formulation in terms of cochains $C^k(\mathcal{S})$ and leads to the following map.

**Definition 21** (de Rham Map)**.** *The de Rham map $R^k$ is defined as*

$$R^k : \left\{ \begin{array}{ccc} H\Lambda^k(M) & \to & C^k(\mathcal{S}) \\ \omega & \mapsto & (T_k \mapsto \int_{\mathcal{T}(T_k)} \omega) \end{array} \right. .$$

For discrete spaces of $k$-forms we essentially require a map $I^k : C^k(\mathcal{S}) \to H\Lambda^k(M)$ that maps the degrees of freedom represented by a $k$-cochain to a corresponding differential form. Compatibility with the de Rham map $R^k \circ I^k = \mathrm{id}_{C^k(\mathcal{S})}$ means that $I^k$ should be a right inverse to the de Rham map $R^k$. Whitney forms and barycentric functions are a constructive way to formulate $I^k$.

**Definition 22** (Local Barycentric Functions)**.** *Let $T = (p_0 \dots p_k)$ be a $k$-simplex. The affine functions $(\lambda_l)_{l=0\dots k}$*

$$\lambda_l : \left\{ \begin{array}{ccc} T & \to & \mathbb{R} \\ x^\mu & \mapsto & \prod_{\mu=1}^n \left(p_l^\mu - x^\mu\right) \end{array} \right.$$

*are called local barycentric functions $\lambda_l$ on $T$ with respective center $p_l^\mu$. The coefficients $(t_l)_{l=0\dots k}$ that satisfy*

$$x = \sum_{l=0}^{k} t_l p_l$$

*are called barycentric coordinates of $x$ on $T$.*

**Definition 23** (Global Barycentric Functions)**.** *The global barycentric functions $\lambda_V : M \to \mathbb{R}$ indexed by vertices $V \in \mathcal{S}_0$ are defined piecewise linear via local ones: for any point $x \in M$ choose any $n$-simplex $T \in \mathcal{S}_n$ such that $x \in T$. If the vertex $V$ belongs to $T$, assign the local barycentric function value, otherwise assign 0.*

These functions $\lambda_V$ are piecewise linear and continuous, and therefore weakly differentiable $\lambda_V \in H\Lambda^0(M)$. A visual example in the case of a two-dimensional mesh is given in figure 2.3.

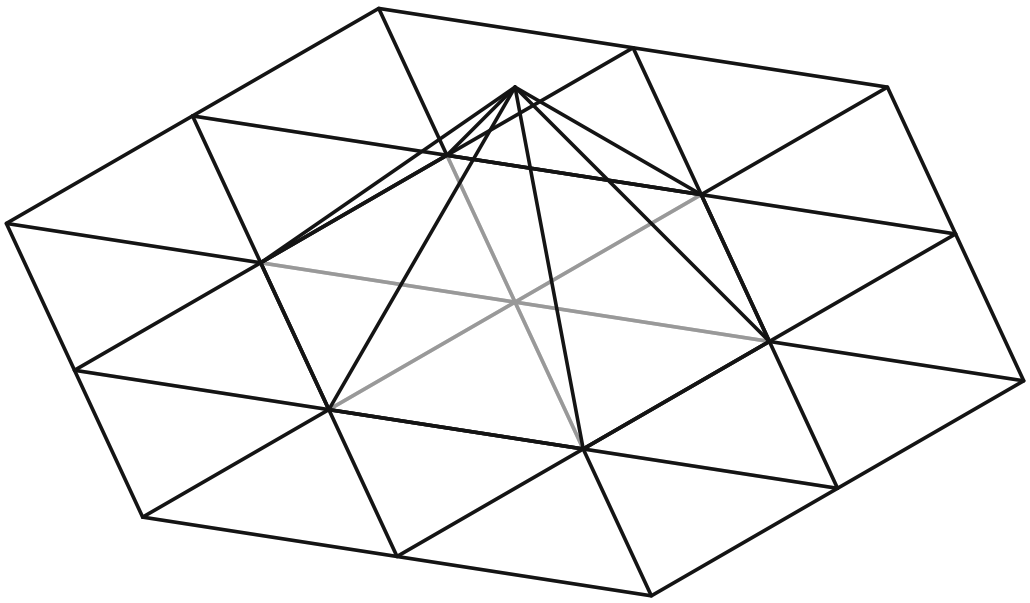

Figure 2.3: An illustration of a piecewise linear global barycentric function associated with a particular vertex in a two-dimensional mesh.

Higher rank differential forms are given by

**Definition 24** (Whitney $k$-Forms)**.** *The Whitney $k$-form $\lambda_{T_k}$ associated to an oriented $k$-simplex $T_k = \langle p_0 \dots p_k \rangle \in \mathcal{S}_k$ is defined via corresponding global barycentric functions $(\lambda_{p_l})_{l=0,\dots,k}$ as in*

$$\lambda_{T_k} := \sum_{\sigma \in \Pi(k+1)} (-1)^{\mathrm{sgn}(\sigma)} \lambda_{p_{\sigma(0)}} \wedge \mathrm{d}\lambda_{p_{\sigma(1)}} \wedge \dots \wedge \mathrm{d}\lambda_{p_{\sigma(k)}}.$$

*The space of Whitney $k$-forms is denoted by $H_{\mathcal{T}}\Lambda^k(M)$.*

The essential property that Whitney $k$-forms $\lambda_T \in H_\mathcal{T}\Lambda^k(M)$ carry is that their integral over any $k$-simplex $T' \in \mathcal{S}_k$ satisfies

$$\int_{T'} \lambda_T = \delta_{T'T} = \begin{cases} 1 & T' = T \\ 0 & T' \neq T \end{cases}$$

and hence the right inverse de Rham map $I^k$ can be given by

$$I^k : \begin{cases} C^k(\mathcal{S}) & \to & H\Lambda^k(M) \\ (\phi_{T_k})_{T_k \in \mathcal{S}_k} & \mapsto & \sum_{T_k \in \mathcal{S}_k} \phi_{T_k} \lambda_{T_k} \end{cases} .$$

While it may not be a left inverse, $I^k \circ R^k$ maps a continuous differential form $\omega \in H\Lambda^k(M)$ to a Whitney form $\omega_h \in H_\mathcal{T}\Lambda^k(M)$ while preserving $\omega$s integrals over $k$-simplices.

**Definition 25** (Whitney Interpolation Operator)**.** *The operator $I_h^k := I^k \circ R^k : H\Lambda^k(M) \to H_\mathcal{T}\Lambda^k(M)$ defines the so-called interpolation operator for Whitney $k$-forms.*

**Example 2.4.2** ($H^1, Hcurl, Hdiv$ Interpolation Operators)**.** *In three spatial dimensions, 0-forms are represented by functions and 1- as well as 2-forms can be interpreted as vector fields using the Hodge star operator $\star : \Lambda^2(M) \to \Lambda^1(M)$ and the musical isomorphism $\sharp : \Lambda^1(M) \to TM$. These can be identified as the so-called scalar $H^1$ functions and $Hcurl$ or $Hdiv$ vector fields respectively.*

*The corresponding Whitney Interpolation operators are given by*

- *point evaluation $f|_V$ of a 0-form $f \in \Lambda^0(M)$ at vertices $V \in \mathcal{S}_0$ followed by linear combinations $\sum_{V \in \mathcal{S}_0} f|_V \lambda_V$ with barycentric vertex functions $\lambda_V$*
- *curve integral $\int_E v$ of a vector field $v \in Hcurl$ along an edge $E \in \mathcal{S}_1$ followed by linear combinations $\sum_{E \in \mathcal{S}_1} \left(\int_E v\right) \lambda_E$ of Whitney 1-form vector fields $\lambda_E$*
- *flux integral $\int_F n \cdot v$ of a vector field $v \in Hdiv$ through a surface $F \in \mathcal{S}_2$ followed by linear combinations $\sum_{F \in \mathcal{S}_2} \left(\int_F n \cdot v\right) (\star\lambda_F)$ of Whitney 2-form vector fields $\star\lambda_F$*

The exterior derivative $\mathrm{d} : H\Lambda^k(M) \to H\Lambda^{k+1}(M)$ is a well defined map on the continuous level and yields the de Rham complex. One appealing property of Whitney forms is their compatibility with this structure.

**Lemma 2.4.3** (Commuting Diagram)**.** *The diagram*

$$\begin{array}{ccc} H\Lambda^k(\mathcal{S}) & \xrightarrow{\mathrm{d}} & H\Lambda^{k+1}(\mathcal{S}) \\ \downarrow{\scriptstyle R^k} & & \downarrow{\scriptstyle R^{k+1}} \\ C^k(\mathcal{S}) & \xrightarrow{\delta} & C^{k+1}(\mathcal{S}) \end{array}$$

*commutes.*

*Proof.* This essentially is Stokes' theorem in disguise. On the one hand we have for $R^{k+1}\mathrm{d}\omega$

$$R^{k+1}\mathrm{d}\omega = \left(\int_{T_{k+1}} \mathrm{d}\omega\right)_{T_{k+1} \in \mathcal{S}_{k+1}} = \left(\int_{\partial T_{k+1}} \omega\right)_{T_{k+1} \in \mathcal{S}_{k+1}}$$

and on the other hand $\delta R^k \omega$ is

$$\delta R^k \omega = \delta \left(\int_{T_k} \omega\right)_{T_k \in \mathcal{S}_k} = \left(\int_{\partial T_{k+1}} \omega\right)_{T_{k+1} \in \mathcal{S}_{k+1}}$$

as $\delta$ is the conjugate map of $\partial$. □

Restricting to Whitney forms $H_{\mathcal{T}}\Lambda^k(\mathcal{S}) \subset H\Lambda^k(\mathcal{S})$ und using $I^k$ as an inverse to $R_k|_{H_{\mathcal{T}}\Lambda^k(M)}$ the diagram commutes in all directions.

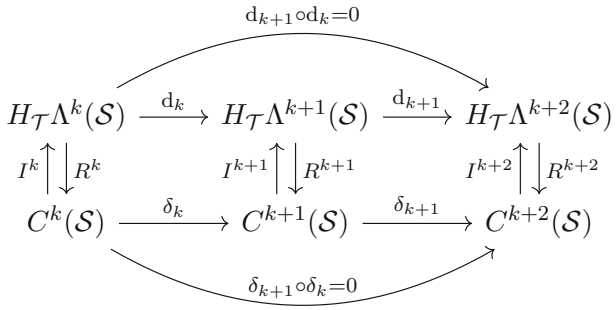


As a consequence we have that the exterior derivative can be interpreted as a well defined map $\mathrm{d} : H_{\mathcal{T}}\Lambda^k(M) \to H_{\mathcal{T}}\Lambda^{k+1}(M)$, which can be evaluated using the linear coboundary operator on $k$-cochain represenations of forms. The latter can be implemented in finite dimensions using a matrix. Same goes for the inner product of Whitney $k$-forms.

**Definition 26** (Mass Matrix)**.** *The mass matrix $M_{TT'}$ indexed via $k$-simplices $T, T' \in \mathcal{S}_k$ is defined via the inner product 5 of two associated Whitney $k$-forms $\lambda_T, \lambda_{T'} \in H_{\mathcal{T}}\Lambda^k(M)$.*

$$M_{TT'} = \langle \lambda_T, \lambda_{T'} \rangle_{\Lambda^k(M)}$$

**Remark 2.4.4.** *The Whitney forms generated by barycentric functions represent finite element spaces of polynomial order one, as they are piecewise linear. These ideas and techniques can be generalized to deliver higher order spaces for differential forms.*

## 2.5 Electrodynamics - a Primer

The theory of electromagnetism was in historical terms the first gauge theory that has been studied, and serves as a gateway towards more general non-Abelian gauge theories. Instead of introducing the formalism as written down by Maxwell with separate time and spatial coordinates, it is beneficial to use a model of combined space and time as introduced in the framework of Special Relativity [41].

**Definition 27.** *The space-time Lorentzian manifold $M$ is the smooth manifold $\mathbb{R}^4$ equipped with a non-degenerate Minkowski metric $g$*

$$g_{\mu\nu} = \begin{pmatrix} -1 & 0 & 0 & 0 \\ 0 & 1 & 0 & 0 \\ 0 & 0 & 1 & 0 \\ 0 & 0 & 0 & 1 \end{pmatrix}_{\mu\nu} \tag{2.2}$$

*with signature $(3, -1)$.*

Most of the quantities in electromagnetism can be identified as differential forms.

**Definition 28** (Gauge Field)**.** *Given the electromagnetic gauge field $A \in \Lambda^1(M)$, the field strength $F \in \Lambda^2(M)$ is defined as $F := \mathrm{d}A$.*

**Definition 29** (Maxwell's Equations)**.** *The relativistic Maxwell's equations read as*

$$\star\, \mathrm{d} \star F = J \tag{2.3}$$
$$\mathrm{d}F = 0 \tag{2.4}$$

*where the 1-form $J \in \Lambda^1(M)$ is called the space-time current.*

**Remark 2.5.1.** *Note that the second equation is automatically fulfilled as the exterior derivative is annihilated if applied twice* $\mathrm{d}F = \mathrm{dd}A = 0$. *Or one may perhaps interpret this the other way around: The ansatz* $F = \mathrm{d}A$ *happens to solve the second equation. Under certain topological conditions, these are, in fact, the only solutions as elaborated by the theory of de Rham cohomology [41].*

**Remark 2.5.2.** *These expressions may be reformulated to yield a more familiar form of equations by expanding objects using generators for forms* $\mathrm{d}x^\mu$.

$$\begin{aligned} J &= J_\mu \mathrm{d}x^\mu \\ A &= A_\mu \mathrm{d}x^\mu \\ F &= F_{\mu\nu} \mathrm{d}x^\mu \wedge \mathrm{d}x^\nu \end{aligned}$$

*Splitting* 3*-dimensional space and time components*

$$J_\mu = \begin{pmatrix} \rho \\ j_x \\ j_y \\ j_z \end{pmatrix}_\mu \quad A_\mu = \begin{pmatrix} \phi \\ A_x \\ A_y \\ A_z \end{pmatrix}_\mu \quad F_{\mu\nu} = \begin{pmatrix} 0 & -E_x & -E_y & -E_z \\ E_x & 0 & B_z & -B_y \\ E_y & -B_z & 0 & B_x \\ E_y & B_y & -B_x & 0 \end{pmatrix}_{\mu\nu}$$

*one would obtain the more familiar electric* $\vec{E}$ *and magnetic fields* $\vec{B}$*, electric potential* $\phi$*, vector potential* $\vec{A}$ *as well as charge* $\rho$ *and spatial current densities* $\vec{j}$*, as they appear in Maxwell's original formulation.*

The gauge symmetry in this formulation of electromagnetism reflects itself in the fact, that gauge fields $A, \tilde{A}$ that differ by an exterior derivative of a function $A - \tilde{A} = \mathrm{d}f$ describe the same field strength.

$$\mathrm{d}A = \mathrm{d}(\tilde{A} + \mathrm{d}f) = \mathrm{d}\tilde{A} + \mathrm{dd}f = \mathrm{d}\tilde{A} \tag{2.5}$$

**Definition 30** (Gauge Transformation)**.** *The addition of a gradient field* $\mathrm{d}f \in \Lambda^1(M)$ *to the gauge field* $A \in \Lambda^1(M)$ *as in equation 2.5 is called an (electromagnetic) gauge transformation.*

**Definition 31** (Continuity Equation)**.** *Given Maxwell's equations in 2.4 there holds the continuity equation*

$$\mathrm{div}J := \star\mathrm{d}\star J = 0. \tag{2.6}$$

*Proof.* This follows from the first Maxwell equation in 2.4 and applying the property of the exterior derivative $\mathrm{d} \circ \mathrm{d} = 0$ as well as $F = \mathrm{d}A$.

$$\mathrm{div}J := \star\mathrm{d}\star J = \star\mathrm{d}\star\star\mathrm{d}\star F = \star\mathrm{dd}\star F = 0$$

□

**Remark 2.5.3.** *The compatibility of discrete Whitney k-forms with the de-Rham chain means that this discretization exactly preserves gauge symmetry and charge conservation of electromagnetism.*

**Remark 2.5.4.** *Note that the only gauge dependent quantity is A. The field strength F and space-time current J are gauge invariant in this theory. It will turn out, that this is not true for generalized non-Abelian gauge theories - here F and J are gauge dependent.*

## 2.6 Gauge Symmetry

### Lie Groups and Lie Algebras

At the center of gauge theories lies the idea of continuous physical symmetries which can be described using Lie groups.

**Definition 32** (Lie Groups and Algebras)**.** *A Lie Group $(G, \circ)$ is a smooth manifold and simultaneously a group, equipped with smooth group product $\circ : G \times G \to G$ and smooth inverse map $(\cdot)^{-1} : G \to G$. The adjoint map $\mathrm{Ad}_g$ with respect to a group element $g \in G$ is defined as*

$$\mathrm{Ad}_g : \left\{ \begin{array}{ccc} G & \to & G \\ h & \mapsto & g \circ h \circ g^{-1} \end{array} \right. .$$

*The associated Lie Algebra $\mathfrak{g}$ is defined as the tangent space at the identity $T_{\mathbb{1}}G$ equipped with the differential geometric Lie Bracket $[\cdot, \cdot] : \mathfrak{g} \times \mathfrak{g} \to \mathfrak{g}$ which satisfies the Jacobi identity*

$$[\tau, [\sigma, \mu]] = [[\tau, \sigma], \mu] + [\sigma, [\tau, \mu]].$$

*The structure constants $c_{klm} \in \mathbb{R}$ of the Lie algebra with respect to a basis $(\tau_k)_{k=1,\dots,\dim\mathfrak{g}}$ are the collection of scalars that represent the Lie bracket via the equation*

$$[\tau_k, \tau_l] = c_{klm}\tau_m. \tag{2.7}$$

*The adjoint map of the Lie group acting on the Lie Algebra is defined as the push-forward $(\mathrm{Ad}_g)_*$*

$$(\mathrm{Ad}_g)_* : \left\{ \begin{array}{ccc} T_{\mathbb{1}}G & \to & T_{\mathbb{1}}G \\ \sigma & \mapsto & (\mathrm{Ad}_g)_*\sigma \end{array} \right. .$$

*The exponential map*

$$\exp : \left\{ \begin{array}{ccc} \mathfrak{g} & \to & G \\ X & \mapsto & \exp\{X\} \end{array} \right.$$

*is defined as follows: Take a Lie algebra element $\sigma \in T_{\mathbb{1}}G = \mathfrak{g}$ and a smooth curve $\sigma : [0, 1] \to G$ representing it as a tangent vector at the identity $\mathbb{1} \in G$. The curve $\gamma_\sigma(t) : [0, 1] \to G$ satisfying*

$$\frac{\mathrm{d}}{\mathrm{d}t}|_{t_0}\gamma_\sigma(t) = \frac{\mathrm{d}}{\mathrm{d}t}|_{t=0}\left(\gamma_\sigma(t_0) \circ \sigma(t)\right) \quad \forall t_0 \in [0, 1],\ \gamma_\sigma(0) = \mathbb{1}$$

*defines the exponential map by $\exp\{\sigma\} := \gamma_\sigma(1)$. It is a local diffeomorphism from the Lie algebra $\mathfrak{g}$ to a neighbourhood of the identity $\mathbb{1} \in G$ in the Lie Group $G$.*

**Remark 2.6.1.** *The type of Lie Groups $G$ and algebras $\mathfrak{g}$ this work will be focussing on are considered to be the "classical" case: matrix Lie groups $G \subset GL(n, \mathbb{C}) \subset \mathbb{C}^{n\times n}$ and associated matrix Lie algebras $\mathfrak{g} \subset \mathfrak{gl}(n, \mathbb{C}) \subset \mathbb{C}^{n\times n}$ (also called linear Lie algebras). Here the group product can be identified as matrix multiplication $g \circ h = gh$ and the Lie Bracket in turn becomes the matrix commutator $[X, Y] = XY - YX$.*

*Furthermore, the push-forward of the adjoint map $(\mathrm{Ad}_g)_*$ can be explicitly evaluated using matrix multiplication of Lie algebra matrices with Lie group matrices $(\mathrm{Ad}_g)_*\sigma = g\sigma g^{-1}$. This is part of the reason why, by slight abuse of notation, this map is often directly referred to as the adjoint map/representation/action $\mathrm{Ad}_g : \mathfrak{g} \to \mathfrak{g}$.*

*Here the (abstract) exponential map $\exp$ also coincides with the matrix exponential map defined via a Taylor Series $e^X := \sum_{n=0}^{\infty} \frac{1}{n!}X^n$. We will reserve $\exp\{X\}$ and $e^X$ for the abstract exponential map and matrix exponential when necessary.*

**Example 2.6.2** (SU(N))**.** *The Lie Group $SU(N)$ consisting of hermitean $\mathbb{C}^{N\times N}$ matrices with unit determinant*

$$SU(N) := \{U \in \mathbb{C}^{N\times N} | UU^\dagger = U^\dagger U = \mathbb{1}, \det U = 1\}$$

*plays a central role in gauge theories. The associated Lie algebra $su(N)$ is the vector space of anti-hermitean traceless $\mathbb{C}^{N\times N}$ matrices*

$$su(N) := \{\tau \in \mathbb{C}^{N\times N} | \tau^\dagger = -\tau, \mathrm{Tr}\,\tau = 0\}.$$

*For more details we refer to section 6.3.1 in the appendix.*

**Remark 2.6.3.** *In physics the Lie algebra $su(N)$ is often defined as the space of hermitean traceless matrices instead. The difference compared to the above definition is accommodated by the inclusion of an $i \in \mathbb{C}$ in the exponential map as in $\tau \mapsto \exp\{i\tau\}$.*

**Remark 2.6.4.** *Even when working with general Lie groups and algebras it may be useful to interpret them as operators on (linear) spaces. Beneficial in this context is the idea of so-called actions and representations.*

**Definition 33** (Group Action)**.** *A group action of a group $(G, \circ)$ onto a set $M$ is a map $\triangleright : G \to End(M)$ (the set of all endomorphisms from $M$ onto itself), that is compatible with the group structure in the sense that*

$$\mathbb{1} \triangleright \psi = \psi, \quad g \triangleright h \triangleright \psi = (g \circ h) \triangleright \psi \quad \forall \psi \in M.$$

**Definition 34** (Group Representation)**.** *A group representation $R : G \to End(V)$ of a group $G$ onto a vector space $V$ over the field $\mathbb{C}$ is a linear group action. In finite dimensions, a representation can be equivalently interpreted as a group homomorphism $R : G \to GL(n, \mathbb{C})$ where $n = \dim V$.*

**Definition 35** (Lie Algebra Representation)**.** *A Lie algebra representation of a Lie algebra $(\mathfrak{g}, [\cdot, \cdot])$ is a linear group homomorphism $\rho : \mathfrak{g} \to \mathbb{C}^{n \times n}$ where the latter is the linear vector space of complex matrices equipped with the matrix commutator $[A, B] = AB - BA$.*

**Remark 2.6.5.** *The definition of Lie algebra representations may be generalized to arbitrary algebra products on the space of complex matrices. However, it is important to note that any (locally diffeomorphic) Lie group representation $R : G \to GL(n, \mathbb{C})$ induces a Lie algebra representation $\rho \equiv R_*|_{\mathbb{1}} : \mathfrak{g} \to \mathfrak{gl}(n, \mathbb{C})$ as the push-forward of $R$ restricted at the identity $\mathbb{1}$: Local diffeomorphisms preserve the (differential geometric) Lie Bracket*

$$R_*([\sigma, \tau]) = [R_*(\sigma), R_*(\tau)] \quad \forall \sigma, \tau \in \mathfrak{g}.$$

*We refer to [35] for a more detailed proof. In 6.3.2 in the appendix we note how Lie group representations $R$ also connect the abstract exponential map $\exp : \mathfrak{g} \to G$ to the more concrete matrix exponential $e^A$ for matrices in $A \in \mathbb{C}^{n \times n}$.*

**Example 2.6.6** (Fundamental Representation)**.** *Any matrix-valued Lie group $G \subset GL(n, \mathbb{C}) \subset \mathbb{C}^{n \times n}$ and Lie algebra $\mathfrak{g} \subset \mathfrak{gl}(n, \mathbb{C}) \subset \mathbb{C}^{n \times n}$ carries the representation given by the embedding $\mathrm{id}_G : G \to GL(n, \mathbb{C})$ or $\mathrm{id}_\mathfrak{g} : \mathfrak{g} \to \mathfrak{gl}(n, \mathbb{C})$. Furthermore, some Lie groups or algebras were historically defined as subsets of matrices $\mathbb{C}^{n \times n}$ to begin with, which is then often reflected in the name the Lie group carries itself. In such cases, the respective representation of the Lie group is also called the fundamental representation.*

**Example 2.6.7** (Adjoint Action onto the Group)**.** *The adjoint map $\mathrm{Ad}. : G \to \mathrm{End}(G)$ is an action of $G$ onto itself.*

**Example 2.6.8** (Adjoint Representation (onto the Lie Algebra))**.** *The push-forward of the adjoint map $(\mathrm{Ad}.)_* : G \to \mathrm{End}(\mathfrak{g})$ defines the co-called adjoint representation onto its associated Lie algebra $\mathfrak{g}$ (a vector space). In the case of a matrix Lie group $G \subset GL(n, \mathbb{C}) \subset \mathbb{C}^{n \times n}$ and associated matrix Lie algebra $\mathfrak{gl}(n, \mathbb{C}) \subset \mathbb{C}^{n \times n}$ we can write down this representation in terms of matrix multiplication*

$$\mathrm{Ad}_*(g) : \begin{cases} \mathfrak{gl}(n, \mathbb{C}) & \to & \mathfrak{gl}(n, \mathbb{C}) \\ \sigma & \mapsto & (\mathrm{Ad}_g)_* \sigma = g \sigma g^{-1} \end{cases} .$$

**Example 2.6.9.** *The adjoint representation of $SU(2)$ onto its three-dimensional Lie algebra is related to $SO(3)$. This is the basis for the famous homomorphism between $SU(2)$ and $SO(3)$ and the phenomena known as the "$4\pi$-symmetry" [1].*

## Global and Local Gauge Symmetry

Lie groups play an essential role in particle physics.

**Example 2.6.10** ($U(1)$ Symmetry of wavefunction)**.** *The complex quantum mechanical wavefunction $\psi : M \to \mathbb{C}$ defined as the solution to the Schrödinger equation*

$$\partial_k \partial^k \psi + V \psi = E \psi$$

*is often used for modelling single particles. While there are many quantities that are observable, such as the probability density function $p := |\psi|^2$, the overall complex phase is unobservable. More concretely, multiplying a wavefunction $\psi$ with a complex phase $e^{i\phi}$ has no effect on physical observables. In other words, the theory exhibits a $U(1) := \{e^{i\phi}, \phi \in \mathbb{R}\}$ symmetry.*

**Example 2.6.11** ($SU(3)$ particle color symmetry)**.** *One basic premise in Quantum ChromoDynamics (QCD) which describes the strong interaction, is that point particles carry an additional property called color. This involves promoting the previously mentioned scalar wavefunction $\psi : M \to \mathbb{C}$ to a vector-valued one $\psi : M \to \mathbb{C}^3$ where each complex entry is interpreted as a different "color". The intuitive requirement that "no color is exceptional" calls for a physical theory which is $SU(3)$ symmetric when multiplying particle wavefunctions $\psi$ with $SU(3)$-rotations $g$ as in $\psi \mapsto g\psi$.*

Often a distinction is made between global and local symmetries. The former one involves multiplying a function $\psi$ with a single constant Lie group element $g \in G$ as in $\psi(\cdot) \mapsto g\psi(\cdot)$, while the latter allows for spatially varying Lie group elements $\psi(\cdot) \mapsto g(\cdot)\psi(\cdot)$.

Complications regarding local symmetries become apparent in terms which involve a derivative. Assume that the Lie group $G$ may act on a color-wavefunction $\psi$ via multiplication $g\psi$. One would like to have that its derivative $\partial_k\psi$ also transforms in the same manner when applying local symmetry transformations $\psi(\cdot) \mapsto \tilde{\psi}(\cdot) = g(\cdot)\psi(\cdot)$. This is obviously not the case as can be seen by using the product rule

$$\partial_k(g(x)\psi(x)) = \partial_k g(x)\psi(x) + g(x)\partial_k\psi(x) \neq g(x)\partial_k\psi(x).$$

Naively reverse engineering the problem and without mathematical rigor, one may try to modify the derivative by adding in another term for compensation. The solution in this case is to add a term $A_k$ which simultaneously transforms with $\psi$ according to $A_k \to \tilde{A}_k = gA_kg^{-1} - \partial_k g g^{-1}$. With the modified derivative $\nabla_k = \partial_k + A_k$ (which now also transforms with $g$!) we get

$$\begin{aligned}
\nabla_k\psi \to \tilde{\nabla}_k\tilde{\psi} &= \partial_k(g\psi) + \tilde{A}_k(g\psi) = \\
&= \partial_k(g\psi) + (gA_kg^{-1} - \partial_k g g^{-1})(g\psi) = \\
&= \partial_k g\psi + g\partial_k\psi + gA_kg^{-1}g\psi - \partial_k g g^{-1}g\psi = \\
&= \partial_k g\psi + g\partial_k\psi + gA_k\psi - \partial_k g\psi = \\
&= g(\partial_k\psi + A_k\psi) = g\nabla_k\psi.
\end{aligned}$$

Hence, the modified derivative $\nabla_k\psi$ transforms in a similar way compared to $\psi$.

The above construction involving $A$ may seem to be a "trick", but it represents a starting point for gauge theories in the context of particle physics. In particular, the special case of the Abelian Lie group $G = U(1)$ simplifies the transformation with an element $g = e^\tau \in U(1)$ and $\tau \in i\mathbb{R}$

$$A_k \to \tilde{A}_k = gA_kg^{-1} - \partial_k g g^{-1} = A_k - \partial_k e^\tau e^{-\tau} = A_k - \partial_k\tau e^\tau e^{-\tau} = A_k - \partial_k\tau$$

down to the addition of the gradient of a function, as is the case in electromagnetism in the last section 2.5.

## 2.7 Non-Abelian Gauge Theories

What follows is a brief introduction to gauge theories with non-Abelian symmetry groups. A mathematically solid foundation can be described using the theory of differential geometry and bundles. We refer to [52] [50] [41] [44] [34] [35] for more detailed perspectives in these directions.

Analogous to the case of Electromagnetism, we define similar quantities of fundamental importance, with one difference being, that they are additionally Lie group- or algebra-valued.

**Definition 36** (Gauge Transformation)**.** *A gauge transformation is represented by a Lie group-valued function $g \in C^\infty(M, G)$, where $G$ is referred to as the gauge group.*

**Remark 2.7.1.** *While the gauge transformation is represented by a function $g \in C^\infty(M, G)$, the way in which it acts can vary depending on the object. In algebraic terms, the action or representation of the Lie group may vary depending on the space it acts upon.*

**Definition 37** (Lie Algebra-Valued Forms)**.** *The space of Lie algebra-valued forms $\Lambda^k(M; \mathfrak{g})$ are fully antisymmetric maps that take $k$ tangent vectors $(v_{(l)})_{l=1,\dots,k}$ and map into the Lie algebra $\mathfrak{g}$.*

Such objects $\phi \in \Lambda^k(M;\mathfrak{g})$ can be decomposed using the tensor product $\mathrm{d}x^\mu \otimes \tau_m$ of generators of the exterior algebra $(\mathrm{d}x^\mu)_{\mu=1,\dots,\dim(M)}$ and a basis of the Lie algebra $(\tau_m)_{m=1,\dots,\dim(\mathfrak{g})}$. In index notation with implied summation this means

$$\phi = \phi^m_\mu \mathrm{d}x^\mu \otimes \tau_m.$$

**Definition 38** (Space-Time Current)**.** *The space-time current $\mathcal{J}$ is a Lie algebra-valued 1-form. It transforms under gauge transformations under the (linear) adjoint representation.*

$$\mathcal{J} \to \mathrm{Ad}_g \mathcal{J} = g\mathcal{J}g^{-1}$$

In order to work with this modified exterior algebra, operations acting on scalar differential forms $\Lambda^k(M)$ have to be suitably extended.

**Definition 39** (Wedge-Bracket)**.** *The Wedge-Bracket $[\omega \wedge \phi]$ of two Lie algebra-valued forms $\omega \in \Lambda^k(M;\mathfrak{g})$ and $\phi \in \Lambda^l(M;\mathfrak{g})$ is defined as the linear extension of*

$$[\mathrm{d}x^\mu \otimes \tau_m \wedge \mathrm{d}x^\nu \otimes \tau_n] := (\mathrm{d}x^\mu \wedge \mathrm{d}x^\nu) \otimes [\tau_m, \tau_n]$$

*where $(\mathrm{d}x^\mu)_{\mu=1,\dots,\dim(M)}$ and $(\tau_m)_{m=1,\dots,\dim(\mathfrak{g})}$ are any basis/set of generators for the space of differential forms and Lie algebra, respectively.*

*It has graded commutativity*

$$[\psi \wedge \phi] = (-1)^{bc+1}[\phi \wedge \psi]$$

*and satisfies a graded product rule*

$$[\omega \wedge [\psi \wedge \phi]] = [[\omega \wedge \psi] \wedge \phi]] + (-1)^{ab}[\psi \wedge [\omega \wedge \phi]]$$

*for forms $\omega \in \Lambda^a(M;\mathfrak{g}), \psi \in \Lambda^b(M;\mathfrak{g}), \phi \in \Lambda^c(M;\mathfrak{g})$ .*

**Definition 40** (Inner Product)**.** *The symmetric linear inner product $\langle \omega, \phi \rangle$ of two Lie algebra-valued forms $\omega \in \Lambda^k(M;\mathfrak{g})$ and $\phi \in \Lambda^l(M;\mathfrak{g})$ is defined as the linear extension of*

$$\langle \mathrm{d}x^\mu \otimes \tau_m, \mathrm{d}x^\nu \otimes \tau_n \rangle := \langle \mathrm{d}x^\mu, \mathrm{d}x^\nu \rangle_{\Lambda^k(M)} \langle \tau_m, \tau_n \rangle_{\mathfrak{g}}$$

*where $(\mathrm{d}x^\mu)_{\mu=1,\dots,\dim(M)}$ and $(\tau_m)_{m=1,\dots,\dim(\mathfrak{g})}$ are any basis/set of generators for the space of differential forms and Lie algebra, respectively.*

*If the inner product $\langle \cdot, \cdot \rangle_{\mathfrak{g}}$ is symmetric and ad-invariant we further have*

$$\langle [\omega \wedge \psi], \phi] \rangle + (-1)^{kl} \langle \psi, [\omega \wedge \phi] \rangle = 0$$

*for forms $\omega \in \Lambda^k(M;\mathfrak{g})), \psi \in \Lambda^l(M;\mathfrak{g})), \phi \in \Lambda^m(M;\mathfrak{g}))$.*

**Definition 41** (Yang-Mills Field)**.** *The Yang-Mills field, otherwise known as connection 1-form $\mathcal{A}$ is a Lie algebra-valued 1-form $\Lambda^1(M;\mathfrak{g})$. Gauge transformations $g \in C^\infty(M,G)$ act on it via*

$$\mathcal{A} \to g\mathcal{A}g^{-1} - \mathrm{d}gg^{-1}.$$

**Definition 42** (Yang-Mills Field Strength)**.** *The Yang-Mills field strength, otherwise known as curvature 2-form $\mathcal{F}$ is a Lie algebra-valued 2-form $\Lambda^2(M;\mathfrak{g})$ defined via the so-called Cartan structure relation*

$$\mathcal{F} = \mathrm{d}\mathcal{A} + \frac{1}{2}[\mathcal{A} \wedge \mathcal{A}].$$

*Gauge transformations $g \in C^\infty(M,G)$ act on it via the (linear) adjoint representation*

$$\mathcal{F} \to \mathrm{Ad}_g \mathcal{F} := g\mathcal{F}g^{-1}.$$

**Remark 2.7.2.** *Although $\mathcal{A}$ is a Lie algebra-valued 1-form, it does not share the transformation behaviour of the space-time currents $\mathcal{J}$. This highlights the fundamental difference between these objects, even though they seem to share the same space. Studying the underlying geometry of principal bundles can further elaborate this distinction: the Yang-Mills field $\mathcal{A}$ represents the connection and captures geometric information, while the space-time current $\mathcal{J}$ is introduced as a physical quantity in the equations of motion.*

*It is remarkable that the curvature 2-form $\mathcal{F}$ transforms similarly to $\mathcal{J}$ under the adjoint representation given that it is defined in terms of $\mathcal{A}$.*

**Remark 2.7.3.** *In a slightly different context of Riemannian geometry, the connection 1-form $\mathcal{A}$ and curvature 2-form $\mathcal{F}$ play a central role in general relativity. Here $\mathcal{A}$ corresponds to the Christoffel symbols, while $\mathcal{F}$ refers to the Riemann 2-form or curvature tensor. The appropriate Lie Algebra is that of the $SO(3,1)$ Lie Group - the group of Lorentz transformations on $3+1$-dimensional space-time.*

The introduced Lie algebra-valued forms can be written down in terms of components

$$\begin{aligned}\mathcal{J} &= \mathcal{J}_\mu \mathrm{d}x^\mu = J^m_\mu \mathrm{d}x^\mu \otimes \tau_m \\ \mathcal{A} &= \mathcal{A}_\mu \mathrm{d}x^\mu = A^m_\mu \mathrm{d}x^\mu \otimes \tau_m \\ \mathcal{F} &= \frac{1}{2}\mathcal{F}_{\mu\nu}\mathrm{d}x^\mu \wedge \mathrm{d}x^\nu = \frac{1}{2}F^m_{\mu\nu}(\mathrm{d}x^\mu \wedge \mathrm{d}x^\nu) \otimes \tau_m\end{aligned}$$

and in section 6.2 of the appendix we additionally write down expressions and equations using these components with index notation.

In order to talk about gradient and divergence of Lie algebra-valued objects, we introduce a modified exterior derivative.

**Definition 43** (Gauge-Covariant Exterior Derivative)**.** *The gauge-covariant exterior derivative $\mathrm{d}_\mathcal{A}\omega$ of Lie algebra-valued forms $\omega \in \Lambda^k(M;\mathfrak{g})$ is defined as*

$$\mathrm{d}_\mathcal{A} : \begin{cases} \Lambda^k(M,\mathfrak{g}) & \to & \Lambda^{k+1}(M,\mathfrak{g}) \\ \omega & \mapsto & \mathrm{d}_\mathcal{A}\omega = \mathrm{d}\omega + [\mathcal{A}\wedge\omega] \end{cases}$$

*with the connection 1-form $\mathcal{A} \in \Lambda^1(M;\mathfrak{g})$. It satisfies the graded product rule*

$$\mathrm{d}_\mathcal{A}[\omega\wedge\phi] = [\mathrm{d}_\mathcal{A}\omega\wedge\phi] + (-1)^k[\omega\wedge\mathrm{d}_\mathcal{A}\phi]$$

*for Lie algebra-valued $k$-forms $\omega \in \Lambda^k(M;\mathfrak{g})$ and $l$-forms $\phi \in \Lambda^l(M;\mathfrak{g})$ and applying it twice yields the curvature $\mathcal{F}$*

$$\mathrm{d}^2_\mathcal{A}\phi = \mathrm{d}_\mathcal{A}\mathrm{d}_\mathcal{A}\phi = [\mathcal{F}\wedge\phi].$$

*Proof.* We compute $\mathrm{d}^2_\mathcal{A}\phi$.

$$\begin{aligned}\mathrm{d}^2_\mathcal{A}\phi &= \mathrm{d}_\mathcal{A}(\mathrm{d}_\mathcal{A}\phi) = \\ &= \mathrm{d}_\mathcal{A}(\mathrm{d}\phi + [\mathcal{A}\wedge\phi]) = \\ &= \mathrm{d}(\mathrm{d}\phi + [\mathcal{A}\wedge\phi]) + [\mathcal{A}\wedge(\mathrm{d}\phi + [\mathcal{A}\wedge\phi])] = \\ &= \mathrm{d}^2\phi + \mathrm{d}[\mathcal{A}\wedge\phi]) + [\mathcal{A}\wedge\mathrm{d}\phi] + [\mathcal{A}\wedge[\mathcal{A}\wedge\phi]] = \\ &= \mathrm{d}[\mathcal{A}\wedge\phi]) + [\mathcal{A}\wedge\mathrm{d}\phi] + [\mathcal{A}\wedge[\mathcal{A}\wedge\phi]] = \\ &= [\mathrm{d}\mathcal{A}\wedge\phi] + (-1)^1[\mathcal{A}\wedge\mathrm{d}\phi]) + [\mathcal{A}\wedge\mathrm{d}\phi] + [\mathcal{A}\wedge[\mathcal{A}\wedge\phi]] = \\ &= [\mathrm{d}\mathcal{A}\wedge\phi] + [\mathcal{A}\wedge[\mathcal{A}\wedge\phi]]\end{aligned} \tag{2.8}$$

The last term can be expressed using the graded product rule

$$[\mathcal{A}\wedge[\mathcal{A}\wedge\phi]] = [[\mathcal{A}\wedge\mathcal{A}]\wedge\phi]] + (-1)^{1\cdot 1}[\mathcal{A}\wedge[\mathcal{A}\wedge\phi]] \tag{2.9}$$

$$[\mathcal{A}\wedge[\mathcal{A}\wedge\phi]] = \frac{1}{2}[[\mathcal{A}\wedge\mathcal{A}]\wedge\phi]] \tag{2.10}$$

so that we get

$$\begin{aligned}\mathrm{d}^2_\mathcal{A}\phi &= [\mathrm{d}\mathcal{A}\wedge\phi] + [\mathcal{A}\wedge[\mathcal{A}\wedge\phi]] = \\ &= [\mathrm{d}\mathcal{A}\wedge\phi] + \frac{1}{2}[[\mathcal{A}\wedge\mathcal{A}]\wedge\phi] = \\ &= [(\mathrm{d}\mathcal{A} + \frac{1}{2}[\mathcal{A}\wedge\mathcal{A}])\wedge\phi] = [\mathcal{F}\wedge\phi].\end{aligned} \tag{2.11}$$

□

**Remark 2.7.4.** *Although the expression in the Cartan structure equation* $\mathrm{d}\mathcal{A}+\frac{1}{2}[\mathcal{A}\wedge\mathcal{A}]$ *shares resemblance with the exterior covariant derivative* $\mathrm{d}_{\mathcal{A}}\mathcal{A}=\mathrm{d}\mathcal{A}+[\mathcal{A}\wedge\mathcal{A}]$*, these should be not confused with each other. The origins of these formulas in differential geometric terms are different.*

A common theme in physics is that governing equations of motion can be derived by applying the variational principle to physical quantities, such as energy and action.

**Definition 44** (Yang-Mills Action)**.** *The Yang-Mills action* $S_{\mathrm{YM}}[\mathcal{A}]$ *for a given space-time current* $\mathcal{J}\in\Lambda^1(M;\mathfrak{g})$ *is defined as*

$$S_{\mathrm{YM}}[\mathcal{A}]=\int_M\langle\mathcal{F},\mathcal{F}\rangle+\langle\mathcal{A},\mathcal{J}\rangle\mathrm{dVol}.$$

Upon variation of the Yang-Mills functional $S_{\mathrm{YM}}[\mathcal{A}]$ with respect to $\mathcal{A}$ one obtains generalized Maxwell's equations.

**Definition 45** (Weak Yang-Mills Equations)**.** *The Yang-Mills equations*

$$\int_M 2\langle\mathcal{F}(\mathcal{A}),\mathrm{d}_{\mathcal{A}}\mathcal{A}'\rangle+\langle\mathcal{J},\mathcal{A}'\rangle\mathrm{dVol}=0$$

*define critical points of the Yang-Mills action.*

*Proof.* We perturb the gauge field $\mathcal{A}+\varepsilon\mathcal{A}'$ within the space of linear space of Lie algebra-valued 1-forms $\Lambda^1(M;\mathfrak{g})$ and form the variation of the Yang-Mills action.

$$\begin{aligned}\mathcal{F}(\mathcal{A}+\varepsilon\mathcal{A}')&=\mathrm{d}\big(\mathcal{A}+\varepsilon\mathcal{A}'\big)+\frac{1}{2}[(\mathcal{A}+\varepsilon\mathcal{A}')\wedge(\mathcal{A}+\varepsilon\mathcal{A}')]=\\&=\mathrm{d}\mathcal{A}+\varepsilon\mathrm{d}\mathcal{A}'+\frac{1}{4}[\mathcal{A}\wedge\mathcal{A}]+\frac{1}{2}\varepsilon[\mathcal{A}\wedge\mathcal{A}']+\frac{1}{2}\varepsilon[\mathcal{A}'\wedge\mathcal{A}]+\frac{1}{2}\varepsilon^2[\mathcal{A}'\wedge\mathcal{A}']=\\&=\mathrm{d}\mathcal{A}+\frac{1}{2}[\mathcal{A}\wedge\mathcal{A}]+\varepsilon(\mathrm{d}\mathcal{A}'+[\mathcal{A}\wedge\mathcal{A}'])+\frac{1}{2}\varepsilon^2[\mathcal{A}'\wedge\mathcal{A}']=\\&=\mathcal{F}+\varepsilon\mathrm{d}_{\mathcal{A}}\mathcal{A}'+\mathcal{O}(\varepsilon^2)\end{aligned}$$

$$\langle\mathcal{F}(\mathcal{A}+\varepsilon\mathcal{A}'),\mathcal{F}(\mathcal{A}+\varepsilon\mathcal{A}')\rangle=\langle\mathcal{F}(\mathcal{A}),\mathcal{F}(\mathcal{A})\rangle+2\varepsilon\langle\mathcal{F}(\mathcal{A}),\mathrm{d}_{\mathcal{A}}\mathcal{A}'\rangle+\mathcal{O}(\varepsilon^2)$$

$$\begin{aligned}\frac{\mathrm{d}}{\mathrm{d}\varepsilon}|_{\varepsilon=0}S_{\mathrm{YM}}[\mathcal{A}+\varepsilon\mathcal{A}']&=\frac{\mathrm{d}}{\mathrm{d}\varepsilon}|_{\varepsilon=0}\int_M\langle\mathcal{F}(\mathcal{A}+\varepsilon\mathcal{A}'),\mathcal{F}(\mathcal{A}+\varepsilon\mathcal{A}')\rangle+\langle\mathcal{J},\mathcal{A}+\varepsilon\mathcal{A}'\rangle\mathrm{dVol}=\\&=\int_M\frac{\mathrm{d}}{\mathrm{d}\varepsilon}|_{\varepsilon=0}\left(\langle\mathcal{F}(\mathcal{A}+\varepsilon\mathcal{A}'),\mathcal{F}(\mathcal{A}+\varepsilon\mathcal{A}')\rangle+\langle\mathcal{J},\mathcal{A}+\varepsilon\mathcal{A}'\rangle\right)\mathrm{dVol}=\\&=\int_M 2\langle\mathcal{F}(\mathcal{A}),\mathrm{d}_{\mathcal{A}}\mathcal{A}'\rangle+\langle\mathcal{J},\mathcal{A}'\rangle\mathrm{dVol}\end{aligned}$$

□

**Remark 2.7.5.** *The Yang-Mills equations in a nutshell take the form of*

$$\star\mathrm{d}_{\mathcal{A}}\star\mathcal{F}=J.$$

*Recalling electromagnetism, there was another equation present which seems to be absent here, but in fact, it is a fundamental identity in differential geoemtry that has its own name: the Bianchi identity* $\mathrm{d}_{\mathcal{A}}\mathcal{F}=0$*. The theory of connections on principal bundles facilitates the proof of this [52] [34] [35].*

In section 6.2.1 of the appendix we convert the weak equations to strong ones by means of partial integration.

**Definition 46** (Non-Abelian Continuity Equation)**.** *Let $\mathcal{A}$ be a critical point of the Yang-Mills action with given space-time current $\mathcal{J}$. Then there holds the non-Abelian continuity equation*

$$\nabla_\mu \mathcal{J}^\mu := \star \mathrm{d}_\mathcal{A} \star \mathcal{J} = 0$$

*where $\nabla_\mu(\cdot)^\mu$ is called the gauge-covariant divergence.*

In coordinates this can be expressed as

$$\nabla_\mu \mathcal{J}^\mu = \partial_\mu \mathcal{J}^\mu + [\mathcal{A}_\mu, \mathcal{J}^\mu]$$

or alternatively by splitting space-time components $\mathcal{J}^0 = \rho, (\mathcal{J}^k)_{k=1,2,3} = (j^k)_{k=1,2,3}$

$$\nabla_\mu \mathcal{J}^\mu = \partial_t \rho + [\mathcal{A}_0, \rho] + \partial_k j^k + [\mathcal{A}_k, j^k] = 0.$$

*Proof.* Note that $\mathrm{d}_\mathcal{A}^2 \tau = [F \wedge \tau]$ for Lie algebra-valued forms $\tau \in \Lambda^p(M, \mathfrak{g})$. Therefore we have

$$\nabla_\mu \mathcal{J}^\mu = \nabla_\mu \nabla_\nu \mathcal{F}^{\mu\nu} = \star \mathrm{d}_A \star \star \mathrm{d}_A \star \mathcal{F} = \star \mathrm{d}_A^2 \star \mathcal{F} = \star [\mathcal{F} \wedge \star \mathcal{F}] = g^{\mu\alpha} g^{\nu\beta} [\mathcal{F}_{\mu\nu}, \mathcal{F}_{\alpha\beta}].$$

Due to symmetry this must be equal to zero.

$$g^{\mu\alpha} g^{\nu\beta} [\mathcal{F}_{\mu\nu}, \mathcal{F}_{\alpha\beta}] = [\mathcal{F}_{\mu\nu}, \mathcal{F}^{\mu\nu}] = -[\mathcal{F}^{\mu\nu}, \mathcal{F}_{\mu\nu}] = -[\mathcal{F}_{\mu\nu}, \mathcal{F}^{\mu\nu}] \Rightarrow \nabla_\mu \mathcal{J}^\mu = 0$$

□

**Example 2.7.6** (Regular Continuity Equation)**.** *In Abelian gauge theories, such as $U(1)$ electromagnetism, the Lie Bracket vanishes and one is left with the regular continuity equation*

$$\nabla_\mu \mathcal{J}^\mu = \partial_\mu \mathcal{J}^\mu + [\mathcal{A}_\mu, \mathcal{J}^\mu] = \partial_\mu \mathcal{J}^\mu = \star \mathrm{d} \star \mathcal{J} = 0.$$

**Remark 2.7.7** (Global vs Local Charge Conservation)**.** *In the Abelian case of electromagnetism, the space-time continuity equation may be integrated over the space-time manifold $M$ after which Stokes' theorem may be applied. By considering boundary-less manifolds or (asymptotically) vanishing boundary currents $\mathcal{J} \to 0$ we get*

$$\int_M \mathrm{div} \mathcal{J} = \int_{\partial M} \mathcal{J} = 0$$

*that the integrated divergence remains zero.*

*Similar to the setting of a space-time manifold $M = \mathbb{R} \times M_S$ that essentially consists of virtually identical slices $M_S$ at different times $t \in \mathbb{R}$ (or a suitable foliation of $M$), we may formulate the total conserved charge $Q(t) := \int_{M_S} \rho(t) \mathrm{d}^3 x$ at time $t \in \mathbb{R}$*

$$\partial_t Q(t) = \partial_t \int_{M_S} \rho(t) \mathrm{d}^3 x = \int_{M_S} \partial_t \rho(t) \mathrm{d}^3 x = \int_{M_S} \partial_k j^k(t) \mathrm{d}^3 x = \int_{\partial M_S} j^k(t) \mathrm{d}^2 x_k = 0.$$

*However, as with general Yang-Mills theories, there exists no such analogue "global" conserved charge: there is no analogue Stokes' theorem for $\mathcal{J}$ or $j$ in this case. Furthermore charges gauge transform according to the adjoint action $\rho \to \mathrm{Ad}_g \rho = g \rho g^{-1}$ and are therefore gauge dependent. Charge conservation should therefore be thought of as a purely local gauge dependent concept described by the gauge-covariant non-Abelian continuity equation.*

The Yang-Mills equations are in general not uniquely solvable unless further suitable restrictions are manually applied. These are known as gauge-fixing and the following one is particularly beneficial for time stepping simulations.

**Definition 47** (Temporal Gauge)**.** *The connection 1-form $\tilde{\mathcal{A}} \in \Lambda^1(M;\mathfrak{g})$ that satisfies $\tilde{\mathcal{A}}_0 = 0$ defines the so-called temporal gauge.*

Given an arbitrary connection 1-form $\mathcal{A} \in \Lambda^1(M;\mathfrak{g})$ reaching the gauge-equivalent connection 1-form in temporal gauge boils down to solving the equation

$$g\mathcal{A}_0 g^{-1} - \partial_0 g g^{-1} = 0.$$

A purely formal solution can be motivated

$$\begin{aligned} &g\mathcal{A}_0 g^{-1} - \partial_0 g g^{-1} = 0 \\ &g\mathcal{A}_t g^{-1} - \partial_t g g^{-1} = 0 \\ &\partial_0 g = a\mathcal{A}_0 \\ &g(t,x^k) = \int_{-\infty}^{t} g(t')\mathcal{A}_t(t',x^k)\mathrm{d}t' \end{aligned}$$

by the so-called ordered exponential

$$g(t,x^k) = \sum_{n=0}^{\infty} \int_{-\infty}^{t} \int_{-\infty}^{t'_n} \int_{-\infty}^{t'_{n-1}} \cdots \int_{-\infty}^{t'_2} \mathcal{A}_0\left(t'_n\right) \cdots \mathcal{A}_0\left(t'_1\right) dt'_1 \cdots dt'_{n-2} dt'_{n-1} dt'_n$$

which will be discussed in more detail in the upcoming section 2.8 and the appendix 6.4.2.

The continuity equation in this gauge takes on the form

$$\nabla_\mu \mathcal{J}^\mu = \partial_t \rho + \nabla_k j^k = \partial_t \rho + \partial_k j^k + [\mathcal{A}_k, j^k] = 0$$

where $\nabla_k(\cdot) = \partial_k(\cdot) + [\mathcal{A}_k, \cdot]$ can be interpreted as the purely spatial gauage covariant derivative.

**Remark 2.7.8.** *No gauge is physically exceptional, meaning that all configurations of $\mathcal{A}$ and $\mathcal{J}$ which are reachable via gauge transformations $g \in C^\infty(M,G)$ are physically equivalent. Choosing a particular gauge may be beneficial for simplifying expressions, equations and calculations.*

A very common approach is to split temporal and spatial parts of equations. We perform this procedure in temporal gauge $\mathcal{A}_0 = 0$ for the the Yang-Mills equations

$$\int_M 2\langle \mathcal{F}(\mathcal{A}), \mathrm{d}_{\mathcal{A}}\mathcal{A}' \rangle + \langle \mathcal{J}, \mathcal{A}' \rangle \mathrm{dVol} = 0$$

in the appendix 6.2.2 to obtain

$$\begin{aligned} &\int_M \langle \mathcal{E}, \mathrm{d}_{\mathcal{A}}\rho' \rangle = \int_M \langle \rho, \rho' \rangle \\ &-\int_M \langle \mathcal{E}, \partial_t \mathcal{E}' \rangle - \int_M \langle 2\mathcal{F}, \mathrm{d}_{\mathcal{A}}\mathcal{E}' \rangle = \int_M \langle j, \mathcal{E}' \rangle \end{aligned}$$

with Lie algebra-valued electric fields $\mathcal{E}$ and spatial field strength $\mathcal{F}$.

**Remark 2.7.9.** *For simulations involving time stepping, the initial conditions posed must satisfy the first equation for $\nu = 0$, which represents a generalized version of the electromagnetic Gauss' law. The second set of equations $\nu = 1,2,3$ can then be used as equations of motion for time evolution of fields.*

**Remark 2.7.10.** *Electromagnetism is a special gauge theory with an underlying Abelian $U(1)$ Lie Group. As a consequence, the corresponding Lie Bracket on the Lie Algebra of imaginary numbers $i\mathbb{R}$ vanishes, and, in short, all algebraic operations commute. Therefore all non-linear terms in the Yang-Mills equations disappear, leaving linear Maxwell equations. The commutative properties furthermore simplify the gauge transformation behaviour, such that the field strength $\mathcal{F}$ and space-time current $\mathcal{J}$ are not affected by gauge transformations.*

## 2.8 Parallel Transport

Gauge theories take inspiration from differential geometry. In particular, the notion of parallel transport plays an important role here.

The upshot is that local quantities belonging to separate points in space(-time) may not be compared directly, even though their types are virtually identical. Vectors from tangent spaces $T_pM$ associated to different points $p \in M$ on a manifold $M$ are a common example in the context of Riemannian geometry - a vector $v \in T_pM$ can not be interpreted as a vector in $T_qM$ for different $q \neq p$. In the case of gauge theories, on the other hand, there exist other physically motivated objects, such as charges, which follow similar rules. In any case, the concept of a connection can define a notion of how to establish a map between such spatially separated yet structurally similar spaces - this idea is known as parallel transport.

**Definition 48** (Parallel Transporter)**.** *Let $\mathcal{A} \in \Lambda^1(M;\mathfrak{g})$ be a Lie algebra-valued connection 1-form and $\gamma : [0,1] \to M$ be a space-time curve. Let $\sigma g := (L_g)_*\sigma \in T_gG$ denote the push-forward of the left translation for any $\sigma \in \mathfrak{g}$. The Lie group-valued function $U \in C^\infty([0,1],G)$ that satisfies the parallel transport equation*

$$\frac{\mathrm{d}}{\mathrm{d}t}U(t) + \mathcal{A}(\dot\gamma(t))U(t) = 0$$

*is called the parallel transporter along $\gamma$. Gauge transformations $g \in C^\infty(M,G)$ act on it via $g(\gamma(t))U(t)g(\gamma(0))$.*

In section 6.4.1 of the appendix we demonstrate how the transformation behaviour of the connection $\mathcal{A}$ implies that of $U(t)$.

The notion of parallel transporters is a useful tool for the next concept.

**Definition 49** (Covariantly Constant)**.** *Let $\psi \in C^\infty(M,V)$ be a $V$-valued function with some linear representation space $V$ on which the Lie group $G$ and Lie algebra $\mathfrak{g}$ may act.*

*Let $\blacktriangleright\colon G \times V \to V$ be the representation under which $\psi \in V$ gauge transform.*

*Let $\triangleright : TG \times V \to V$ be the corresponding representation that satisfies*

$$\left(\frac{\mathrm{d}}{\mathrm{d}t}g(t)\right) \triangleright \psi = \frac{\mathrm{d}}{\mathrm{d}t}\left(g(t) \blacktriangleright \psi\right) \quad \forall g(\cdot) \in C^\infty([0,1],G).$$

*The differential operator*

$$\nabla_{\mathcal{A}}\psi := \mathrm{d}\psi + \mathcal{A} \triangleright \psi$$

*is called covariant derivative. $\psi$ is said to be covariantly constant along a curve $\gamma : [0,1] \to M$ if the $\psi$-parallel transport equation*

$$\nabla_{\mathcal{A}}\psi(\dot\gamma(t)) = \mathrm{d}\psi(\dot\gamma(t)) + \mathcal{A}(\dot\gamma(t)) \triangleright \psi = 0$$

*holds for all $t \in [0,1]$.*

**Remark 2.8.1.** *The covariant exterior derivative $\mathrm{d}_{\mathcal{A}} : \Lambda^k(M;\mathfrak{g}) \to \Lambda^{k+1}(M;\mathfrak{g})$ would be an example with the linear action $\mathcal{A} \triangleright \psi = [\mathcal{A},\psi]$ on the Lie algebra $V = \mathfrak{g}$. We only mention that the above definition of the covariant derivative is a more general one and may be applied to other quantities such as charges.*

Figure 2.4 shows an illustration of parallel transport along a curve involving an object on a unit circle.

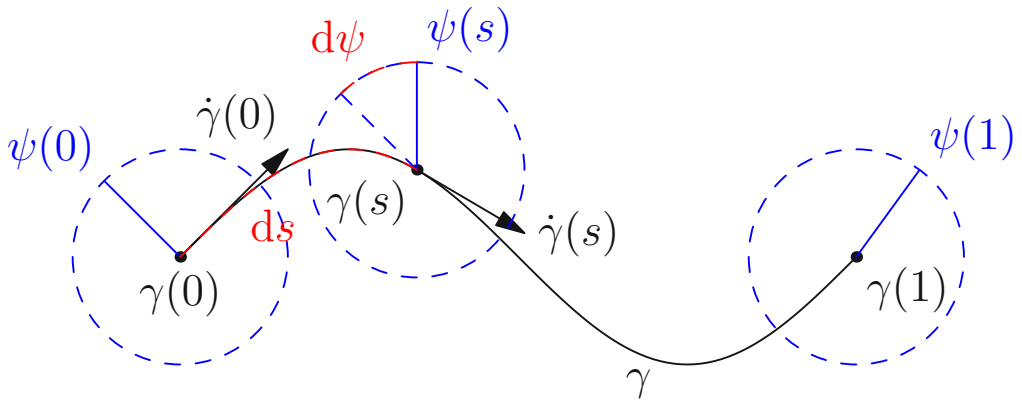


Figure 2.4: Sketch of the setting involving parallel transport of a quantity $\psi(0)$ living on the dashed unit circle along a curve $\gamma$. While each dashed circle along the curve $\gamma$ is virtually identical, they should be thought of as distinct "spaces". A connection prescribes how to interpret objects *psi*$(0)$ in one spatial location, as ones of different locations $\psi(1)$ by means of "continuous" transformations along a curve $\gamma$.

**Lemma 2.8.2.** *In the above setting, an initial value $\psi_x \in V$ at $x \in M$ can be covariantly constantly extended to a function $\psi : [0,1] \to V$ along $\gamma : [0,1] \to M$ using the parallel transporter $U : [0,1] \to G$*

$$\psi(t) := U(t) \blacktriangleright \psi_x.$$

*Proof.* We use the linear and defining property of the Lie group/algebra actions. we first note that any Lie algebra vector $\tau \in \mathfrak{g}$ represents a curve $\gamma_\tau : [0,1] \to G$ on $G$. Hence we have for any Lie group element $g$

$$\begin{aligned}
\tau \triangleright g \blacktriangleright \psi = = \left(\frac{\mathrm{d}}{\mathrm{d}t}|_{t=0}\gamma_\tau(t)\right) \triangleright g \blacktriangleright \psi = \\
= \frac{\mathrm{d}}{\mathrm{d}t}|_{t=0} \left(\gamma_\tau(t) \blacktriangleright g \blacktriangleright \psi\right) = \\
= \frac{\mathrm{d}}{\mathrm{d}t}|_{t=0} \left(\gamma_\tau(t) g \blacktriangleright \psi\right) = \\
= \left(\frac{\mathrm{d}}{\mathrm{d}t}|_{t=0}(\gamma_\tau(t) g)\right) \blacktriangleright \psi = \\
= (\tau g) \triangleright \psi.
\end{aligned}$$

Applying this to $U$ we obtain

$$\begin{aligned}
\frac{\mathrm{d}}{\mathrm{d}t}\psi(t) = \frac{\mathrm{d}}{\mathrm{d}t}\left(U(t) \blacktriangleright \psi_x\right) = \\
= \left(\frac{\mathrm{d}}{\mathrm{d}t}U(t)\right) \triangleright \psi = \\
= (-\mathcal{A}(\dot\gamma(t))U(t)) \triangleright \psi = \\
= -\mathcal{A}(\dot\gamma(t)) \triangleright U(t) \blacktriangleright \psi = \\
= -\mathcal{A}(\dot\gamma(t)) \triangleright \psi(t) = \\
\Rightarrow \frac{\mathrm{d}}{\mathrm{d}t}\psi(t) + \mathcal{A}(\dot\gamma(t)) \triangleright \psi(t) = 0.
\end{aligned}$$

□

**Example 2.8.3.** *Color charges $\rho_x \in \mathfrak{g}$ located at some points $x \in M$ transform under the adjoint action $g \blacktriangleright \rho := \mathrm{Ad}_g\rho = g\rho g^{-1}$ of the Lie group. The corresponding linear action of the Lie Algebra $\mathcal{A} \triangleright \rho$ is the*

*Lie Bracket.*

$$\begin{aligned}\left(\frac{\mathrm{d}}{\mathrm{d}t}\left(g(t)\rho g^{-1}(t)\right)\right)|_{t=0} &= \left(\frac{\mathrm{d}}{\mathrm{d}t}g(t)\rho g^{-1}(t) + g(t)\rho\frac{\mathrm{d}}{\mathrm{d}t}g^{-1}(t)\right)|_{t=0} = \\ &= \left(\frac{\mathrm{d}}{\mathrm{d}t}|_{t=0}g(t)\rho g^{-1}(t) + g(t)\rho(-g^{-1}(t)\frac{\mathrm{d}}{\mathrm{d}t}g(t)g^{-1}(t))\right)|_{t=0} = \\ &= \left(\frac{\mathrm{d}}{\mathrm{d}t}|_{t=0}g(t)\rho g^{-1}(t) - g(t)\rho g^{-1}(t)\frac{\mathrm{d}}{\mathrm{d}t}g(t)g^{-1}(t)\right)|_{t=0} = \\ &= \frac{\mathrm{d}}{\mathrm{d}t}g(0)\rho - \rho\frac{\mathrm{d}}{\mathrm{d}t}g(0) = [\frac{\mathrm{d}}{\mathrm{d}t}g(0), \rho]\end{aligned}$$

*Hence $U(t) \blacktriangleright \rho_x = U(t)\rho_x U^{-1}(t)$ solves $\rho$'s parallel transport equation with $\mathcal{A}(\dot\gamma(t)) \triangleright \rho = [\mathcal{A}(\dot\gamma(t)), \rho]$.*

The parallel transporter $U(t)$ may act as a Lie group element on objects to enable the comparison of spaces that formerly belong to distinct points in space-time.

**Definition 50** (Parallel Transport Map)**.** *Let $V$ be linear representation space $V$ on which the Lie group $G$ and Lie algebra $\mathfrak{g}$ may act linearly, as in the above setting. The parallel transport map for a curve $\gamma : [0,1] \to M$ connecting points $\gamma(0) = x$ and $\gamma(1) = x'$ is defined via the parallel transporter $U \in C^\infty([0,1], G)$ as*

$$U_{x\to x'} : \left\{ \begin{array}{ccc} V & \to & V \\ \psi & \mapsto & U_{x\to x'}\psi = U(1) \blacktriangleright \psi \end{array} \right. .$$

It is important to note that the result depends on the the entire curve trajectory. Parallel transporters associated to different curves which share the same starting and endpoints may deliver different values in general.

So far we have reframed the solution of parallel transport equations of objects in linear representation spaces $\psi \in V$ to that of the parallel transporters $U \in G$. The equation that defines the latter can be formally solved by using the path ordered exponential.

**Definition 51** (Path Ordered Exponential)**.** *Let $\gamma : [0,1] \to M$ be a smooth curve $\gamma \in C^\infty([0,1], M)$ connecting points $x, x' \in M$. The path ordered exponential*

$$U(t) = \mathcal{P}\left\{\exp\left\{\int_0^t \mathcal{A}(\dot\gamma(t'))\mathrm{d}t'\right\}\right\} \tag{2.12}$$

$$:= \sum_{n=0}^{\infty}\int_0^1\int_0^{t'_n}\int_0^{t'_{n-1}}\cdots\int_0^{t'_2}\mathcal{A}(\dot\gamma(t'_n))\cdots\mathcal{A}(\dot\gamma(t'_1))\mathrm{d}t'_1\cdots\mathrm{d}t'_n \tag{2.13}$$

*solves the parallel transporter equations*

$$\frac{\mathrm{d}}{\mathrm{d}t}U(t) + A(\dot\gamma(t))U(t) = 0.$$

We mention elements of the proof in section 6.4.2 of the appendix.

**Example 2.8.4.** *In the case where individual $\mathcal{A}$'s commute the path ordered exponential reduces to the regular exponential as shown in the appendix 6.4.2. This is for instance the case in Abelian gauge theories, such as Electromagnetism with the $U(1)$ group, or if $\mathcal{A}$ is constant along $\gamma$.*

Parallel transporters along closed curves play a special role: their transformation behaviour is purely local $U[\gamma] \to g(\gamma(0))U[\gamma]g^{-1}(\gamma(0))$.

**Definition 52** (Wilson Loop)**.** *Let $U[\gamma]$ be the parallel transporter along a closed curve $\gamma : [0,1] \to M$, $\gamma(0) = \gamma(1)$. The gauge invariant trace is called the Wilson loop $W[\gamma] = \mathrm{Tr}\{U[\gamma]\}$.*

Gauge invariance follows from cyclicity of the trace and the gauge transformation of parallel transporters for closed loops.

$$W[\gamma] = \mathrm{Tr}\{U[\gamma]\} \to \mathrm{Tr}\{g(\gamma(0))U[\gamma]g^{-1}(\gamma(0))\} = \mathrm{Tr}\{g^{-1}(\gamma(0))g(\gamma(0))U[\gamma]\} = \mathrm{Tr}\{U[\gamma]\} = W[\gamma]$$

The fact that Wilson loops are invariant under gauge transformations, suggests that they represent physical observables. Indeed, there is a link to the Yang-Mills field strength $\mathcal{F}$.

**Example 2.8.5.** *Take a small closed loop of dimension $\varepsilon << 1$ in space-time and expand its respective parallel transporter $U$ in terms of $\varepsilon$. Following the calculation 6.4.3 in the appendix we obtain an expression directly related to the components of the Yang-Mills field strength $\mathcal{F}_{\mu\nu}$*

$$U = \mathbb{1} + \varepsilon^2 \mathcal{F}_{\mu\nu} \dot{\gamma}^{\mu}_{(1)} \dot{\gamma}^{\nu}_{(2)} + \mathcal{O}(\varepsilon^3). \tag{2.14}$$

*Therefore the field strength components $\mathcal{F}_{\mu\nu}$ can be intuitively thought of as representing the infinitesimal parallel transport along an infinitesimal loop located in the plane spanned by $\mu$- and $\nu$-coordinate directions.*

**Remark 2.8.6.** *In electromagnetism, an Abelian gauge theory, the above result can be more concretely obtained by using Stokes' theorem on a surface $S$ in the form of*

$$\exp\left\{\int_S \mathcal{F} \mathrm{d}A\right\} = \exp\left\{\oint_{\partial S} \mathcal{A} \mathrm{d}t\right\}.$$

*There also exist non-Abelian versions of this theorem tailored towards $\mathcal{F} = \mathrm{d}\mathcal{A} + \frac{1}{2}[\mathcal{A} \wedge \mathcal{A}]$ and $\mathcal{A}$, which are partly based on the Taylor expansion procedure outlined in the above example [11].*

This forms the basis for the current state-of-the-art discretization of gauge theories.

## 2.9 Lattice Gauge Theory (LGT)

Lattice gauge theory (LGT) is a framework for discretizing gauge theories while respecting nuances and properties present in the continuum [22]. It is a finite difference approach, in which space-time is discretized onto a discrete lattice where some functions, such as charges, are associated to vertices while other objects, such as currents, belong to edges connecting these vertices. In particular, the continuous Yang-Mills field $\mathcal{A} \in \Lambda^1(M; \mathfrak{g})$ is replaced with a discrete set of parallel transporters $(U_{x,\mu})_{x \in M, \mu=0,\dots,3} \in G$ called gauge links that connect vertices $x$ and $x + \hat{\mu}$. Based on the Taylor expansion formula that resembles Stokes' theorem, the Yang-Mills field strength $\mathcal{F} \in \Lambda^2(M; \mathfrak{g})$ will be associated to parallel transporters $U_{\square}$ along lattice loops $\square$ that can be formed with these gauge links $(U_{x,\mu})_{x \in M, \mu=0,\dots,3} \in G$.

As we did for continuous gauge theories, we will build the basics of lattice gauge theory separately but will not study the convergence towards the former in the continuum limit.

**Definition 53** (LGT Space-Time Lattice)**.** *The discrete space-time lattice $\mathbb{M}$ consists of a hypercubic lattice with even spacing $(a^\mu)_{\mu=0,\dots,3} \in \mathbb{R}^4$*

$$\mathbb{M} := \left\{ x \in \mathbb{R}^4 | x = \sum_{\mu=0}^{3} n_\mu a^\mu, \quad n_\mu \in \mathbb{Z} \right\}$$

*equipped with the Minkowski metric*

$$g_{\mu\nu} = \begin{pmatrix} -1 & 0 & 0 & 0 \\ 0 & 1 & 0 & 0 \\ 0 & 0 & 1 & 0 \\ 0 & 0 & 0 & 1 \end{pmatrix}_{\mu\nu}.$$

*We denote the point reachable from a vertex $x \in \mathbb{M}$ going one step $a^\mu$ into the $\mu$th coordinate direction as $x + \hat{\mu}$. The edge going from $x \in \mathbb{M}$ to $x + \hat{\mu}$ is $E_{x,\mu} \in \mathbb{E}$. We denote a small rectangular loop that starts at a vertex $x \in \mathbb{M}$ and is spanned by coordinate directions $\mu$ and $\nu$ as in the path $x \to x+\hat{\mu} \to x+\hat{\mu}+\hat{\nu} \to x+\hat{\nu} \to x$ via $F_{v,\mu\nu} \in \mathbb{F}$.*

**Definition 54** (LGT Gauge Transformation)**.** *A discrete gauge transformation in LGT is represented by a Lie group-valued function $g : \mathbb{M} \to G$.*

**Definition 55** (LGT Space-Time Current)**.** *The discrete space-time current $\mathcal{J}$ in LGT is represented by a Lie algebra-valued function $J : \mathbb{E} \to \mathfrak{g}$. It transforms under gauge transformations $g : \mathbb{M} \to G$ at the starting point $v \in \mathbb{M}$ of each edge $E_v \in \mathbb{E}$ under the (linear) adjoint representation.*

$$\mathcal{J}_{x,\mu} \to \mathrm{Ad}_{g_x} \mathcal{J}_{x,\mu} = g_x \mathcal{J}_{x,\mu} g_x^{-1}$$

**Remark 2.9.1.** *The choice of whether the discrete current transforms at the edge's starting or endpoint is a mere convention.*

**Definition 56** (LGT Gauge Links)**.** *The discrete connection in LGT is represented by Lie group-valued Gauge Links* $(U_{E_v})_{E_v \in \mathbb{E}}$ *- that describe a function* $U : \mathbb{E} \to G$*. It transforms under gauge transformations* $g : \mathbb{M} \to G$ *as in*

$$U_{x,\mu} \to g_x U_{x,\mu} g^{-1}_{x+\hat{\mu}}.$$

*Parallel transporters* $U_\gamma$ *along lattice paths* $\gamma \equiv ((x_k, \mu_k))_{k=0,\dots,n}$ *are constructed using Gauge Links via*

$$U_\gamma := \prod_{k=0}^{n} U_{x_k,\mu_k} = U_{x_0,\mu_0} U_{x_1,\mu_1} \dots U_{x_n,\mu_n}.$$

**Remark 2.9.2.** *The order of multiplication of gauge links follows the Lattice Gauge Theory convention which differs from the regular application of matrices on vectors. In the latter case the above multiplication should be performed in the opposite direction, starting on the right with the first parallel transporter.*

$$U_\gamma = \dots U_{x_n,\mu_n} \dots U_{x_1,\mu_1} U_{x_0,\mu_0}$$

*The transition from continuum to LGT parallel transporters can be consistently achieved by inversion*

$$U_{cont} \to U_{LGT} = U^{-1}_{cont} = U^{\dagger}_{cont}.$$

**Definition 57** (Plaquette)**.** *A Plaquette* $W_{x,\mu\nu}$ *belonging to a face* $F_{x,\mu\nu}$ *is the smallest rectangular loop parallel transporter starting at* $x \in \mathbb{M}$ *which is spanned by coordinate directions* $\hat{\mu}$ *and* $\hat{\nu}$*.*

$$W_{x,\mu\nu} := U_{x,\mu} U_{x+\hat{\mu},\nu} U_{x+\hat{\mu}+\hat{\nu},-\mu} U_{x+\hat{\nu},-\nu}$$

Examples of parallel transporters and plaquettes are illustrated in figure 2.5.

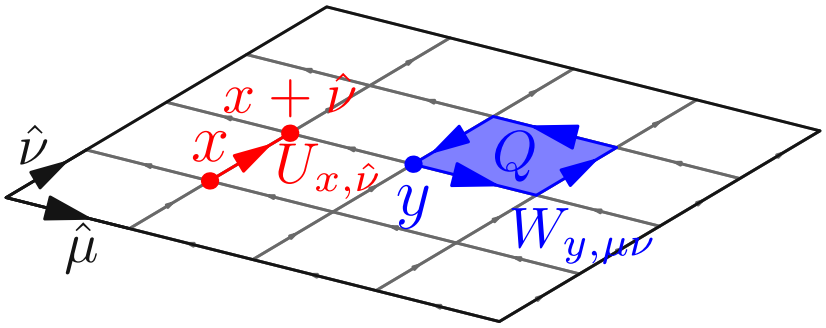


Figure 2.5: Illustration of a parallel transporter $U_{x,\nu}$ and plaquette variables $W_{y,\mu\nu}$ on a two dimensional square lattice.

We now seek a discretization of the Yang-Mills action $S_{YM} = 2\langle \mathcal{F}, \mathcal{F} \rangle + \langle \mathcal{J}, \mathcal{A} \rangle$. Assuming that the gauge links $U_{x,\mu}$ and in turn the plaquettes $U_{x,\mu\nu}$ are close enough to the identity $U \simeq \mathbb{1}$ we may formally take the logarithms $\ln U_{x,\mu}$ and $\ln U_{x,\mu\nu}$.

**Definition 58** (LGT Gauge Field)**.** *The discrete gauge field in LGT* $\mathcal{A}$ *is represented by a Lie algebra-valued function* $\mathcal{A} : \mathbb{E} \to \mathfrak{g}$*.*

$$\mathcal{A} \equiv \mathcal{A}_{x,\mu} = \frac{1}{a^\mu} \ln U_{x,\mu} \simeq \frac{1}{a^\mu}(\mathbb{1} - U_{x,\mu})$$

**Definition 59** (LGT Field Strength)**.** *The discrete field strength in LGT* $\mathcal{F}$ *is represented by a Lie algebra-valued function* $\mathcal{F} : \mathbb{F} \to \mathfrak{g}$*.*

$$\mathcal{F} \equiv \mathcal{F}_{x,\mu\nu} = \frac{1}{a^\mu a^\nu} \ln W_{x,\mu\nu} \simeq \frac{1}{a^\mu a^\nu}(\mathbb{1} - W_{x,\mu\nu})$$

*It transforms under gauge transformations* $g : \mathbb{M} \to G$ *at each plaquette's* $U_{x,\mu\nu}$ *starting point* $X \in \mathbb{M}$ *under the (linear) adjoint representation.*

$$\mathcal{F}_{x,\mu\nu} \to g_x \mathcal{F}_{x,\mu\nu} g^{-1}_x$$

**Definition 60** (Wilson Action)**.** *The discretely gauge invariant Wilson action with current source terms*

$$S_W := \sum_{x\in\mathbb{M}}\sum_{\mu,\nu=0}^{3} g^{\mu\mu}g^{\nu\nu}\frac{1}{(a^\mu a^\nu)^2}\operatorname{Tr}\{(\mathbb{1}-W_{x,\mu\nu})(\mathbb{1}-W_{x,\mu\nu}^\dagger)\}+ \\ +\sum_{x\in\mathbb{M}}\sum_{\mu,\nu=0}^{3} g^{\mu\nu}\operatorname{Tr}\{\mathcal{J}_{x,\mu}\mathcal{A}_{x,\nu}^\dagger\}$$

*is a LGT approximation of the Yang-Mills action.*

**Remark 2.9.3.** *Sometimes the trace term is reformulated using*

$$\begin{aligned}\operatorname{Tr}\{(\mathbb{1}-W_{x,\mu\nu})(\mathbb{1}-W_{x,\mu\nu}^\dagger)\} &= \operatorname{Tr}\{\mathbb{1}-W_{x,\mu\nu}-W_{x,\mu\nu}^\dagger+W_{x,\mu\nu}W_{x,\mu\nu}^\dagger)\} = \\ &= \operatorname{Tr}\{\mathbb{1}-W_{x,\mu\nu}-W_{x,\mu\nu}^\dagger+\mathbb{1}\} = \\ &= \operatorname{Tr}\{\mathbb{1}-W_{x,\mu\nu}-W_{x,\mu\nu}^\dagger+\mathbb{1}\} = \\ &= \operatorname{Tr}\{2-W_{x,\mu\nu}-W_{x,\mu\nu}^\dagger\}.\end{aligned}$$

**Remark 2.9.4.** *The natural discretization of $\langle\mathcal{F},\mathcal{F}\rangle$ would be one*

$$\sum_{\mu,\nu,\alpha,\beta=0}^{3} g^{\mu\alpha}g^{\nu\beta}\frac{1}{a^\mu a^\nu}\frac{1}{a^\alpha a^\beta}\operatorname{Tr}\{\ln W_{x,\mu\nu}(\ln W_{x,\alpha\beta})^\dagger\}$$

*where distinct plaquettes $W_{x,\mu\nu}$ and $W_{x,\alpha\beta}^\dagger$ with $(\mu,\nu)\neq(\alpha,\beta)$ encounter each other. The Wilson action takes one approximation step further and discards such terms. In a FEM context this can be interpreted as mass lumping [14].*

In the case of continuous Yang-Mills theory, the Yang-Mills action may be varied with respect to the gauge field $\mathcal{A}\in\Lambda^1(M;\mathfrak{g})$ which lives in the linear space of Lie algebra-valued forms. In lattice gauge theory, on the other hand, $\mathcal{A}$ is replaced by parallel transporters $U\in G$ which reside in the Lie group manifold. We therefore need to find a suitable notion of variation for this case.

One idea might involve the parametrization of gauge group elements $U\in G$ using the exponential map $U=\exp\{\mathcal{A}\}$ where $\mathcal{A}\in\mathfrak{g}$ may be straightforwardly varied $\mathcal{A}+t\delta\mathcal{A}\in\mathfrak{g}$. Thinking in terms of representations and power series of matrices the variation of the matrix exponential takes on

$$\frac{\mathrm{d}}{\mathrm{d}t}|_{t=0}\sum_{n=0}^{\infty}a_n(\mathcal{A}+t\delta\mathcal{A})^n = \sum_{n=0}^{\infty}a_n\frac{\mathrm{d}}{\mathrm{d}t}|_{t=0}(\mathcal{A}+t\delta\mathcal{A})^n = \tag{2.15}$$

$$= \sum_{n=0}^{\infty}a_n\left(\sum_{k=1}^{n}(\mathcal{A}+t\delta\mathcal{A})^k\frac{\mathrm{d}}{\mathrm{d}t}(\mathcal{A}+t\delta\mathcal{A})(\mathcal{A}+t\delta\mathcal{A})^{n-k}\right)|_{t=0} = \tag{2.16}$$

$$= \sum_{n=0}^{\infty}a_n\sum_{k=1}^{n}\mathcal{A}^k\delta\mathcal{A}\mathcal{A}^{n-k} \tag{2.17}$$

a rather cumbersome form. Rearranging the order of $\mathcal{A}$ and $\delta\mathcal{A}$ is in general not possible due to non-commutativity.

A more general and slightly different approach to variations in the context of Lie group manifolds can be constructed using the group multiplication. $\delta\mathcal{A}\in\mathfrak{g}$ as a Lie algebra element represents a tangent vector $\delta\mathcal{A}\in T_{\mathbb{1}}G$ at the Lie group's identity $\mathbb{1}\in G$. $\exp\{t\delta\mathcal{A}\}$ is a smooth curve representative which can give rise to a translated curve $\exp\{t\delta\mathcal{A}\}\circ g$ located at $g\in G$ by means of group multiplication. It is then possible to evaluate the corresponding directional derivatives of functions.

**Definition 61** (Group Derivative)**.** *Let $f\in C^1(G;V)$ be a smooth function from the Lie group $G$ onto a linear space $V$. The directional derivative of $f$ at $g\in G$ into the direction $\mathcal{A}'\in\mathfrak{g}$*

$$\delta_{\mathcal{A}'}f(g) := \frac{\mathrm{d}}{\mathrm{d}t}|_{t=0}f(\exp\{t\mathcal{A}'\}\circ g)$$

*is called the group derivative of $f$ in the direction $\mathcal{A}'\in\mathfrak{g}$ at $g\in G$.*

**Remark 2.9.5.** *As the group multiplication with a group element $g \in G$ from the right $h \mapsto R_g h := h \circ g$ is a diffeomorphic map, its push forward $(R_g)_* : T_{\mathbb{1}}G \to T_gG$ bijectively maps the Lie algebra $\mathfrak{g} \simeq T_{\mathbb{1}}G$ to the tangent space $T_gG$ at $g$. This intuitively means that the group derivative covers "all directions" that originate from $g \in G$ and that criticality of a function $f$ at $g \in G$ corresponds to a vanishing group derivative $\delta_{\mathcal{A}'} f(g) = 0$ in all directions $\mathcal{A}' \in \mathfrak{g}$.*

**Example 2.9.6** (Group Derivative for Representations)**.** *In our case we will apply group derivative to Lie groups which themselves consist of matrices, meaning that we look at the so-called representations $R : G \to GL(n, \mathbb{C})$. The derivative of such a representation $R$ is worked out in section 6.3.3 of the appendix.*

As the group derivative is based on a derivative, it can be shown that common differentiation rules hold, including the product rule. Numerical implementations will often directly work with representations and $R$ itself is often symbolically hidden away in practice.

**Remark 2.9.7.** *Variation of the Wilson action with respect to gauge links using the group derivative would yield discrete analogue Yang-Mills equations used in Lattice Gauge Theory. We leave this step here out as we will deal with a generalization of the Wilson action later in section 4.4.*

## 2.10 Gauge Theories vs. General Relativity

Gauge theories are often compared to general relativity - both can be understood using concepts of differential geometry on manifolds, in particular connections and curvature of bundles as well as Lie groups [44] [52] [50]. In this section we breifly highlight similarities and differences between the two theories.

In the case of Yang-Mills theories the symmetry group $SU(N)$ acts on "colored" objects (such as particle wavefunctions or charges) with the requirement that physics is invariant under such transformations. As color in this context represents an additional degree of freedom objects carry, this symmetry is often referred to as an "internal symmetry".

In general relativity, however, the Poincare group $P$ of coordinate transformations acts simultaneously on coordinates and components of tensorial objects in a particular space-time coordinate system. Therefore the Poincaré symmetry here is not a purely internal one, but associated to space-time. The "gauge symmetry" in this context can be identified as the freedom of choice involving charts. While this choice itself is arbitrary and there is no reason to prefer one chart over the other, all calculations and operations may be performed in a suitable one given that they are well defined on the level of manifolds.

Furthermore, the Levi-Civita connection used in general relativity is tied to a space-time metric $g$, of which there does not exist any analogue in general gauge theories.

The Yang-Mills field strength $\mathcal{F}_{\mu\nu}$ and Riemann curvature tensor $R^{\alpha}{}_{\beta\mu\nu}$ are identical objects in the sense that both describe the Lie algebra-valued curvature 2-form. $\mathcal{F}_{\mu\nu}$ is $su(N)$-valued whereas $\mu$- and $\nu$-components in $(R^{\alpha}{}_{\beta})_{\mu\nu} \equiv \mathcal{R}_{\mu\nu}$ are $so(3,1)$-valued.

In both cases, the physical action of interest can be constructed using the curvature 2-form $\mathcal{F}$ or $\mathcal{R}$. One example could involve an inner product on the appropriate Lie algebra combined with that of 2-forms

$$S_{\mathcal{F}} \sim \int_M \langle \mathcal{F}_{\mu\nu}, \mathcal{F}^{\mu\nu} \rangle_{\mathfrak{g}} \quad S_{\mathcal{R}} \sim \int_M \langle \mathcal{R}_{\mu\nu}, \mathcal{R}^{\mu\nu} \rangle_{\mathfrak{g}}$$

which indeed is how the Yang-Mills action is formed. However, instead of the term $\langle \mathcal{R}_{\mu\nu}, \mathcal{R}^{\mu\nu} \rangle_{\mathfrak{g}} := R_{\alpha\beta\mu\nu} R^{\alpha\beta\mu\nu}$ known as the Kretschmann scalar in general relativity, the Ricci scalar $R$ is used to formulate the Einstein-Hilbert action $S_{\text{EH}}$ for gravity

$$S_{\text{EH}} := \int_M R \quad R := R^{\alpha\beta}{}_{\alpha\beta}.$$

Notice, that this involves mixing Lie algebra- and form-valued-indices which is in general not possible in the case of gauge theories. Furthermore the Einstein-Hilbert action can be understood as the integral of a scalar curvature, as opposed to the Yang-Mills action which contains the inner product of the curvature with itself.

## 2.11 Regge Calculus and Distributional Connections

Regge Calculus is a framework aimed at discretizing (pseudo-)Riemannian manifolds. It has been studied and extended not only by communities in differential geometry but also those in numerics [24] [17]. Because of this, it has found traction in numerical relativity - a field which aims to study aspects of general relativity and gravity using numerical simulations [23] [45] [9] [7]. While the original formulation first proposed by Tullio Regge [47] focusses on the (discrete) space-time metric $g$, there is a perspective of Regge Calculus expressed in terms of Lie group-valued parallel transporters - similar to lattice gauge theories.

As is the case with FEM, we start with a triangulation of the space-time manifold in terms of a simplicial complex $\mathcal{S} = \bigcup_{k=0}^{4} \mathcal{S}_k$. Similar to the spirit of gauge theories, we also fix a symmetry group in this context.

**Definition 62** (Poincaré Group)**.** *Let $(\mathbb{R}^4, \eta)$ be the four dimensional space-time manifold with the Minkwoski metric $\eta = \mathrm{diag}(-1, 1, 1, 1)$. The Poincare Group $P$ is defined as the set of space-time isometries $\Lambda : \mathbb{R}^4 \to \mathbb{R}^4$, that are diffeomorphic and length preserving maps in the sense of $\eta(\Lambda_* v, \Lambda_* v)) = \eta(v, v)$ where $\Lambda_* : T\mathbb{R}^4 \to T\mathbb{R}^4$ is the appropriate map for tangent vectors $v \in T\mathbb{R}^4$ (push forward or Jacobian).*

Some examples of elements this group includes are space-time translations, spatial rotations in $\mathbb{R}^3$ (which define the Lie group $SO(3)$) and the so-called Lorentz boosts [12]. These can be interpreted as transformations between coordinate systems of different physical observers, which we also call frames. The overall physical outcome should be independent of the frame chosen. The theory of relativity from the view of space-time coordinates therefore has the Poincare group as a symmetry group. In mathematical terms Riemannian geometry can be differential geometrically reinterpreted using the so-called frame bundle, which can be intuitively understood as the collection of all possible choices of frames which may vary across the manifold [44]. For Regge Calculus in particular, we attach a frame to each 4-simplex.

**Definition 63** (Frame Coordinate Transformation)**.** *A discrete frame coordinate transformation in Regge calculus is represented by a function $\Lambda : \mathcal{S}_4 \to P$ that maps to each simplex $T \in \mathcal{S}_4$ of maximal degree a Poincare group element $\Lambda(T) \in P$.*

This means that the frame in each 4-simplex may be virtually transformed in a different manner.

One appropriate notion of connection that is compatible with this discrete concept of coordinate transformations can be given by discrete connection as defined below.

**Definition 64** (Parallel Transporters and Discrete Connection)**.** *The discrete connection is defined via parallel transporters $U_{TT'} \in P$ between neighbouring simplices $T, T' \in \mathcal{S}_4$ which share a face $F = T \cap T' \in \mathcal{S}_3$. Frame coordinate transformations $\Lambda \equiv (\Lambda_T)_{T \in \mathcal{S}_4}$ act on it as in*

$$U_{T,T'} \to \Lambda_T U_{T,T'} \Lambda_{T'}^{-1}.$$

The discrete connection therefore lives on 3-faces and additionally carries a sense of orientation which points from one 4-simplex to its neighbour. For this reason it is often referred to as a distributional connection. A two-dimensional example involving a mesh of triangles (or maximal 2-simplices) is depicted in figure 2.6. In this case, the parallel transporters $U_{TT'}$ can be represented by an arrow perpendicular to the edge $E = T \cap T'$ (or 1-face) shared by both triangles $T$ and $T'$ (2-simplices). It represents the spatial 2D-rotation necessary to parallel transport objects, for instance frames, across the edge. The parallel transport process of a single vector across such an element border is depicted in figure 2.7.

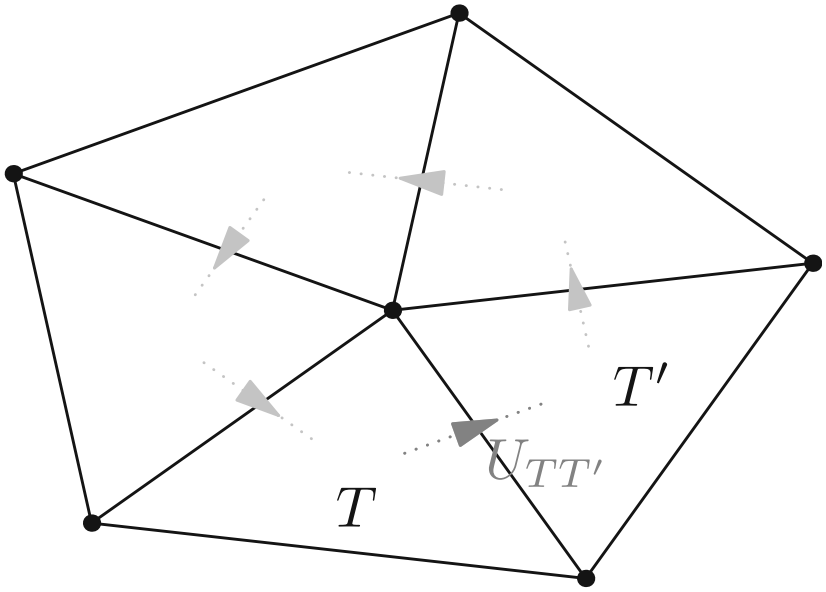


Figure 2.6: The distributional connection consisting of parallel transporters $U_{TT'}$ connecting elements $T$ and $T'$ illustrated in the two dimensional case.

It is always possible to find frame transformations $\Lambda_T$ and $\Lambda_{T'}$ for two simplices $T$ and $T'$ such that the local parallel transporter $U_{TT'}$ transforms to the identity $U_{T,T'} \to \mathbb{1}$. The individual matrix representations of $U_{T,T'}$ in a connection therefore depend on the choice of frames in $T$ and $T'$.

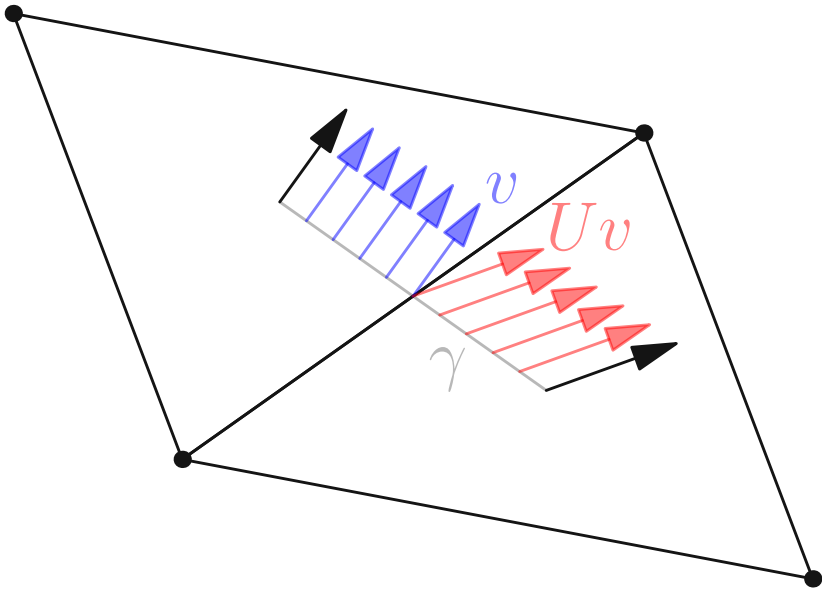


Figure 2.7: Illustration of the parallel transport of a tangent vector $v$ along a curve $\gamma$ that crosses an edge using the distributional connection. The vector field along the curve is piece-wise constant with a "discontinuity" at the edge resulting from the parallel transporter $U$.

**Definition 65** (Plaquette)**.** *Let $B \in \mathcal{S}_2$ be a 2-simplex with surrounding 4-simplices $(T_i)_{0=1,\dots,k} \subseteq \mathcal{S}_4$ indexed in a loop such that $T_i \cap T_{i+1} \neq \emptyset$ and $T_k = T_0$. The parallel transporter $W_{T_0,B} = \prod_{i=0}^{k} U_{T_i,T_{i+1}}$ obtained by multiplying individual $U_{T_i,T_j} \in P$ is called a plaquette $W_{T,B}$ starting at the simplex $T_0 \in \mathcal{S}_4$ centered around the bone/hinge $B \in \mathcal{S}_2$.*

In the 2D example of figure 2.8 involving triangles, the bones/hinges are represented by points and plaquettes by spatial rotations in two dimensions.

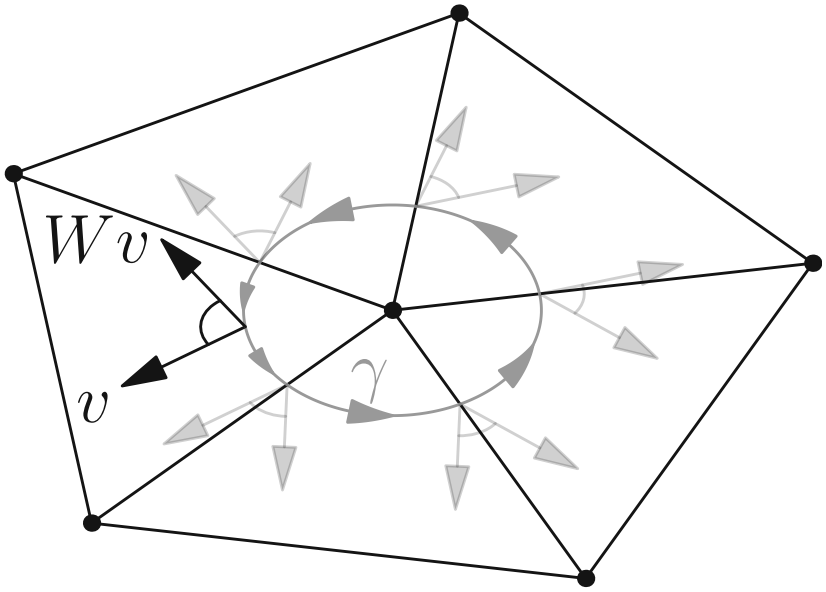


Figure 2.8: Parallel transportation of a tangent vector $v$ around a loop curve $\gamma$. At each element interface the connection prescribes a rotation of the vector. The final result $Wv$ involving the plaquette $W$ may differ from the starting vector $v$.

Plaquettes transform locally in one element $W_{T,B} \to (\Lambda^*)_T W_{T,B} (\Lambda^*)_T^{-1}$ and represent the deficit when parallel transporting along a loop, which is a measure of curvature. In the case of the discrete connection, only successive loop parallel transports which encircle bones have the potential to be non-trivial. All others are trivial and are represented by the identity $\mathbb{1} \in P$. This suggests the idea that the curvature of the connection is concentrated in all bones $B \in \mathcal{S}_2$ and leads to the discretization of the Einstein-Hilbert action in general relativity

$$S_{\text{EH}} := \int_M R \text{dVol} \quad R := g^{\beta\mu} R^{\alpha}{}_{\beta\alpha\mu}$$

where $(R^{\alpha}{}_{\beta})_{\mu\nu}$ stands for the Riemannian curvature tensor [47] [55].

**Definition 66** (Regge Action)**.** *The Regge action is defined as the sum over all bones $B \in \mathcal{S}_2$ and corresponding plaquette $W_{T,B} \equiv (W_{T,B})^{\mu}_{\nu}$ variables*

$$\sum_{B \in \mathcal{S}_2} (V_B)_{\mu\nu} (W_{T,B})^{\mu\nu}$$

*weighed with the area of each bone $(V_B)_{\mu\nu}$ expressible using the coordinates of points $(x_B^{(i)})_{i=1,\dots,n-2}$ which span the $n-2$-simplex $B$ [13].*

$$(V_B)_{\mu_1\mu_2} = \varepsilon_{\mu_1\mu_2\mu_3\mu_4} \prod_{i=1}^{2} (x_B^{(i)} - x_B^{(i+1)})^{\mu_{i+2}}$$

# 3 Finite Element Method (FEM)

## 3.1 Standard FEM Time Stepping

To investigate different discretizations and their behaviour in simulating Yang-Mills fields, we study time evolution simulations in which non-Abelian effects become relevant. As such computations can be resource intensive, we will not simulate the full $3+1$-dimensional simulation of $SU(3)$ gauge theory (the setting for the strong nuclear interaction in space-time) but use a simplified model instead. We therefore fix the gauge group $SU(2)$ with the three–dimensional Lie Algebra $su(2)$. We will simulate in two spatial dimensions or set symmetric initial conditions in three spatial dimensions which enable an effective two-dimensional simulation. In this section we deploy periodic boundary conditions in space and time.

Recall the weak Yang-Mills equations in temporal gauge $\mathcal{A}_0 = 0$ with $\mathcal{E}_n = -\partial_t \mathcal{A}$ in the space-time split form derived in section 6.2.2 of the appendix

$$\begin{aligned} \int_M \langle \mathcal{E}, \mathrm{d}_{\mathcal{A}} \rho' \rangle &= \int_M \langle \rho, \rho' \rangle && \forall \rho' \in \Lambda^0(M; \mathfrak{g}) \\ -\int_M \langle \mathcal{E}, \partial_t \mathcal{E}' \rangle - \int_M \langle \mathcal{F}, \mathrm{d}_{\mathcal{A}} \mathcal{E}' \rangle &= \int_M \langle j, \mathcal{E}' \rangle && \forall \mathcal{E}' \in \Lambda^1(M; \mathfrak{g}) \end{aligned}$$

where $M$ denotes the space-time manifold. For simplicity we assume a temporal foliation in terms of $M = \cup_{t \in I_t} M_t$ in which all spatial sub-manifolds $M_t$ that represent the time-slices at times $t \in I_t$ can be identified with one spatial domain $M_S$. In short this means that $M$ is equivalent to the cartesian product $M = I_t \times M_S$. We furthermore assume that all space-time functions can be viewed as differentiable functions in time. We therefore represent space-time $k$-forms as spatial $k$-form-valued differentiable functions $C^1(I_t; \Lambda^k(M_S; \mathfrak{g}))$.

With partial integration with integration over the temporal boundary in time we redistribute the temporal derivative as in

$$\begin{aligned} \int_M \langle \mathcal{E}, \partial_t \mathcal{E}' \rangle &= \int_M \partial_t \langle \mathcal{E}, \mathcal{E}' \rangle - \int_M \langle \partial_t \mathcal{E}, \mathcal{E}' \rangle = \\ &= \underbrace{\int_{\partial_t M} \langle \mathcal{E}, \mathcal{E}' \rangle}_{=0} - \int_M \langle \partial_t \mathcal{E}, \mathcal{E}' \rangle = -\int_M \langle \partial_t \mathcal{E}, \mathcal{E}' \rangle \end{aligned}$$

$$\begin{aligned} \int_M \langle \mathcal{E}, \mathrm{d}_{\mathcal{A}} \rho' \rangle &= \int_M \langle \rho, \rho' \rangle && \forall \rho' \in C^1(I_t; \Lambda^0(M_S; \mathfrak{g})) \\ \int_M \langle \partial_t \mathcal{E}, \mathcal{E}' \rangle - \int_M \langle \mathcal{F}, \mathrm{d}_{\mathcal{A}} \mathcal{E}' \rangle &= \int_M \langle j, \mathcal{E}' \rangle && \forall \mathcal{E}' \in C^1(I_t; \Lambda^1(M_S; \mathfrak{g})). \end{aligned}$$

It suffices to restrict the formulation over each time-slice $M_t$.

$$\begin{aligned} \int_{M_t} \langle \mathcal{E}, \mathrm{d}_{\mathcal{A}} \rho' \rangle &= \int_{M_t} \langle \rho, \rho' \rangle && \forall \rho' \in \Lambda^0(M_S; \mathfrak{g}) \\ \int_{M_t} \langle \partial_t \mathcal{E}, \mathcal{E}' \rangle - \int_{M_t} \langle \mathcal{F}, \mathrm{d}_{\mathcal{A}} \mathcal{E}' \rangle &= \int_M \langle j, \mathcal{E}' \rangle && \forall \mathcal{E}' \in \Lambda^1(M_S; \mathfrak{g}) \end{aligned}$$

The second equation may be used for time steps and the first equation can be used to track the change in charge at each step.

We choose an explicit leapfrog scheme: The goal of this scheme is to update values $(\mathcal{E}^-, \mathcal{A}^-)$ to new ones $(\mathcal{E}^+, \mathcal{A}^+)$ using successive updates to obtain first $\mathcal{A}^+$ using $\mathcal{E}^-$

$$\mathcal{A}^+ = \mathcal{A}^- - \tau \mathcal{E}^-$$

and then $\mathcal{E}^+$ using $\mathcal{A}^+$

$$\mathcal{E}^+ = \mathcal{E}^- + \tau\Delta\mathcal{E} \quad \langle \Delta\mathcal{E}, \mathcal{E}' \rangle - \langle \mathcal{F}(\mathcal{A}^+), \mathrm{d}_{\mathcal{A}^+}\mathcal{E}' \rangle = \langle j, \mathcal{E}' \rangle \quad \forall \mathcal{E}' \in \Lambda^1(M_S; \mathfrak{g}).$$

We evaluate the new charge density in the next step $\rho^+$ using $\mathcal{E}^+$ and $\mathcal{A}^+$

$$\langle \rho^+, \rho' \rangle = \langle \mathcal{E}^+, d_{\mathcal{A}^+}\rho' \rangle \quad \forall \rho' \in \Lambda^0(M_S; \mathfrak{g}).$$

## 3.2 Charge Conservation

We examine whether charge is conserved in the continuous formulation and then attempt to translate this into the discrete setting using finite element spaces.

For simplification we assume the absence of spatial currents $j = 0$ with the goal of examining this setting in the absence of charges and currents. During one time step, we can rewrite the defining equations for a charge update from $\rho^-$ to $\rho^+$

$$\begin{aligned}
\langle \rho^+, \rho' \rangle &= \langle \mathcal{E}^+, d_{\mathcal{A}^+}\rho' \rangle = \\
&= \langle \mathcal{E}^- + \tau\Delta\mathcal{E}, d_{\mathcal{A}^+}\rho' \rangle = \\
&= \langle \mathcal{E}^-, d_{\mathcal{A}^+}\rho' \rangle + \tau\langle \Delta\mathcal{E}, d_{\mathcal{A}^+}\rho' \rangle = \\
&= \langle \mathcal{E}^-, d_{\mathcal{A}^- - \tau\mathcal{E}^-}\rho' \rangle + \tau\langle \Delta\mathcal{E}, d_{\mathcal{A}^+}\rho' \rangle = \\
&= \langle \mathcal{E}^-, d_{\mathcal{A}^-}\rho' \rangle - \tau\langle \mathcal{E}^-, [\mathcal{E}^- \wedge \rho'] \rangle + \tau\langle \Delta\mathcal{E}, d_{\mathcal{A}^+}\rho' \rangle = \\
&= \langle \rho^-, \rho' \rangle + \tau \underbrace{\left( \langle \Delta\mathcal{E}, d_{\mathcal{A}^+}\rho' \rangle - \langle \mathcal{E}^-, [\mathcal{E}^- \wedge \rho'] \rangle \right)}_{=: \langle \Delta\rho, \rho' \rangle}
\end{aligned}$$

to identify the second term as the one responsible for drifts in charge $\Delta\rho$. Stationary charge density would translate to $\Delta\rho = 0$. The second term vanishes due to the algebraic properties of operations which imply $\langle [\rho \wedge E], E \rangle = 0$.

$$\begin{aligned}
&\langle [\rho \wedge E], E \rangle = (-1)^{0\cdot 1+1}\langle E, [\rho \wedge E] \rangle = -\langle [\rho \wedge E], E \rangle \\
&\Rightarrow \langle [\rho \wedge E], E \rangle = -\langle E, [\rho \wedge E] \rangle = 0
\end{aligned}$$

For the first term, we utilize the time stepping equation that $\Delta\mathcal{E}$ satisfies

$$\langle \Delta\mathcal{E}, \mathcal{E}' \rangle - \langle \mathcal{F}(\mathcal{A}^+), \mathrm{d}_{\mathcal{A}^+}\mathcal{E}' \rangle = \langle j, \mathcal{E}' \rangle \quad \forall \mathcal{E}' \in \Lambda^1(M_S; \mathfrak{g})$$

and can insert $d_{\mathcal{A}^+}\rho' = \mathcal{E}'$ with $\rho' \in \Lambda^0(M_S; \mathfrak{g})$ as a viable test function to use $d^2_{\mathcal{A}}(\cdot) = [\mathcal{F}(\mathcal{A}) \wedge \cdot]$.

$$\begin{aligned}
\langle \Delta\rho, \rho' \rangle &= \langle \Delta\mathcal{E}, \underbrace{d_{\mathcal{A}^+}\rho'}_{\mathcal{E}'} \rangle = \\
&= \langle \mathcal{F}(\mathcal{A}^+), d_{\mathcal{A}^+}d_{\mathcal{A}^+}\rho' \rangle = \\
&= \langle \mathcal{F}(\mathcal{A}^+), d^2_{\mathcal{A}^+}\rho' \rangle = \\
&= \langle \mathcal{F}(\mathcal{A}^+), [\mathcal{F}(\mathcal{A}^+) \wedge \rho'] \rangle \\
&= (-1)^{2\cdot 2}\langle \underbrace{[\mathcal{F}(\mathcal{A}^+) \wedge \mathcal{F}(\mathcal{A}^+)]}_{=0}, \rho' \rangle = 0
\end{aligned}$$

thus showing charge conservation.

We now turn to the discrete case where we replace continuous forms $\Lambda^k(M_S; \mathfrak{g})$ with Whitney forms $\Lambda^k_h(M_S; \mathfrak{g})$ and therefore need to re-evaluate the above line of reasoning. One key property that reflects the compatibility of continuous and discrete de-Rham complexes is the Interpolation commutation relation $\mathrm{d} \circ I^p_h = I^{p+1}_h \circ \mathrm{d}$. The same can not be directly said for the exterior covariant derivative

$$\mathrm{d}_{\mathcal{A}} : \left\{ \begin{array}{ccc} \Lambda^k(M_S; \mathfrak{g}) & \to & \Lambda^{k+1}(M_S; \mathfrak{g}) \\ \omega & \mapsto & \mathrm{d}_{\mathcal{A}}\omega = \mathrm{d}\omega + [\mathcal{A} \wedge \omega] \end{array} \right.$$

and Whitney forms $\Lambda_h^k(M_S;\mathfrak{g})$. The multiplicative operation $\omega \to [\mathcal{A}\wedge\omega]$ does not fit into the discrete de-Rham chain

$$\mathrm{d}: \begin{cases} \Lambda_h^k(M_S;\mathfrak{g}) & \to & \Lambda_h^{k+1}(M_S;\mathfrak{g}) \\ \omega & \mapsto & \mathrm{d}\omega \end{cases}.$$

In terms of numerical implementation, the first thing that comes to mind may be to interpolate the expression on the right side using the operator $I_h^k : \Lambda^k(M_S;\mathfrak{g}) \to \Lambda_h^k(M_S;\mathfrak{g})$, such that the discrete covariant derivative $\delta_{\mathcal{A}}$ takes on the form $\delta_{\mathcal{A}} = I_h^k \circ \mathrm{d}_{\mathcal{A}}$.

$$\delta_{\mathcal{A}}: \begin{cases} \Lambda_h^k(M_S;\mathfrak{g}) & \to & \Lambda_h^{k+1}(M_S;\mathfrak{g}) \\ \omega & \mapsto & I_h^k \mathrm{d}_{\mathcal{A}}\omega = \mathrm{d}\omega + I_h^k[\mathcal{A}\wedge\omega] \end{cases}$$

Therefore the property $d_{\mathcal{A}}^2(\cdot) = [\mathcal{F}(\mathcal{A})\wedge\cdot]$ is not guaranteed to persist in the discrete setting and we need to evaluate $I_h^2 \circ \mathrm{d}_{\mathcal{A}} \circ I_h^1 \circ \mathrm{d}_{\mathcal{A}}$.

We introduce some shorthand notations: $\rho_h, \mathcal{A}_h, \mathcal{F}_h(\mathcal{A})$ will be interpolations of $\rho, \mathcal{A}, \mathcal{F}$ respectively

$$\rho_h = I_h^0\rho, \quad \mathcal{A}_h = I_h^1\mathcal{A}, \quad \mathcal{F}_h(\mathcal{A}) = I_h^2\mathcal{F}(\mathcal{A})$$

where we note the differences between $\mathcal{F}_h(\mathcal{A}), \mathcal{F}(\mathcal{A}_h), \mathcal{F}_h(\mathcal{A}_h)$. We write down the variational formulation, as from a discretized perspective using $\delta_{\mathcal{A}_h}$

$$\begin{aligned} &\langle \mathcal{E}_h, \delta_{\mathcal{A}_h}\rho_h'\rangle = \langle \rho_h, \rho_h'\rangle && \forall \rho_h' \in \Lambda_h^0(M_S;\mathfrak{g}) \\ &\langle \dot{\mathcal{E}}_h, \mathcal{E}_h'\rangle - \langle \mathcal{F}_h(\mathcal{A}_h), \delta_{\mathcal{A}_h}\mathcal{E}_h'\rangle = \langle j_h, \mathcal{E}_h'\rangle && \forall \mathcal{E}_h' \in \Lambda_h^1(M_S;\mathfrak{g}) \end{aligned}$$

with time stepping

$$\langle \Delta\mathcal{E}_h, \mathcal{E}_h'\rangle - \langle \mathcal{F}_h(\mathcal{A}_h^-), \delta_{\mathcal{A}_h^-}\mathcal{E}_h'\rangle = \langle j_h, \mathcal{E}_h'\rangle \quad \forall \mathcal{E}_h' \in \Lambda_h^1(M_S;\mathfrak{g}).$$

Performing identical steps for $\delta\rho_h$ as before and dropping the minus sign in $\mathcal{A}_h^- = \mathcal{A}_h$

$$\begin{aligned} \langle \Delta\rho_h, \rho_h'\rangle &= \langle \Delta\mathcal{E}_h, \underbrace{\delta_{\mathcal{A}_h}\rho_h'}_{\mathcal{E}_h'}\rangle = \\ &= \langle \mathcal{F}_h(\mathcal{A}_h), \delta_{\mathcal{A}_h}\delta_{\mathcal{A}_h}\rho_h'\rangle = \\ &= \langle \mathcal{F}_h(\mathcal{A}_h), I_h^2\mathrm{d}_{\mathcal{A}_h}I_h^1\mathrm{d}_{\mathcal{A}_h}\rho_h'\rangle \end{aligned}$$

$$\begin{aligned} \mathrm{d}_{\mathcal{A}_h}I_h^1J &= \mathrm{d}I_h^1J + [\mathcal{A}_h\wedge I_h^1J] = \\ &= I_h^2\mathrm{d}J + I_h^2[\mathcal{A}_h\wedge I_h^1J] - I_h^2[\mathcal{A}_h\wedge I_h^1J] + [\mathcal{A}_h\wedge I_h^1J] = \\ &= I_h^2\mathrm{d}_{\mathcal{A}_h}J + \underbrace{\left([\mathcal{A}_h\wedge I_h^1J] - I_h^2[\mathcal{A}_h\wedge I_h^1J]\right)}_{\varepsilon(\mathcal{A}_h,J_h)} \end{aligned}$$

$$I_h^2\mathrm{d}_{\mathcal{A}_h}I_h^1\mathrm{d}_{\mathcal{A}_h}\rho_h' = I_h^2I_h^2\mathrm{d}_{\mathcal{A}_h}\mathrm{d}_{\mathcal{A}_h}\rho_h' + \varepsilon(\mathcal{A}_h,J) = I_h^2[\mathcal{F}(\mathcal{A}_h)\wedge\rho_h'] + \varepsilon(\mathcal{A}_h,\rho_h')$$

we "reverse engineer" the expression to match the continuous case.

$$\begin{aligned} \langle \Delta\rho_h, \rho_h'\rangle &= \langle \mathcal{F}_h(\mathcal{A}_h), I_h^2\mathrm{d}_{\mathcal{A}_h}I_h^1\mathrm{d}_{\mathcal{A}_h}\rho_h'\rangle = \\ &= \langle \mathcal{F}_h(\mathcal{A}_h), I_h^2[\mathcal{F}(\mathcal{A}_h)\wedge\rho_h'] + \varepsilon(\mathcal{A}_h,\rho_h')\rangle = \\ &= \langle \mathcal{F}_h(\mathcal{A}_h), I_h^2[\mathcal{F}(\mathcal{A}_h)\wedge\rho_h']\rangle + \langle \mathcal{F}_h(\mathcal{A}_h), \varepsilon(\mathcal{A}_h,\rho_h')\rangle = \\ &= \langle \mathcal{F}_h(\mathcal{A}_h), [I_h^2\mathcal{F}(\mathcal{A}_h)\wedge\rho_h']\rangle - \langle \mathcal{F}_h(\mathcal{A}_h), [I_h^2\mathcal{F}(\mathcal{A}_h)\wedge\rho_h']\rangle + \\ &+ \langle \mathcal{F}_h(\mathcal{A}_h), I_h^2[\mathcal{F}(\mathcal{A}_h)\wedge\rho_h']\rangle + \langle \mathcal{F}_h(\mathcal{A}_h), \varepsilon(\mathcal{A}_h,\rho_h')\rangle = \\ &= \underbrace{\langle \mathcal{F}_h(\mathcal{A}_h), [\mathcal{F}_h(\mathcal{A}_h)\wedge\rho_h']\rangle}_{=0} - \langle \mathcal{F}_h(\mathcal{A}_h), [I_h^2\mathcal{F}(\mathcal{A}_h)\wedge\rho_h']\rangle + \\ &+ \langle \mathcal{F}_h(\mathcal{A}_h), I_h^2[\mathcal{F}(\mathcal{A}_h)\wedge\rho_h']\rangle + \langle \mathcal{F}_h(\mathcal{A}_h), \varepsilon(\mathcal{A}_h,\rho_h')\rangle = \\ &= \left(\langle \mathcal{F}_h(\mathcal{A}_h), I_h^2[\mathcal{F}(\mathcal{A}_h)\wedge\rho_h']\rangle - \langle \mathcal{F}_h(\mathcal{A}_h), [I_h^2\mathcal{F}(\mathcal{A}_h)\wedge\rho_h']\rangle\right) + \langle \mathcal{F}_h(\mathcal{A}_h), \varepsilon(\mathcal{A}_h,\rho_h')\rangle = \\ &= \langle \mathcal{F}_h(\mathcal{A}_h), \underbrace{I_h^2[\mathcal{F}(\mathcal{A}_h)\wedge\rho_h'] - [I_h^2\mathcal{F}(\mathcal{A}_h)\wedge\rho_h']}_{\varepsilon(\mathcal{F}(\mathcal{A}_h),\rho_h')}\rangle + \langle \mathcal{F}_h(\mathcal{A}_h), \varepsilon(\mathcal{A}_h,\rho_h')\rangle = \\ &= \langle \mathcal{F}_h(\mathcal{A}_h), \varepsilon(\mathcal{F}(\mathcal{A}_h),\rho_h')\rangle + \langle \mathcal{F}_h(\mathcal{A}_h), \varepsilon(\mathcal{A}_h,\rho_h')\rangle \end{aligned}$$

$\varepsilon$ stands for the difference generated by interpolating before and after the wedge product for $k$ and $l$-forms $K$ and $L$

$$\varepsilon(K, L) = I_h^{k+l}[K \wedge L] - [I_h^k K \wedge I_h^l L].$$

If the forms $\varepsilon$ acts upon are already in a finite element space (as is the case in the second term $\varepsilon(\mathcal{A}_h, \rho_h)$ responsible for the drift in charge) a part of the error boils down to comparison of a function with its interpolated counterpart as in

$$\|\varepsilon(\mathcal{A}_h, \rho_h)\|_{L^2} = \|I_h^1(\mathcal{A}_h \wedge \rho_h) - \mathcal{A}_h \wedge \rho_h\|_{L^2}.$$

The argument in standard FEM theory for proving convergence of such errors towards zero in the continuum limit, makes the assumptions that the functions involved have sufficiently high regularity. However, the product of these two $\mathcal{A}_h \wedge \rho_h$ functions may fail to deliver such regularity, yielding a distribution. The situation becomes even less clear with the second error term $\varepsilon(\mathcal{F}(\mathcal{A}_h), \rho_h')$ involving the curvature, as the terms $I_h^2[\mathcal{F}(\mathcal{A}_h) \wedge \rho_h'], [I_h^2\mathcal{F}(\mathcal{A}_h) \wedge \rho_h']$ and $I_h^2[I_h^2\mathcal{F}(\mathcal{A}_h) \wedge \rho_h']$ mean different things.all mean different things. Therefore this error term $\varepsilon(\mathcal{F}(\mathcal{A}_h), \rho_h')$ does not exactly match the form required for being able to apply the standard FEM convergence argument.

Leaving that aside, we may try to inspect and write down said error terms for gaining insight. As an example we look at $\varepsilon(\mathcal{A}_h, \rho_h)$ for a 1-form $\mathcal{A}_h$ and 0-form $\rho_h$.

$$\begin{aligned}
\mathcal{A} \in \Lambda^1(M_S; \mathfrak{g}) \quad &\longrightarrow \quad \mathcal{A}_h = \mathcal{A}^{(ij)}\lambda_{(ij)} \in \Lambda_h^1(M_S; \mathfrak{g}) \quad \mathcal{A}^{(ij)} = \int_{E_{(ij)}} \mathcal{A} \cdot \mathrm{d}s \\
\rho \in \Lambda^0(M_S; \mathfrak{g}) \quad &\longrightarrow \quad \rho_h = \rho^{(k)}\lambda_{(k)} \in \Lambda_h^0(M_S; \mathfrak{g}) \quad \rho^{(k)} = \rho|_{V_{(k)}}
\end{aligned}$$

$$\begin{aligned}
[\mathcal{A}_h \wedge \rho_h] &= [\mathcal{A}^{(ij)}\lambda_{(ij)} \wedge \rho^{(k)}\lambda_{(k)}] = \\
&= [\mathcal{A}^{(ij)}, \rho^{(k)}]\lambda_{(ij)} \wedge \lambda_{(k)} = \\
&= \left([\mathcal{A}^{(ij)}, \rho^{(k)}]\lambda_{(k)}\right)\lambda_{(ij)} = \\
&= \left([A_l^{(ij)}t_l, \rho^{(k)}]\lambda_{(k)}\right)\lambda_{(ij)} = \\
&= \left(A_l^{(ij)}[t_l, \rho^{(k)}]\lambda_{(k)}\right)\lambda_{(ij)} = \\
&= \left(\int_{E_{(ij)}} A_l \cdot \mathrm{d}s[t_l, \rho^{(k)}]\lambda_{(k)}\right)\lambda_{(ij)} = \\
&= \left(\lambda_{(k)}\int_{E_{(ij)}} A_l \cdot \mathrm{d}s\right)[t_l, \rho^{(k)}]\lambda_{(ij)} = \\
&= \left(\lambda_{(k)}\int_{E_{(ij)}} (A_h)_l \cdot \mathrm{d}s\right)[t_l, \rho^{(k)}]\lambda_{(ij)}
\end{aligned}$$

$$\begin{aligned}
I_h^1[\mathcal{A}_h \wedge \rho_h] &= ([\mathcal{A}_h \wedge \rho_h])^{(ij)}\lambda_{(ij)} = \\
&= \int_{E_{(ij)}} [\mathcal{A}_h \wedge \rho_h] \cdot \mathrm{d}s\lambda_{(ij)} = \\
&= \int_{E_{(ij)}} [\mathcal{A}_h \wedge \rho^{(k)}\lambda_{(k)}] \cdot \mathrm{d}s\lambda_{(ij)} = \\
&= \int_{E_{(ij)}} [A_h^l t_l \wedge \rho^{(k)}\lambda_{(k)}] \cdot \mathrm{d}s\lambda_{(ij)} = \\
&= \left(\int_{E_{(ij)}} \lambda_{(k)}A_h^l \cdot \mathrm{d}s[t_l, \rho^{(k)}]\right)\lambda_{(ij)} = \\
&= \left(\int_{E_{(ij)}} \lambda_{(k)}A_h^l \cdot \mathrm{d}s\right)[t_l, \rho^{(k)}]\lambda_{(ij)}
\end{aligned}$$

$$\varepsilon(\mathcal{A}_h, \rho_h) = \left( \lambda_{(k)} \int_{E_{(ij)}} A_h^l \cdot \mathrm{d}s - \int_{E_{(ij)}} \lambda_{(k)} A_h^l \cdot \mathrm{d}s \right) [t_l, \rho^{(k)}] \lambda_{(ij)}$$

The above equation basically compares a regular average with a $\lambda$-weighted one. While terms involving forms of higher ranks are bound to be more complicated, it is reasonable to expect qualitatively similar expressions due to the nature of Whitney interpolation operators.

The two operations involved in the covariant exterior derivative $\mathrm{d}_\mathcal{A}$ are, intuitively speaking, of different nature: a derivative d and a product $[\mathcal{A} \wedge \cdot]$.

$$\mathrm{d}_\mathcal{A} B = \mathrm{d}B + [\mathcal{A} \wedge B]$$

Thinking in terms of piecewise polynomials, as is frequently done in FEM, the derivative lowers the polynomial degree, whereas the wedge bracket increases it. Therefore getting a desirable chain of discrete spaces connected with $\mathrm{d}_\mathcal{A}$ (similar to the de-Rham chain with d) that fulfil $\mathrm{d}_\mathcal{A} \circ \mathrm{d}_\mathcal{A} = [\mathcal{F}_\mathcal{A} \wedge \cdot]$ becomes a challenge. In particular, there is no analogue to Stokes' theorem in this case.

## 3.3 Simulation Using Exterior Finite Elements - Observations

The linear terms in the Yang-Mills equations resemble a wave equation for the gauge field $\mathcal{A}$. Therefore given the right initial conditions, a peak in $\mathcal{A}$ will start to propagate as a wave over time. In the wave equation the superposition principle applies which is why the waves of multiple peaks will pass through each other without hindrance, as is the case in the Abelian gauge theory of electromagnetism 2.5. However, the non-linear terms in the Yang-Mills equations 45 generate some kind of interaction. It is precisely this scenario, two propagating peaks colliding and interacting, that we will simulate using finite elements, with the expectation that at the collision point the non-linear and non-Abelian nature of the gauge theory can be probed.

In this spirit we implement the time stepping simulation of propagating flux-tubes described in section 6.5 of the appendix using the ngsolve library [49]. In particular we use Exterior finite elements $H_\mathcal{T}\Lambda^k(M)$ [4] [2] [3] to represent components of Lie algebra-valued $k$-forms as in [15]. In contrast to the work in [15] where charge conservation is added as an additional constraint in the variational formulation, we evaluate and track the violation of this constraint equation at each step. The basis of the Lie algebra is chosen such that the Lie bracket represents the cross product of vector-valued components (and the structure constants 2.7 become the three-dimensional Levi Civita symbol 6.2). We use appropriate exterior finite element interpolation operators and higher order integration methods to deal with non-linear operations, such as the Lie Bracket and the application of gauge transformations. All computations are performed using the ngsolve library [49].

The initial conditions $\mathcal{E}_z$ for two flux-tubes as well as an illustration of the gauge invariant energy densities $\mathcal{H}$ in the simulation are depicted in figures 3.1 and 3.2. We plot the integrated energies of equations 6.7 in 3.3 and notice an oscillation between longitudinal and transversal components as expected from a wave-like equation.

We now examine the reconstructed charge density at each time step. If the initial charge density is zero then it should remain zero in the continuous case. However, this was not observed during the FEM simulation. In locations where fields $\mathcal{A}$ and $\mathcal{E}$ with multiple distinct colors are present non-vanishing charge oscillations become noticeable near element borders. These spikes grow larger with time and are depicted in figure 3.5. While the integrated norm of the charge is not a physically conserved quantity, it may serve here as a metric for the violation of the charge conservation as in figure 3.4.

In a parameter scan trying out various combinations of time step sizes $\tau$, mesh sizes $h$ and finite element space orders $n$, a decrease in the charge error mentioned above is not observable in figure 3.6. The total charge violation seems to increase with finer meshes for orders $n > 1$ and time steps seem to have less impact. In figure 3.7 we plot the integrated charge violation against the mesh size in the case of lowest order $n = 1$, and notice a very slight decrease with mesh granularity.

The effects of gauge transformations on initial conditions $\mathcal{E} \to \mathrm{Ad}_g \mathcal{E}, \mathcal{A} \to \mathrm{Ad}_g \mathcal{A} - \mathrm{d}g g^{-1}$ in the simulation were also examined. We make sure to apply gauge transformations only to simulations with higher order finite element spaces to make sure, that the gauge transformed initial conditions can be represented

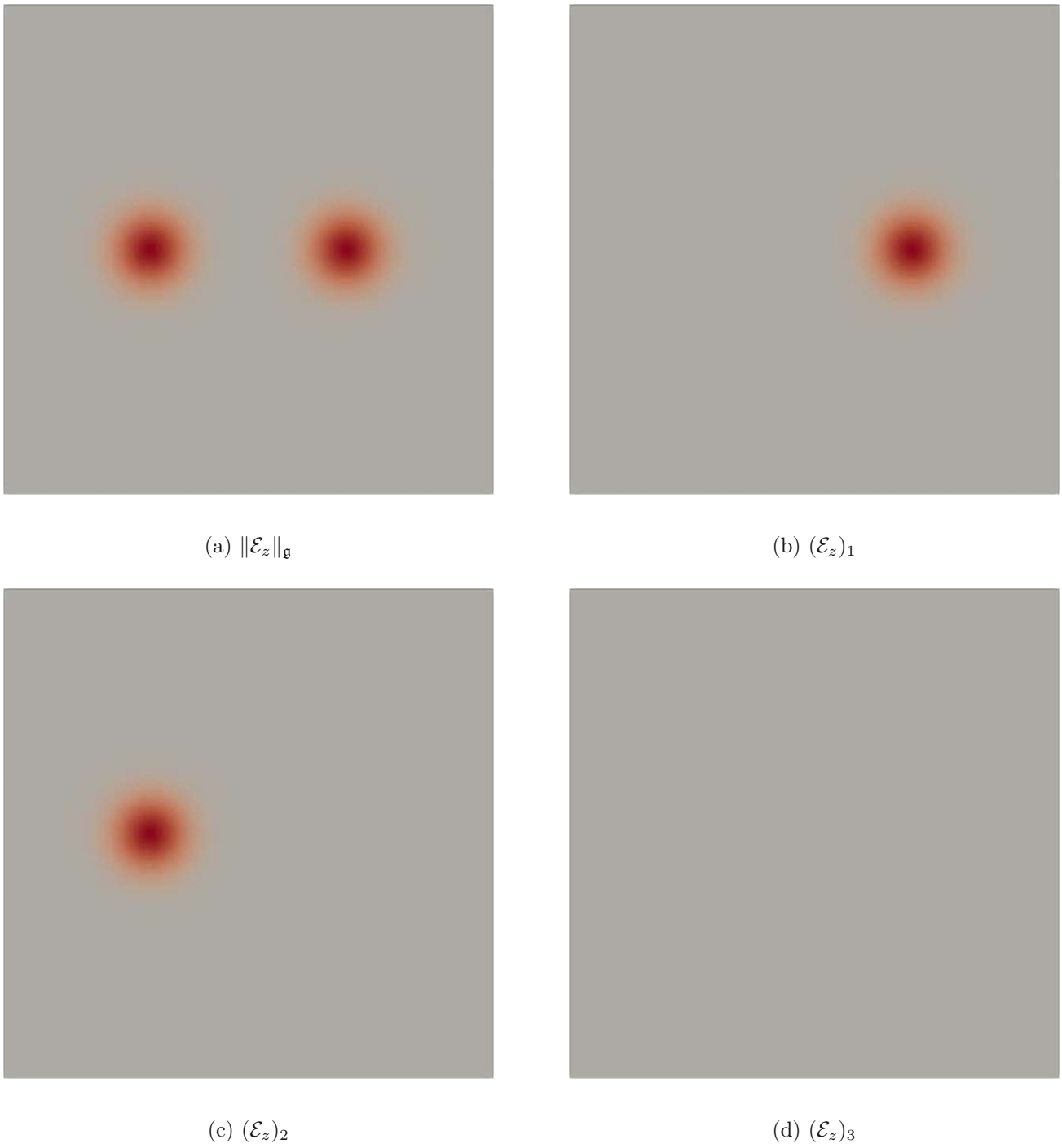

(a) $\|\mathcal{E}_z\|_{\mathfrak{g}}$ (b) $(\mathcal{E}_z)_1$

(c) $(\mathcal{E}_z)_2$ (d) $(\mathcal{E}_z)_3$

Figure 3.1: Visualization of the initial conditions for two differently "colored" flux-tubes. Grey, blue and red correspond to vanishing, negative and positive values respectively. Each flux-tube has a color associated to the first $(\mathcal{E}_z)_1$ and second $(\mathcal{E}_z)_2$ component respectively. Therefore each Gauss peak pops up in a different color component.

accurately. In figure 3.8 a set of initial conditions in finite element spaces of order $n = 6$ are visualized where the gauge transformation of equation 3.1 is applied

$$g(x) = e^{\phi(x)t_3} \quad \phi(x) = C\left(e^{-\frac{\|\vec{r}-\vec{p}_1\|^2}{2\sigma^2}} - e^{-\frac{\|\vec{r}-\vec{p}_2\|}{2\sigma^2}}\right) \tag{3.1}$$

with the "$SU(2)$-rotation angle" $\phi$. This has the effect that each Gauss peak in the initial conditions will mix in different color components of $\mathcal{E}_z$. While the time evolution of the energy densities of both regular initial conditions $\mathcal{E}_z(t = 0)$ and gauge initial conditions $\mathrm{Ad}_g\mathcal{E}_z(t = 0)$ are numerically similar, there are noticeable

(a) $\mathcal{H}_{\mathcal{E},L}$ (b) $\mathcal{H}_{\mathcal{E},T}$

(c) $\mathcal{H}_{\mathcal{B},L}$ (d) $\mathcal{H}_{\mathcal{B},T}$

Figure 3.2: Visualization of the energy densities in the simulation using exterior finite elements. Blue and red correspond to vanishing and high values respectively The self-interaction of the color fields in the form of non-linear terms gives rise to a non-vanishing transversal electric energy density $\mathcal{H}_{\mathcal{E},T}$ and longitudinal magnetic energy density $\mathcal{H}_{\mathcal{B},L}$.



differences in the evaluated charge densities. The previously observed charge violation becomes prevalent and widespread across the spatial domain from the start of the simulation. One explanation for this is that gauge transformations mix different color components and therefore activate the non-linear terms.

However, the charge violation forming at the later stage where the two wave fronts collide, is larger by several magnitudes. One notices, that the effect of the gauge transformation is six magnitudes smaller than the charge violation. Figure 3.9 illustrates the temporal evolution of charge violations for both simulations using ungauged and gauged initial conditions, respectively. To examine this further, we scale the initial conditions $\lambda\mathcal{E}_z(t=0)$ with a small factor $0 < \lambda < 1$ and rerun the simulation. Here the scale tips and the

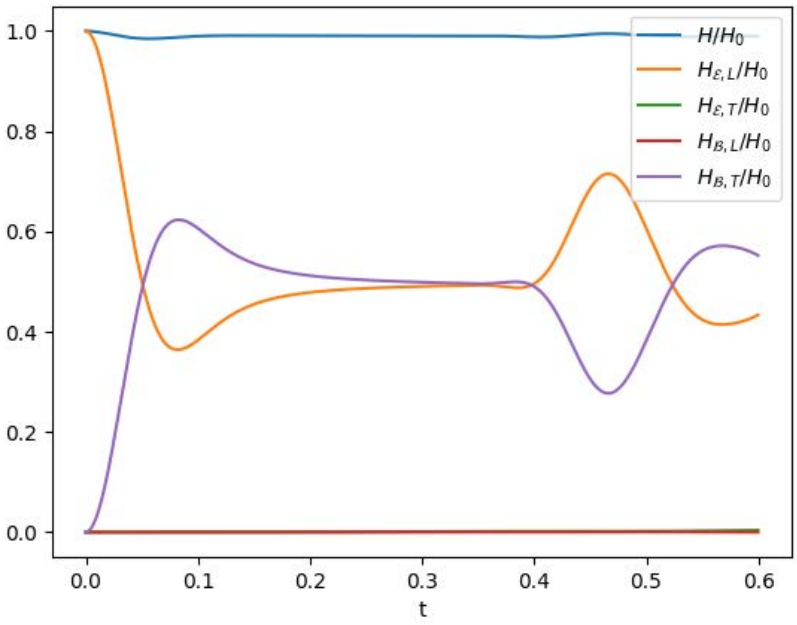


Figure 3.3: Plot of the different energy densities integrated over the domain and normalized with respect to the total initial energy $H_0$.

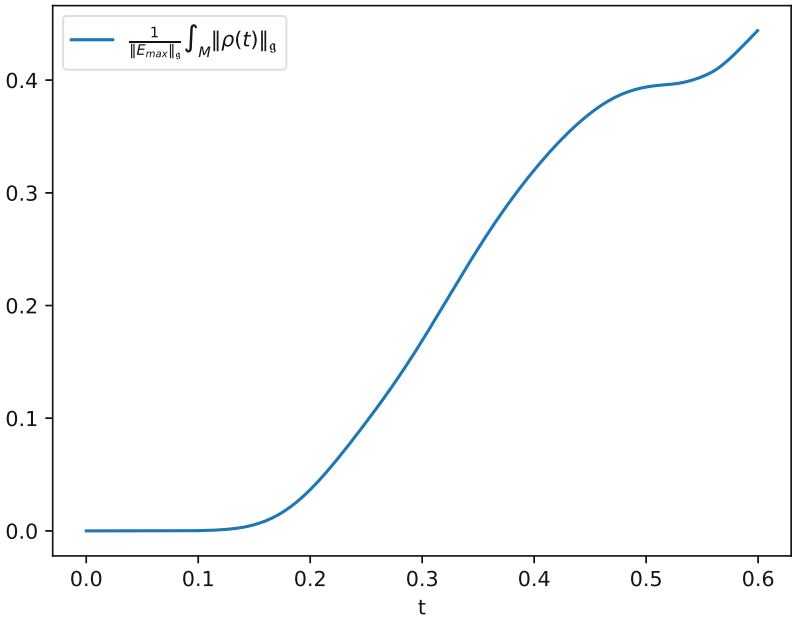


Figure 3.4: A plot of the charge violation integrated over the domain and normalized with respect to the maximum electric field derivative $E_{max}$. While this plot stems from a simulation with time step size $\tau = 0.0005$, mesh size $h = 0.03$ and order $n = 4$, it was observed, that the graph's shape looks virtually identical for other parameters.

effect of the gauge transformation outweighs the charge violation at the point of collision. An illustration of this is given in figure 3.11. A similar plot to 3.9 for the $\lambda$-scaled case with $\lambda = 0.001$ is given by 3.10.

From these observations we conclude that the FEM simulation only exhibits an approximate gauge symmetry if field components are large enough. In the examined scenario with two differently colored flux-tube

Figure 3.5: Visualization of one component $\rho_3$ of the charge density throughout the simulation. Grey, blue and red correspond to vanishing, negative and positive values respectively. The defects in the form of rapid oscillations appear at the spatial locations where two differently colored wave fronts collide.

initial conditions with low amplitudes, gauge transformations create numerical charge violations. Furthermore, this was also observed with purely Abelian initial conditions for $\mathcal{E}_z$: In this case the simulation exhibits discrete charge conservation (up to numerical precision) as everything reduces to an effectively electromagnetic scenario. Gauge transforming these initial conditions then again introduces charge violations as in 3.11, save those at the wave collision point. In short, wherever fields with different color component directions come into contact, localized numerical charge violations are observable.

Charge and current densities are, in general, gauge dependent objects and the idea of simulations that respect the non-Abelian continuity equation is directly linked to understanding and respecting gauge symmetries. Otherwise, having discrete charge conservation in one gauge does not guarantee the same in all other ones, even though they should be physically equivalent.

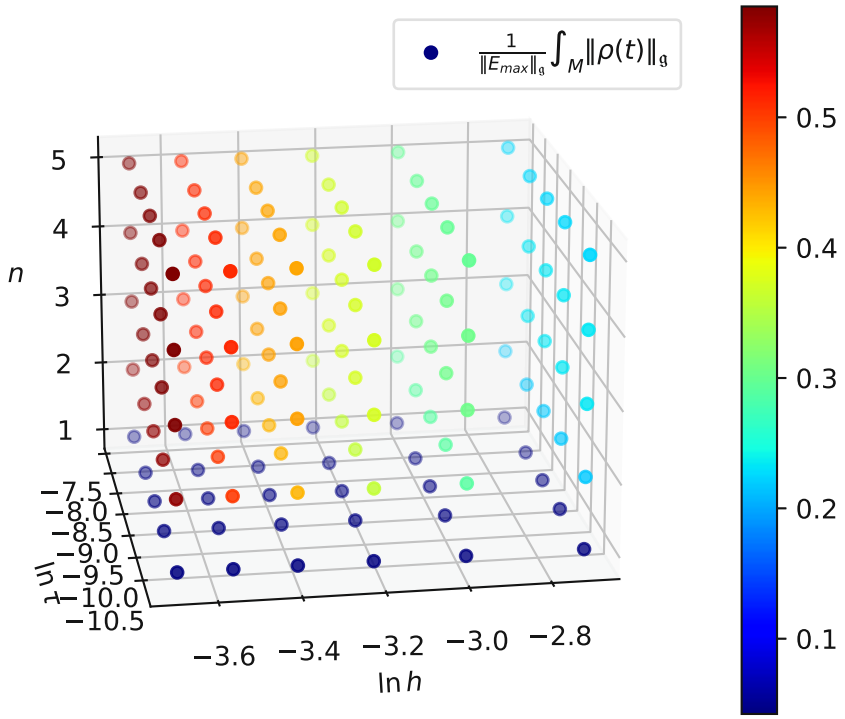


Figure 3.6: Colored scatter plot showcasing the dependence of charge violation on the simulation parameters: time step size $\tau$, mesh size $h$ and finite element space order $n$.

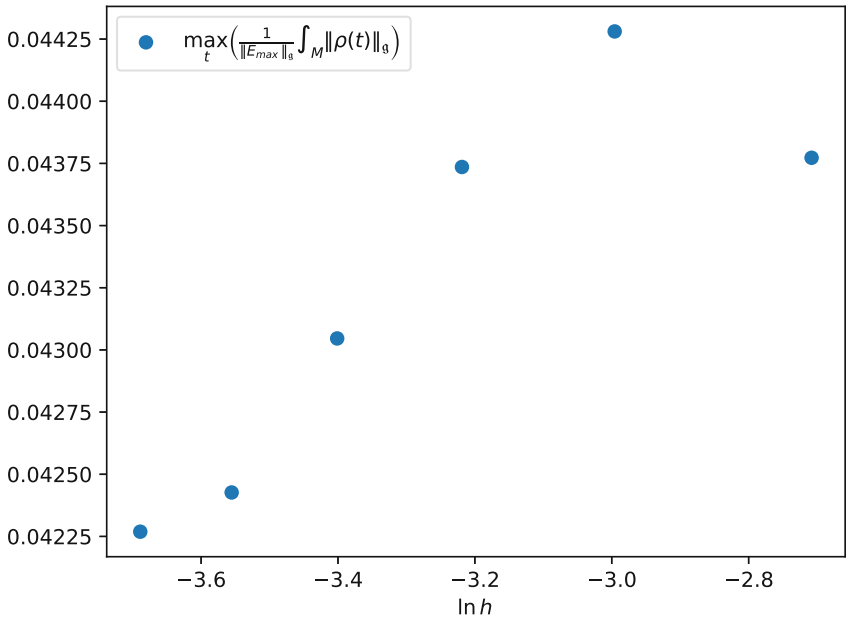


Figure 3.7: Scatter plot showcasing the behaviour of the charge violation with respect to the mesh size $h$ at fixed time step size $\tau = 0.005$ and order $n = 0$.

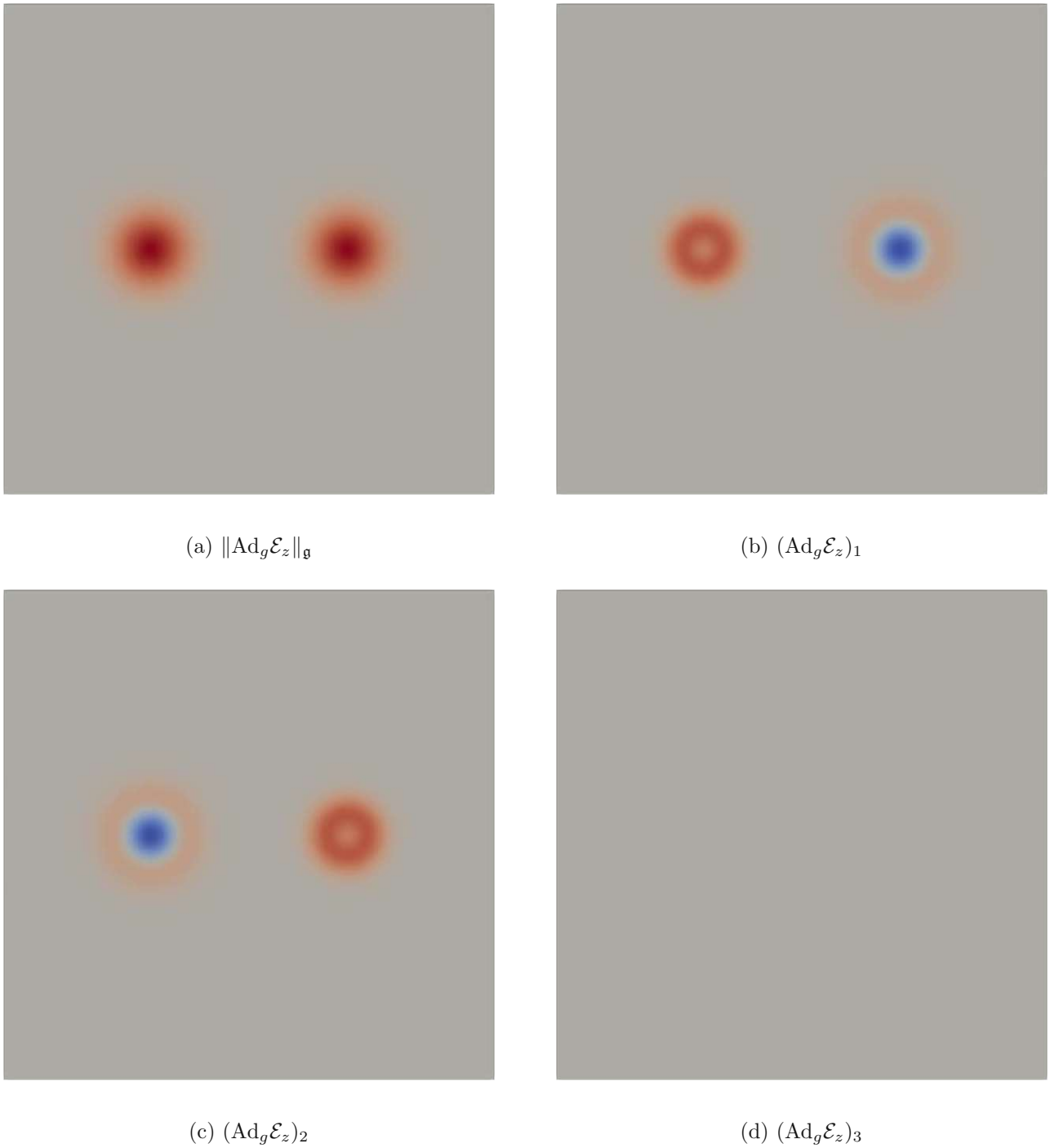

(a) $\|\mathrm{Ad}_g \mathcal{E}_z\|_{\mathfrak{g}}$ (b) $(\mathrm{Ad}_g \mathcal{E}_z)_1$

(c) $(\mathrm{Ad}_g \mathcal{E}_z)_2$ (d) $(\mathrm{Ad}_g \mathcal{E}_z)_3$

Figure 3.8: A visualization of flux-tube initial conditions gauge transformed using 3.1. Grey, blue and red correspond to vanishing, negative and positive values respectively. The Gauss peaks that initially were restricted to one color component, $(\mathcal{E}_z)_1$ or $(\mathcal{E}_z)_2$, are now mixed in contrast to figure 3.1.

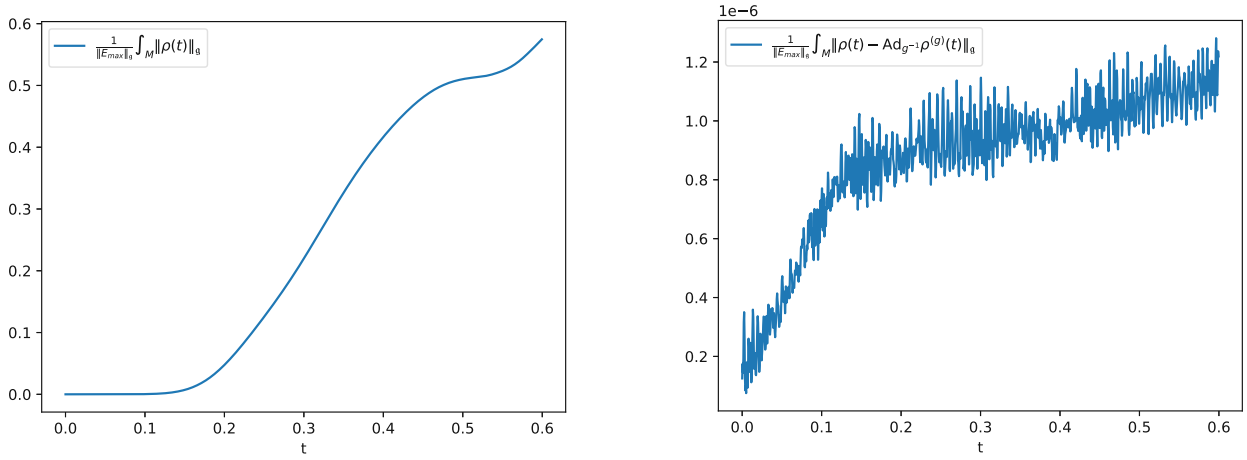


(a) $\frac{1}{\|E_{max}\|_{\mathfrak{g}}}\int_M \|\rho\|_{\mathfrak{g}}$ (b) $\frac{1}{\|E_{max}\|_{\mathfrak{g}}}\int_M \|\rho - \mathrm{Ad}_{g^{-1}}\rho^{(g)}\|_{\mathfrak{g}}$

Figure 3.9: Time evolution plots of charge violation $\frac{1}{\|E_{max}\|_{\mathfrak{g}}}\int_M \|\rho\|_{\mathfrak{g}}$ in figure 3.9a and $\frac{1}{\|E_{max}\|_{\mathfrak{g}}}\int_M \|\rho - \mathrm{Ad}_{g^{-1}}\rho^{(g)}\|_{\mathfrak{g}}$ in figure 3.9b. $\rho$ and $\rho^{(g)}$ are charge densities obtained using ungauged and gauged initial conditions, respectively. The quantities are normalized using the maximum value of the electric field $\|E_{max}\|$.

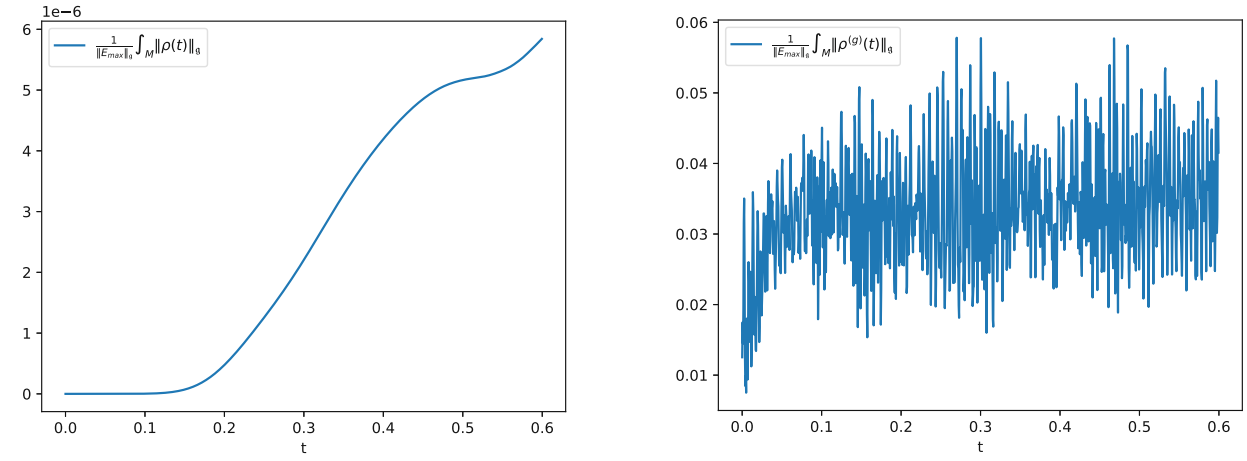


(a) $\frac{1}{\|E_{max}\|_{\mathfrak{g}}}\int_M \|\rho\|_{\mathfrak{g}}$ (b) $\frac{1}{\|E_{max}\|_{\mathfrak{g}}}\int_M \|\rho^{(g)}\|_{\mathfrak{g}}$

Figure 3.10: Time evolution plots of charge violations $\frac{1}{\|E_{max}\|_{\mathfrak{g}}}\int_M \|\rho\|_{\mathfrak{g}}$ in figure 3.10a and $\frac{1}{\|E_{max}\|_{\mathfrak{g}}}\int_M \|\rho^{(g)}\|_{\mathfrak{g}}$ in figure 3.10b. $\rho$ and $\rho^{(g)}$ are charge densities obtained using ungauged and gauged initial conditions respectively. The quantities are normalized using the maximum value of the electric field $\|E_{max}\|$. As opposed to figure 3.9 the initial conditions for the $z$-components of electric fields have been scaled $\lambda\mathcal{E}_z(t=0)$ using $\lambda = 0.001$.

Figure 3.11: A visualization of one component $\rho_3^{(g)}$ of the charge density throughout the simulation with gauged and scaled initial conditions $\lambda \mathrm{Ad}_g \mathcal{E}_z$ and $\lambda = 0.001$. Grey, blue and red correspond to vanishing, negative and positive values respectively. The defects in the form of rapid oscillations are visible throughout the mesh.

# 4 Lattice Gauge Theoretic Finite Element Method

There are efforts towards charge and symmetry preserving Finite Element Methods for Yang-Mills theories. The works of Droniu et al. [20] and Christiansen et al. [15] include the non-Abelian continuity equation in the weak formulation by using Lagrange multipliers. The work of Berchenko-Kogan et al. [8] aims towards a different formulation using Discontinous Galerkin (DG) [16] methods to obtain charge conservation per element. A method which uses concepts from Lattice Gauge Theory (LGT) has been proposed by Christiansen and Halvorsen et al. in [14] and [27].

The role that gauge transformations play in this context has not been fully worked out until now. This may be important not only for preserving the intrinsic symmetry itself but also gauge-dependant charges. In the following we would like to address this by constructing a discretization that exhibits notions of gauge symmetry and charge conservation. We will use LGT [22], Regge Calculus [47], DG [16] and the works in [14] [27] as sources of inspiration.

## 4.1 Lie Group Valued Elements

For the reasons presented in the last section 3.3 it would be beneficial to construct Lie group-valued finite element spaces for discretizing gauge transformations. For instance, the use of geodesic finite elements is a means for creating well defined Lie group-valued functions [48]. We additionaly require suitable FEM spaces that fit within the structure of gauge theories, which also includes the group multiplication. In other words, the discrete subset of Lie group-valued functions we seek $C_h(M,G) \subset C(M,G)$ should be closed with respect to the Lie group multiplication.

We stay within the case of compact Lie groups (such as $SU(N)$) where we may parametrize elements using the exponential map $\exp : \mathfrak{g} \to G$. A function $g \in C(M,G)$ can be then described using Lie Algebra elements $\phi \in C(M,\mathfrak{g})$.

**$U(1)$:**

To start with, we first look at the one dimensional Abelian $U(1)$ group and the spatial domain $M$ corresponding to a line segment. The group product of two elements (in this case complex unit numbers) $g = e^{i\phi}$ and $h = e^{i\psi}$ can be evaluated using addition in the Lie Algebra (in this case imaginary numbers) $gh = e^{i\phi}e^{i\psi} = e^{i\phi+i\psi} = e^{i(\phi+\psi)}$ . This means we can build a desired Lie group-valued functions using the space $C(M;\mathfrak{g}) = C(M;i\mathbb{R})$ and a suitable linear discretization which is fully consistent with the group product.

**$SU(2)$:**

Now let us move on to the non-Abelian $SU(2)$ group, where there exists a closed formula for the exponential map

$$\exp\{i\vec{\alpha}\cdot\hat{\sigma}\} = \exp\{i\alpha\hat{\alpha}\cdot\hat{\sigma}\} = \cos\alpha\mathbb{1} + i\sin\alpha\hat{\alpha}\cdot\hat{\sigma}$$

with three-dimensional unit vectors $\hat{\alpha} \in \mathbb{R}^3$, magnitude (angle of rotation) $\alpha \in [0, 2\pi]$ and set of Pauli matrices $\hat{\sigma} = (\sigma_k)_{k=1,2,3} \in \mathbb{C}^{2\times 2}$. We again assume that two discrete functions $a = \exp\{i\vec{\alpha}\cdot\hat{\sigma}\}$ and $b = \exp\left\{i\vec{\beta}\cdot\hat{\sigma}\right\}$ are parametrized in terms of coefficients $\vec{\alpha} \in C(M,\mathbb{R}^3)$ and $\vec{\beta} \in C(M,\mathbb{R}^3)$. Performing the group multiplication of $a$ with $b$ we get

$$ab = \left(\cos\alpha\cos\beta - \sin\alpha\sin\beta\hat{\alpha}\cdot\hat{\beta}\right)\mathbb{1} + i\left(\sin\alpha\cos\beta\hat{\alpha} + \cos\alpha\sin\beta\hat{\beta}\right)\cdot\hat{\sigma}$$

that the coefficients $\vec{\phi} = \phi\hat{\phi} \in C(M, \mathbb{R}^3)$ representing the product $ab \in C(M, G)$ are

$$\cos\phi = \cos\alpha\cos\beta - \sin\alpha\sin\beta\hat{\alpha}\cdot\hat{\beta}$$
$$\hat{\phi} = \frac{1}{\sin\phi}\left(\sin\alpha\cos\beta\hat{\alpha} + \cos\alpha\sin\beta\hat{\beta}\right).$$

If $\alpha$ and $\beta$ are parametrized in some FEM space (for instance using polynomials), it is not clear that the above group element represented by $\vec{\phi} = \phi\hat{\phi}$ falls under the same parametrization in general. Moreover, a suitable parametrization in the specific case of $SU(2)$ does not guarantee existence of other ones.

In summary, it is difficult to find a group homomorphism between Lie group-valued functions $C(M;G)$ and a discretely parametrized subset $C_h(M;G)$. Following this line of reasoning, a notion of discrete gauge invariance with FEM functions that is self-consistent seems to be difficult to achieve at first glance.

While this shows a part of the problem, it also presents a part of the solution. There is one simple case in which the parametrization is compatible with the group structure - the space representing constant functions. Abandoning the notion of continuity, the next best compromise would be having piecewise constant functions, which would be a step closer to LGT.

## 4.2 A Simplicial Gauge Theory [14] [27]

In this section we want to briefly outline the works of Christiansen and Halvorsen et al. in [14] [27] which aim towards creating a discretization of Yang-Mills theories that follows principles of LGT. In particular we approximate the Yang-Mills action

$$S = \int_M F \wedge \star F = \int_M \mathrm{Re}\,\mathrm{Tr}\{F_{\mu\nu}F^{\mu\nu}\}$$

on a triangulation of the space-time manifold $M$, which for simplicity we will assume to be 3-dimensional.

A discrete gauge transformation is defined to be a Lie group-valued function $g : \mathcal{S}_0 \to G$, that maps to each vertex $V \in \mathcal{S}_0$ a gauge group element $g(V) \in G$. The discrete connection in this case is given by Parallel transporters $(U_E)_{E\in\mathcal{S}_1}$ along edges $E \in \mathcal{S}_1$ in the triangulation that connect vertices. Similar to lattice gauge theory, the field strength variables then correspond to plaquette variables $W_{V,F}$ belonging to faces $F \in \mathcal{S}_2$ which start at vertices $V \in \mathcal{S}_0$. Using Whitney 2-forms with basis functions $(\lambda_F)_{F\in\mathcal{S}_2}$ one may construct an approximate field strength $\mathcal{F}_h$ using

$$\mathcal{F}_h = \sum_{F\in\mathcal{S}_2} (\mathcal{F}_h)_F \lambda_F$$
$$(\mathcal{F}_h)_F = \ln W_{V,F} \simeq \mathbb{1} - W_{V,F}.$$

The degrees of freedom $(\mathcal{F}_h)_F$ belong to faces $F \in \mathcal{S}_2$ with a distinguished orientation and starting point for the plaquette $V \in \mathcal{S}_1$. The combination of the three together is referred to as a pointed oriented face in [14]. As a consequence, the variables $(\mathcal{F}_h)_F$ gauge-transform locally in respective vertices $V$.

The action corresponding to $\mathcal{F}_h$ can be then evaluated using mass matrices $M_{FF'}$ for basis functions $(\lambda_F)_{F\in\mathcal{S}_2}$.

$$\begin{aligned}
S &\simeq \int_M \langle \mathcal{F}_h, \mathcal{F}_h\rangle = \\
&= \int_M \langle \sum_F (\mathcal{F}_h)_E \lambda_F, \sum_{F'} (\mathcal{F}_h)^\dagger_{F'} \lambda_{F'}\rangle = \\
&= \int_M \sum_{F,F'} \mathrm{Re}\,\mathrm{Tr}\Big\{(\mathcal{F}_h)_F (\mathcal{F}_h)^\dagger_{F'}\Big\}\langle\lambda_F, \lambda_{F'}\rangle = \\
&= \sum_{F,F'} \int_M \langle\lambda_F, \lambda_{F'}\rangle\,\mathrm{Re}\,\mathrm{Tr}\Big\{(\mathcal{F}_h)_F (\mathcal{F}_h)^\dagger_{F'}\Big\} = \\
&= \sum_{F,F'} M_{FF'}\,\mathrm{Re}\,\mathrm{Tr}\Big\{(\mathcal{F}_h)_F (\mathcal{F}_h)^\dagger_{F'}\Big\}
\end{aligned}$$

Replacing the curvature variables $(\mathcal{F}_h)_F$ with their approximations we obtain

$$S \simeq \sum_{F,F'} M_{FF'} \operatorname{Re}\operatorname{Tr}\Big\{(\mathcal{F}_h)_F(\mathcal{F}_h)^\dagger_{F'}\Big\} \simeq \sum_{F,F'} M_{FF'} \operatorname{Re}\operatorname{Tr}\Big\{(\mathbb{1}-W_{V,F})(\mathbb{1}-W_{V',F'})^\dagger\Big\}.$$

Note that this expression as it stands may not be not gauge invariant in general: vertices $V$ and $V'$ may be different. Christiansen et al. therefore manually included additional parallel transporters $U_{VV'}$

$$S \simeq \sum_{F,F'} M_{FF'} \operatorname{Re}\operatorname{Tr}\Big\{(\mathcal{F}_h)_F(\mathcal{F}_h)^\dagger_{F'}\Big\} \simeq \sum_{F,F'} M_{FF'} \operatorname{Re}\operatorname{Tr}\Big\{U_{VV'}(\mathbb{1}-W_{V,F})U_{V'V}(\mathbb{1}-W_{V',F'})^\dagger\Big\}.$$

This inclusion is necessary to repair gauge symmetry of the action. Care must be taken to create a consistent discretization that does not depend on the choice of orientations and starting points of plaquettes. Hence, a systematic ordering and pairing of terms has to thought of. We refer to section 4.4 where we further elaborate this point for a slightly different yet qualitatively similar action we introduce in equation 4.4.

It is also mentioned, that only picking out diagonal terms in the sum (also called "mass-lumping" in the FEM context)

$$\begin{aligned} S &\simeq \sum_{F,F'} M_{FF'} \operatorname{Re}\operatorname{Tr}\Big\{U_{VV'}(\mathbb{1}-W_{V,F})U_{V'V}(\mathbb{1}-W_{V',F'})^\dagger\Big\} \simeq \\ &\simeq \sum_{F} M_{FF} \operatorname{Re}\operatorname{Tr}\Big\{(\mathbb{1}-W_{V,F})(\mathbb{1}-W_{V,F})^\dagger\Big\} \end{aligned}$$

leads to a modified Wilson action with different weights $M_{FF}$.

In summary, the above approach takes some further steps from the standard FEM discretization towards LGT. In particular, the continuous connection 1-form $\mathcal{A}$ is replaced by discrete parallel transporters $(U_F)_{E\in\mathcal{S}_1}$. One may note that both weights of curvature variables, $V/(a^\mu a^\nu)^2$ in the Wilson action and $M_{FF}$ here, scale qualitatively identically in terms of the mesh size.

## 4.3 Regge Calculus and Lattice Gauge Theory

The connection between Regge Calculus and Lattice Gauge Theory is mentioned in the literature [13] [6]. In order to construct a gauge symmetric FEM discretization of Yang-Mills theories we may take inspiration from both which share some features and ideas.

While in the case of Riemannian geometry parallel transport is a notion tied to objects of space-time geometric nature (such as tangent vectors), gauge theories apply this idea to different kinds of quantities. In Yang-Mills theories objects that carry a property called color (not associated to space-time) need to be parallel transported using the $SU(N)$ Lie group which rotates color spaces. With this idea, the concept of distributional connections as envisioned in Regge Calculus may be reinterpreted for (lattice) gauge theories as depicted in figure 4.1.

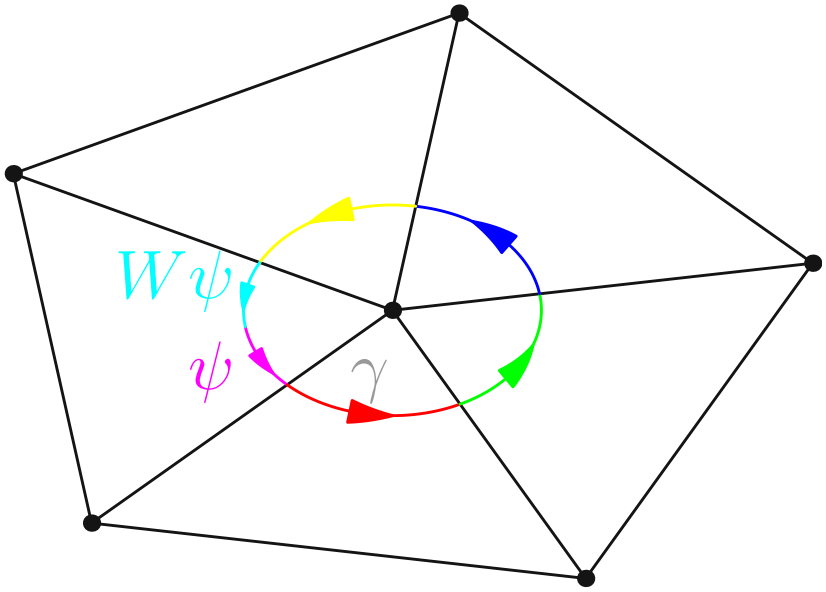


Figure 4.1: Illustration of the parallel transport of a colored object $\psi$ along a curve $\gamma$ that crosses edges using the distributional connection in two dimensions. The "colors" of $\psi$ along the curve are piecewise constant with discontinuities at edges $E$ resulting from respective parallel transporter $U \in G$.

The fact, that colors and associated $SU(N)$-transformations in gauge theories are decoupled from space-time, would translate in the case of Regge calculus to element-wise transformations that affect the connection but do not touch any space-time components. This is comparable to the case of LGT, where a gauge transformation can be individually defined on each vertex separately.

This brings us to the next difference between Regge calculus and LGT, which stems from the definitions of connections themselves. In the Regge case they are defined as Lie group-valued objects connecting elements and are therefore located perpendicular to element interfaces (which are codimension-1-simplices), whereas in the LGT case they consist of Lie group-valued objects connecting vertices and therefore go along respective edges (which are 1-simplices). Both can be qualitatively seen as the same concept but belonging to respective dual lattices. In three dimensions for instance, the connections in Regge calculus and LGT belong to faces (2-simplices) or edges (1-simplices) respectively. This is illustrated in figures 4.2a and 4.2b. The approximation procedure outlined in the Colored-Particle-In-Cell (CPIC) [51] [40] approach also hints at the connection between the two perspectives.

As a consequence, the plaquette variables of respective formalisms that are formed by parallel transport along closed paths, are associated to mutually dual mesh objects: codimension-2-simplices and 2-simplices in Regge calculus and LGT respectively. In 3 dimensions for instance, the curvature in Regge calculus lives on edges (1-simplices) while in LGT it lives on the faces (2-simplices). Figures 4.2c and 4.2d showcase this example.

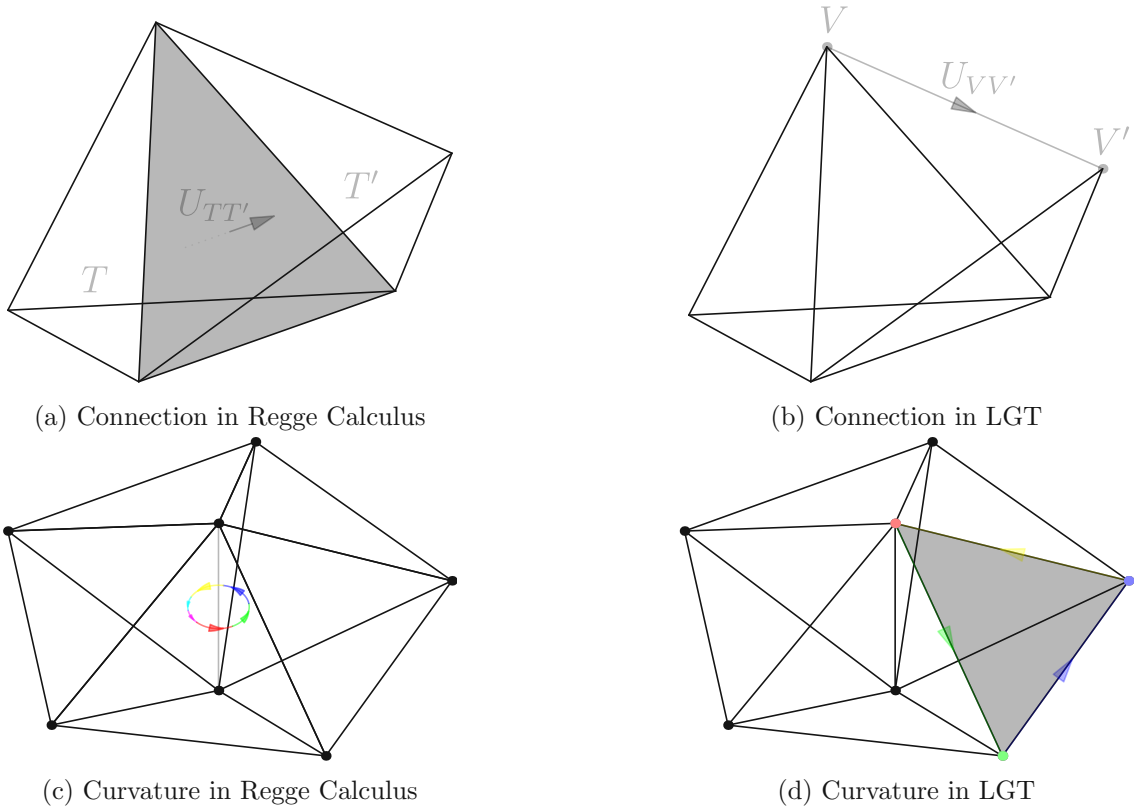


(a) Connection in Regge Calculus

(b) Connection in LGT

(c) Curvature in Regge Calculus

(d) Curvature in LGT

Figure 4.2: Illustration of the connections and curvature contributions of both Regge calculus and Lattice Gauge Theory (LGT) on a three dimensional mesh.

The curvature in the context of Regge calculus can be viewed as a distribution with support at the skeleton $\mathcal{S}_{n-2}$ formed by codimension-2-simplices. The corresponding Regge action can then be accounted for as the Einstein-Hilbert action of the associated discrete distributional curvature with an approximate volume form [39].

However, the Yang-Mills action contains the quadratic curvature term $\langle \mathcal{F}_{\mu\nu}, \mathcal{F}^{\mu\nu} \rangle_{\mathfrak{g}}$. The line of reasoning for the Regge actions does not directly work in this case, as the product of these two singular distributions, $\mathcal{F}$ with itself, would be ill-defined. We would therefore like to investigate suitable discretizations of this action.

## 4.4 Dual Wilson Action

As noted before, the approach to the connections used in Regge calculus can be interpreted as lattice gauge theory on the dual lattice. This means that connection and curvature will be associated to dual mesh objects. We now want to apply the Regge formulation of discrete connections to Yang-Mills theories to motivate and construct a modified Wilson action on the dual mesh - a dual Wilson action so to speak. For simplicity we will remain in three dimensions throughout this section.

While plaquettes still suggest the existence of non-trivial curvature, the identification with curvature variables in LGT was so far motivated by the Stokes-like formula 2.14. The use of this argument is now hindered, as each parallel transporter does not belong to a particular edge and no definitive mesh area can be assigned to each plaquette. In fact, parallel transport along any loop that encloses one particular bone will deliver the same plaquette variable as illustrated in figure 4.3.

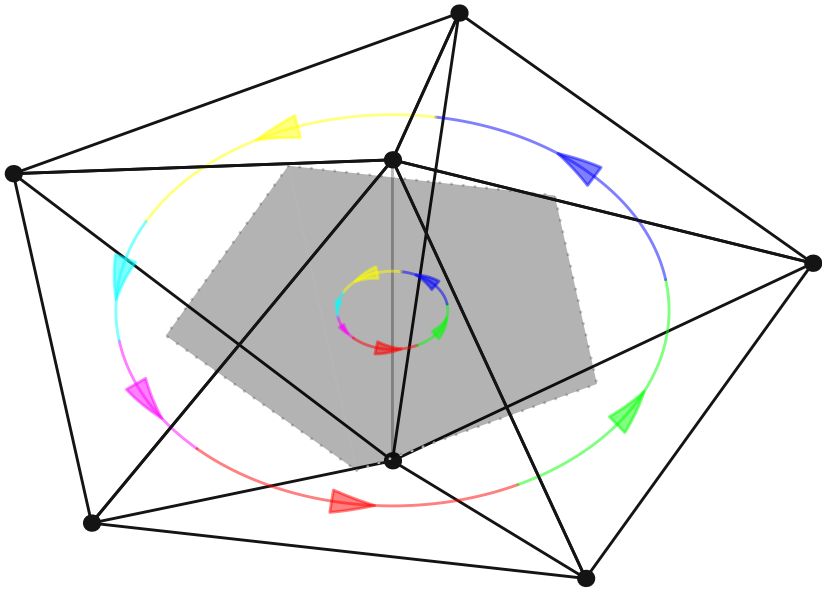

Figure 4.3: The plaquettes belonging to both the small and large loops are identical and therefore both represent the curvature concentrated in the bone edge. The corresponding loop area in the dual lattice is shaded in grey.

Heuristically speaking, we need to weigh the plaquette with an inverse area to qualitatively obtain a viable notion of curvature in the continuum limit. A compromise that naturally comes to ones mind would be to use the plaquette area represented in the dual lattice. This is also mentioned in the work of Miller [39] which motivates the Regge action from first principles.

In more precise terms, we seek to reconstruct the Hodge dual curvature $(\star\mathcal{F})|_E$ living on the edges of the lattice $E \in \mathcal{S}_1$ from the variables $\mathcal{F}|_{F^*}$ describing curvature associated to faces $F^*$ in the dual lattice. A discrete Hodge star operator that achieves this is mentioned by Desbrun et al. in [19] and stands in line with the idea of using the area in the dual lattice. We interpret the formula that defines the discrete Hodge star operator in [19] on a three dimensional mesh as

$$\frac{1}{|E|}\int_E \star\mathcal{F} = \frac{1}{|E^*|}\int_{E^*} \mathcal{F} \tag{4.1}$$

where $E$ stands for the edge with curvature $\star\mathcal{F}$ we would like to describe, and $E^*$ represents the respective dual mesh area with the associated curvature $\mathcal{F}$. $|E|$ and $|E^*|$ refer to the length and area of respective geometrical objects measured according to the space-time metric $g_{\mu\nu}$. We note that these are not necessarily positive if objects align with the time direction. Motivated by formula 2.14 we identify the surface integral $\int_{E^*}\mathcal{F} \simeq \ln W_E$ using the plaquette $W_E$. Assuming that the curvature $\star\mathcal{F}$ is constant along the edge $E$ we obtain

$$\begin{aligned}
\frac{1}{|E|}\int_E \star\mathcal{F} &= \frac{1}{|E^*|}\int_{E^*}\mathcal{F} \\
\frac{1}{|E|}(\star\mathcal{F})|_E\int_E &= \frac{1}{|E^*|}\ln W_E \\
\frac{1}{|E|}(\star\mathcal{F})|_E|E| &= \frac{1}{|E^*|}\ln W_E \\
(\star\mathcal{F})|_E &= \frac{1}{|E^*|}\ln W_E.
\end{aligned}$$

This result is qualitatively similar to lattice gauge theory, where the curvature is weighed with an inverse area.

Continuing in this spirit we can try to adapt the derivation in [39] to approximate the Yang-Mills action. This involves integrating the bones' curvature contributions $(\star\mathcal{F})|_E$ over the volumes $V_E$ associated to each bone $E$.

$$S_{YM} \simeq \sum_E V_E\langle(\star\mathcal{F})|_E, (\star\mathcal{F})|_E\rangle_{\mathfrak{g}} = \sum_E \frac{V_E}{|E^*|^2}\langle\ln W_E, \ln W_E\rangle_{\mathfrak{g}} \tag{4.2}$$

Equation 4.2 represents the standard Wilson action of LGT interpreted on the dual lattice.

Looking back at the Yang-Mills action, we notice that it consists of the inner product of the curvature with itself $\langle \mathcal{F}, \mathcal{F} \rangle$. In an orthonormal coordinate system (where the components $g_{\mu\nu}$ of the metric $g$ essentially become the identity matrix), the individual contributions decompose into a sum of quadratic terms.

$$\begin{aligned}\langle \mathcal{F}, \mathcal{F} \rangle &= \langle \mathcal{F}_{\mu\nu}, \mathcal{F}^{\mu\nu} \rangle_{\mathfrak{g}} = \\ &= \underbrace{g_{\mu\alpha}}_{=\delta_{\mu\alpha}} \underbrace{g_{\nu\beta}}_{=\delta_{\nu\beta}} \langle \mathcal{F}^{\alpha\beta}, \mathcal{F}^{\mu\nu} \rangle_{\mathfrak{g}} = \\ &= \langle \mathcal{F}^{\mu\nu}, \mathcal{F}^{\mu\nu} \rangle_{\mathfrak{g}} = \sum_{\mu,\nu} \langle \mathcal{F}^{\mu\nu}, \mathcal{F}^{\mu\nu} \rangle_{\mathfrak{g}}\end{aligned}$$

The Wilson action merely replaces each $\mathcal{F}^{\mu\nu}$ with the plaquette $W_{x,\mu\nu}$ corresponding to $\mu$-$\nu$-coordinate plane in a regularly ordered cubic grid. As this lattice is orthogonal, the Wilson action containing no cross terms which couple different plaquettes is assumed to be a good approximation.

Simplicial lattices however, do not have orthogonal lattice directions, which is why off-diagonal terms may be crucial for constructing a discrete action. The idea of Christiansen and Halvorsen et al. in [14] and [27] could be a way to proceed here: symbolically interpolate the distributional curvature in the space of Whitney codimension-2-forms $(\lambda_E)_{E \in \mathcal{S}_{n-2}}$, where the degrees of freedom $(\star F)_E = \int_E \star F$ are given by the integral of the dual curvature along respective simplices $E \in \mathcal{S}_{n-2}$. Using the discrete Hodge star operator in equation 4.1 this translates in three dimensions to

$$\begin{aligned}(\star \mathcal{F})_h &= \sum_{E \in \mathcal{S}_1} (\star \mathcal{F})_E \lambda_E \\ (\star \mathcal{F})_E &= \int_E \star \mathcal{F} = \frac{|E|}{|E^*|} \int_{E^*} \mathcal{F} \simeq \frac{|E|}{|E^*|} \ln W_E\end{aligned}$$

and forming the inner product using mass matrices

$$\begin{aligned}S^{(\mathrm{FEM})}_{W^*} &= \langle \mathcal{F}_h, \mathcal{F}_h \rangle = \\ &= \langle \sum_{E \in \mathcal{S}_1} (\star \mathcal{F})_E \lambda_E, \sum_{E' \in \mathcal{S}_1} (\star \mathcal{F})_{E'} \lambda_{E'} \rangle = \\ &= \sum_{E,E' \in \mathcal{S}_1} \langle \lambda_E, \lambda_{E'} \rangle \langle (\star \mathcal{F})_E, (\star \mathcal{F})_{E'} \rangle = \\ &= \sum_{E,E' \in \mathcal{S}_1} M_{EE'} \langle \frac{|E|}{|E^*|} \ln W_E, \frac{|E'|}{|(E')^*|} \ln W_{E'} \rangle_{\mathfrak{g}} = \\ &= \sum_{E,E' \in \mathcal{S}_1} M_{EE'} \frac{|E|}{|E^*|} \frac{|E'|}{|(E')^*|} \langle \ln W_E, \ln W_{E'} \rangle_{\mathfrak{g}} \simeq \\ &\simeq \sum_{E,E' \in \mathcal{S}_1} M_{EE'} \frac{|E|}{|E^*|} \frac{|E'|}{|(E')^*|} \langle \mathbb{1} - W_E, \mathbb{1} - W_{E'} \rangle_{\mathfrak{g}}\end{aligned}$$

we obtain a dual Wilson action

$$S^{(\mathrm{FEM})}_{W^*} = \sum_{E,E' \in \mathcal{S}_1} M_{EE'} \frac{|E|}{|E^*|} \frac{|E'|}{|(E')^*|} \langle \ln W_E, \ln W_{E'} \rangle_{\mathfrak{g}} \simeq \tag{4.3}$$

$$\simeq \sum_{E,E' \in \mathcal{S}_1} M_{EE'} \frac{|E|}{|E^*|} \frac{|E'|}{|(E')^*|} \langle \mathbb{1} - W_E, \mathbb{1} - W_{E'} \rangle_{\mathfrak{g}} \tag{4.4}$$

with couplings of different plaquettes as well as modified respective weights. Note that the lengths $|E|$, areas $|E^*|$ and the mass matrix $M_{EE'} = \langle \lambda_E, \lambda_{E'} \rangle$ in definition 26 implicitly contain the mesh geometry as well as the space-time metric $g$. We will sometimes abbreviate the prefactors in the action 4.4 using weights $C_{EE'}$ as in

$$S^{(\mathrm{FEM})}_{W^*} = \sum_{E,E' \in \mathcal{S}_1} C_{EE'} \langle \ln W_E, \ln W_{E'} \rangle_{\mathfrak{g}} \quad C_{EE'} = M_{EE'} \frac{|E|}{|E^*|} \frac{|E'|}{|(E')^*|}.$$

### Symmetry of the Dual Wilson Action

As this action suffers from the similar problem mentioned by Christiansen et al. in [14] we will elaborate a way to render the action gauge invariant. To start with we aim to justify why this action does not depend on any specific mesh topology in the form of simplex ordering and orientation. As an equivalent alternative to the manual inclusion of parallel transporters, we reframe the repair restoring gauge symmetry through a deliberate choice of suitably pairable plaquettes. This is possible as the adjoint map $W \mapsto UWU^{-1}$ with a parallel transporter $U$ that already occurs in $W$ basically cyclically reorders the terms in $W$. For the corresponding logarithm we also have Ad-invariance

$$\ln\left(UWU^{-1}\right) = U \ln W U^{-1}$$

if $U \in G$ and $W \in G$ are close enough near the identity $\mathbb{1}$. This is also true for the approximation

$$\mathbb{1} - UWU^{-1} = U\mathbb{1}U^{-1} - UWU^{-1} = U(\mathbb{1} - W)U^{-1}.$$

The gauge-symmetry breaking here boils down to the fact, that the pair of distinct plaquettes $W_E$ and $W_{E'}$ start at different elements $El$ and $El'$. We capture this in notation by adding the element index to the plaquette as in

$$S^{(\mathrm{FEM})}_{W^*} = \sum_{E,E' \in \mathcal{S}_1} C_{EE'} \langle \ln W_{El,E}, \ln W_{El',E'} \rangle_{\mathfrak{g}}. \tag{4.5}$$

The first idea that comes to mind, is to fix a common element $El_{E,E'}$ for both loops, such that both start and end in the same element.

$$S^{(\mathrm{FEM})}_{W^*} = \sum_{E,E' \in \mathcal{S}_1} C_{EE'} \langle \ln W_{El_{E,E'},E}, \ln W_{El_{E,E'},E'} \rangle_{\mathfrak{g}}$$

The natural question that arises is, whether this arbitrary choice has an impact on the action. In other words, if a different starting element $El'_{E,E'}$ was chosen, do we obtain an identical action? One can confirm (at least in two and three dimensions) that the action remains identical. This is because the suitable starting elements $El_{E,E'}$ and $El'_{E,E'}$ of plaquettes are located next to each other in such a manner that they are connected via a parallel transporter $U$ contained in both plaquettes $W_{El_{E,E'},E}$ and $W_{El_{E,E'},E'}$ of interest. Therefore we have something similar to

$$W_{El'_{E,E'},E} = U W_{El_{E,E'},E} U^{-1} \quad W_{El'_{E,E'},E'} = U W_{El_{E,E'},E'} U^{-1} \tag{4.6}$$

and due to Ad-invariance we obtain identical terms

$$\begin{aligned}
&\langle \ln W_{El'_{E,E'},E}, \ln W_{El'_{E,E'},E'} \rangle_{\mathfrak{g}} = \\
&= \langle \ln\left(U W_{El_{E,E'},E} U^{-1}\right), \ln\left(U W_{El_{E,E'},E'} U^{-1}\right) \rangle_{\mathfrak{g}} = \\
&= \langle U \ln W_{El_{E,E'},E} U^{-1}, U \ln W_{El_{E,E'},E'} U^{-1} \rangle_{\mathfrak{g}} = \\
&= \langle \ln W_{El_{E,E'},E}, \ln W_{El_{E,E'},E'} \rangle_{\mathfrak{g}}.
\end{aligned}$$

This means that the common element $El_{E,E'}$ for both edges $E$ and $E'$ may be chosen freely. The action is invariant under discrete gauge transformations $(g_T)_{T \in \mathcal{S}_3}$ which constitute of one Lie group rotation $g_T \in G$ per element $T \in \mathcal{S}_3$.

Another freedom plaquettes possess in this formulation is their orientation. Hence we must ask the same question: can the orientation of plaquettes be chosen arbitrarily? It is important to note, that the basis Whitney forms $(\lambda_E)_{E \in \mathcal{S}_1}$ in the mass matrix $M_{EE'}$ carry an orientation. It is therefore plausible, that we need to consistently match the orientation of both Whitney forms and plaquettes. To examine this further, we individually look at the mass matrix $M_{EE'} = \langle \lambda_E, \lambda_{E'} \rangle$ and the pairing term $\langle \ln W_{El_{E,E'},E}, \ln W_{El_{E,E'},E'} \rangle_{\mathfrak{g}}$. Flipping the orientation of Whitney codimension-2-forms $\lambda_E$ (or vector fields in the three dimensional case)

amounts to a minus sign $\lambda_E \to -\lambda_E$. The mass matrix $M_{EE'}$ therefore also inherits this on the off-diagonal part.

$$\begin{aligned} M_{E''E'} &= \langle \lambda_{E''}, \lambda_{E'} \rangle \to \\ &\to \langle (-1)^{\delta_{EE''}} \lambda_{E''}, (-1)^{\delta_{EE'}} \lambda_{E'} \rangle = \\ &= (-1)^{\delta_{EE''}} (-1)^{\delta_{EE'}} \langle \lambda_{E''}, \lambda_{E'} \rangle = (-1)^{\delta_{EE''} + \delta_{EE'}} M_{E''E'} \end{aligned}$$

Flipping the orientation of a plaquette $W_{El_{E,E'},E}$ while keeping the starting element $El_{E,E'}$ means taking the inverse $W_{El_{E,E'},E} \to W^{-1}_{El_{E,E'},E}$. The logarithm $\ln W_{El_{E,E'},E}$ will therefore also get a minus sign

$$\ln W_{El_{E,E'},E} \to \ln\Big(W^{-1}_{El_{E,E'},E}\Big) = -\ln W_{El_{E,E'},E}$$

and in total the action remains invariant.

$$\begin{aligned} &S^{(\mathrm{FEM})}_{W^*} = \\ &= \sum_{E'',E' \in \mathcal{S}_1} C_{E''E'} \langle \ln W_{El_{E'',E'},E}, \ln W_{El_{E'',E'},E'} \rangle_{\mathfrak{g}} = \\ &= \sum_{E'',E' \in \mathcal{S}_1} M_{E''E'} \frac{|E''|}{|(E'')^*|} \frac{|E'|}{|(E')^*|} \langle \ln W_{El_{E'',E'},E}, \ln W_{El_{E'',E'},E'} \rangle_{\mathfrak{g}} \to \\ &\to \sum_{E'',E' \in \mathcal{S}_1} (-1)^{\delta_{EE''} + \delta_{EE'}} M_{E''E'} \frac{|E''|}{|(E'')^*|} \frac{|E'|}{|(E')^*|} \langle (-1)^{\delta_{EE''}} \ln W_{El_{E'',E'},E''}, (-1)^{\delta_{EE'}} \ln W_{El_{E'',E'},E'} \rangle_{\mathfrak{g}} = \\ &= \sum_{E'',E' \in \mathcal{S}_1} M_{E''E'} \frac{|E''|}{|(E'')^*|} \frac{|E'|}{|(E')^*|} \langle \ln W_{El_{E'',E'},E''}, \ln W_{El_{E'',E'},E'} \rangle_{\mathfrak{g}} = \\ &= \sum_{E'',E' \in \mathcal{S}_1} C_{E''E'} \langle \ln W_{El_{E'',E'},E''}, \ln W_{El_{E'',E'},E'} \rangle_{\mathfrak{g}} = S^{(\mathrm{FEM})}_{W^*} \end{aligned}$$

We check whether the same argument for the approximation of the logarithm via computation

$$\mathrm{Tr}\Big\{(\mathbb{1} - W_E)(\mathbb{1} - W_{E'})^\dagger\Big\} = \mathrm{Tr}\Big\{\mathbb{1} - W_E - (W_{E'})^\dagger + W_E (W_{E'})^\dagger\Big\} \tag{4.7}$$

$$\begin{aligned} \mathrm{Tr}\Big\{(\mathbb{1} - W_E^{-1})(\mathbb{1} - W_{E'})^\dagger\Big\} &= \mathrm{Tr}\Big\{\mathbb{1} - W_E^{-1} - (W_{E'})^\dagger + W_E^{-1} (W_{E'})^\dagger\Big\} && (4.8) \\ &= \mathrm{Tr}\Big\{\mathbb{1} - (W_E)^\dagger - (W_{E'})^\dagger + (W_E)^\dagger (W_{E'})^\dagger\Big\} \neq && (4.9) \\ &\neq \pm \mathrm{Tr}\Big\{\mathbb{1} - W_E - (W_{E'})^\dagger + W_E (W_{E'})^\dagger\Big\} \quad E \neq E' && (4.10) \end{aligned}$$

and see, that this is not the case for $E \neq E'$ in general. Therefore, the approximation of the logarithm $\ln W \simeq \mathbb{1} - W$ in the dual Wilson action in equation 4.5 would break the symmetry under examined orientation flips. However, for $E = E'$ we note that both terms, the regular one and the one where $E$'s orientation is flipped, are identical as as $W_E (W_E)^\dagger = \mathbb{1}$. The diagonal of the mass matrix $M_{EE}$ also does not obtain a sign during the flip. This means, that after applying the approximation of the logarithm $\ln W \simeq \mathbb{1} - W$ in combination with mass-lumping this symmetry remains preserved.

Christiansen et al. note in [14] that their action is consistent in the continuum limit. While we do not prove this here, it is reasonable to assume, that their proof carries over to the motivated dual Wilson action in 4.4. Merely the occurence of mesh lengths and areas may require additional arguments.

The theory and research up until now specifically uses the Voronoi dual lattice assuming that the original lattice satisfies the Delauney property. From a practical point of view, the barycentric dual lattice may be used as an approximate substitute so that the last Delauney requirement could be dropped.

As a first step, we will settle upon the approximate mass-lumped dual Wilson action in the form of a sum over all bones

$$S := \sum_{E\in} C_{EE}\langle(\mathbb{1} - W_E)(\mathbb{1} - W_E)^\dagger\rangle_{\mathfrak{g}} \tag{4.11}$$

with the weights $C_{EE} = M_{EE}\frac{|E|^2}{|E^*|^2}$ chosen as before and the approximate logarithm $\ln W \simeq \mathbb{1} - W$.

## 4.5 Charge Evolution

For evolving charges and currents with time, we need to solve a discrete analogue of the non-Abelian continuity equation in 46 involving the current $\mathcal{J}$,

$$\nabla_{\mathcal{A}} \cdot \mathcal{J} = \star \mathrm{d}_{\mathcal{A}} \star \mathcal{J} = \nabla_\mu \mathcal{J}^\mu = \partial_\mu \mathcal{J}^\mu + [\mathcal{A}_\mu, \mathcal{J}^\mu] = 0$$

that intuitively describes respective infinitesimal parallel transport along its own direction. For the sake of simplicity we assume that the spatial current $j^k = \rho u^k$ can be modeled by the product of the charge density $\rho = \mathcal{J}^0$ and a vector field $u^k$ that represents a "charge carrying wind". We further neglect any Lorentz-type forces the gauge field exerts on charges. We use temporal gauge $\mathcal{A}_0 = 0$ and write down the equation in weak form using partial integration

$$\nabla_\mu \mathcal{J}^\mu = \partial_t \rho + \nabla_k j^k = \partial_t \rho + \partial_k(\rho u^k) + [\mathcal{A}_k, \rho u^k] = 0$$

$$\int_M \langle \partial_t \rho, \phi\rangle_{\mathfrak{g}} + \int_M \langle \partial_k(\rho u^k), \phi\rangle_{\mathfrak{g}} + \int_M \langle [\mathcal{A}_k, \rho u^k], \phi\rangle_{\mathfrak{g}} = 0 \tag{4.12}$$

$$\int_M \langle \partial_t \rho, \phi\rangle_{\mathfrak{g}} + \int_M \partial_k \langle \rho u^k, \phi\rangle_{\mathfrak{g}} - \int_M \langle \rho u^k, \partial_k \phi\rangle_{\mathfrak{g}} + \int_M \langle [\mathcal{A}_k, \rho u^k], \phi\rangle_{\mathfrak{g}} = 0 \tag{4.13}$$

$$\int_M \langle \partial_t \rho, \phi\rangle_{\mathfrak{g}} + \int_{\partial M} n_k u^k \langle \rho, \phi\rangle_{\mathfrak{g}} - \int_M u^k \langle \rho, \partial_k \phi\rangle_{\mathfrak{g}} + \int_M u^k \langle [\mathcal{A}_k, \rho], \phi\rangle_{\mathfrak{g}} = 0 \tag{4.14}$$

where we again note, that the conservation should be thought of as purely local. In the appendix section 6.7.1 we further elaborate this particular scenario.

However, in the case of the distributional connection, the continuous connection 1-form $\mathcal{A} \in \Lambda^1(M;\mathfrak{g})$ (describing infinitesimal parallel transport) is replaced with gauge links $U_{TT'} \in G$ and it is not directly clear how to discretize this equation.

### DG-Upwinding

A source of inspiration is the Discontinuous Galerkin (DG) upwinding scheme for the regular continuity equation with charge $\rho$ and spatial current $j^k = u^k \rho$ with given wind $u$. We start with the regular continuity equation in strong form

$$\partial_t \rho + \partial_k(u^k \rho) = 0.$$

In weak form with a generic test function $\phi$ it reads as

$$\int_M \partial_t \rho \phi + \partial_k(u^k \rho)\phi = 0.$$

Splitting the integral into element-wise parts

$$\sum_T \int_T \partial_t \rho \phi + \partial_k(u^k \rho)\phi = 0$$

and performing partial integration

$$\int_T \partial_k(u^k \rho)\phi = \int_{\partial T} n_k u^k \rho \phi - \int_T u^k \rho \partial_k \phi$$

we arrive at a formulation in which $\rho$ does not explicitly require spatial differentiability, thus enabling the potential use of discontinuous function spaces.

$$\sum_T \int_T \partial_t \rho\phi + \int_{\partial T} n_k u^k \rho\phi - \int_T u^k \rho \partial_k \phi = 0$$

If $\rho$ becomes properly discontinuous, the above equation reduces to an element-wise one and there remains the question how the flow between neighbouring elements is mediated. Rearranging the expression for each element $T$ into

$$\int_T \partial_t \rho\phi = \int_T u^k \rho \partial_k \phi - \int_{\partial T} n_k u^k \rho\phi \quad \forall \phi \in L^2$$

makes it clear that the temporal evolution of $\rho$ on each element $T$ is governed by the weak gradient of the current (first term RHS) and the flux through the border (second term RHS). The latter term may be modified to incorporate fluxes from other elements. This is precisely the idea behind the so-called upwinding DG discretization of the transport equation [16].

$$\int_T \partial_t \rho\phi = \int_T u^k \rho \partial_k \phi - \int_{\partial T} n_k u^k \hat{\rho}\phi$$

Here, all border fluxes $\int_{\partial T} n_k u^k \rho\phi$ are set to their upwind values $u^k\hat{\rho}$ which are defined as follows: if the wind $u^k$ flows out of an element, then $\hat{\rho}$ coincides with the $\rho$-value inside this element at the interface ("inner $\rho$ limit"), else $\hat{\rho}$ is chosen to be the value from the neighbouring element sharing the interface ("outer $\rho$ limit"). If the element of interest is $T$ and its respective neighbouring interface is $T'$ then we may write it as

$$(\hat{\rho})_T = \begin{cases} \rho_T & u^k (n_T)_k \geq 0 \\ \rho_{T'} & u^k (n_T)_k < 0 \end{cases}.$$

This naturally fits the idea of parallel transporting charges: the wind dictates how charges flow from one element to the next. Using the discrete connection in the form of gauge links $U_{TT'}$ one can modify this upwinding prescription to account for parallel transport accross element interfaces as in

$$(\hat{\rho})_T = \begin{cases} \rho_T & u^k (n_T)_k \geq 0 \\ \mathrm{Ad}_{U_{T'T}} \rho_{T'} & u^k (n_T)_k < 0 \end{cases}. \tag{4.15}$$

The weak formulation of the DG-assisted parallel transport equation then includes charges that are in addition color-valued $(\rho_c)_{c=1,\dots,\dim \mathfrak{g}}$ which is why an additional Lie algebra inner product $\langle \cdot, \cdot \rangle_{\mathfrak{g}}$ is needed

$$\int_T \langle \partial_t \rho, \phi \rangle_{\mathfrak{g}} = \int_T u^k \langle \rho, \partial_k \phi \rangle_{\mathfrak{g}} - \int_{\partial T} n_k u^k \langle \hat{\rho}, \phi \rangle_{\mathfrak{g}} \quad \forall \phi \in L^2(M; \mathfrak{g}), T \subset \mathcal{S}(M) \tag{4.16}$$

where we specify the Lie algebra-valued discontinuous test function space $L^2(M;\mathfrak{g})$ and assume that charge densities $\rho \in C^1([t_0, t_1], L^2(M, \mathfrak{g}))$ are sufficiently differentiable with respect to the time interval $[t_0, t_1]$. The gradient of test functions $\partial_k \phi$ should be seen as an element-wise quantity.

### Charge Conservation

We examine whether in this setting we can demonstrate charge conservation. The standard argument for $\int_M \rho$ in the DG context is to decompose the domain $M = \cup_T T$ into individual elements $T$ and examine the change in the associated charge with respect to time $\partial_t \int_T \rho_a$. Assuming that $\rho_a$ is bounded we may pull in the temporal derivative $\partial_t \int_T \rho_a = \int_T \partial_t \rho_a$ and notice that this term is equivalent to testing the left side of the variational formulation $\int_T \partial_t \rho_a = \int_T \langle \partial_t \rho, \phi \rangle$ with a suitable (colored!) index test function $\phi_{a'} = c^{-1}_{aa'} \mathbb{1}_T \in L^2(M, \mathfrak{g})$ on the element $T$. Here $c_{aa'} = \langle \tau_a, \tau_b \rangle_{\mathfrak{g}}$ stands for the matrix representing the Lie

algebra inner product in the chosen color basis $(\tau_k)_{k=1,\dots,\dim \mathfrak{g}}$.

$$\begin{aligned}\partial_t \int_T \rho_a &= \int_T \langle \partial_t \rho, \phi \rangle_{\mathfrak{g}} = \\ &= \int_T u^k \langle \rho \underbrace{\partial_k \phi}_{=0} \rangle_{\mathfrak{g}} - \int_{\partial T} n_k u^k \langle \hat{\rho}, \phi \rangle_{\mathfrak{g}} = \\ &= -\int_{\partial T} n_k u^k \langle \hat{\rho}, \phi \rangle_{\mathfrak{g}} = -\int_{\partial T} n_k u^k \hat{\rho}_a\end{aligned}$$

This equation may be interpreted as charge conservation $Q^a_T(t) = \int_T \rho_a(t)$ of each color component $a$ on each triangle $T$ with boundary fluxes

$$\partial_t Q^a_T = -\int_{\partial T} n_k u^k \hat{\rho}_a.$$

While one might be tempted to sum up all charge contributions of individual triangles, it is important to keep in mind, that this would lead to an expression which does not consistently gauge transform as color spaces associated to each triangle can be rotated individually. The sum would therefore be first of all not well defined. We remember that there is no well defined notion of intergrated charge in Yang-Mills theories in genereal. One reason why the purely local charge conservation in the form of the differential non-Abelian continuity equation can be extended to a notion of integrated charge conservation per element may be due to the discrete nature of the connection represented by gauge links between elements. As the connection inside each element behaves effectively Abelian we may integrate charges over these domains.

### Numerical Time Stepping for Charges

For numerical time evolution of the charge $\rho$ using initial conditions $\rho(t=0) = \rho_0$ we approximate the temporal derivative $\partial_t \rho$ using a finite difference with time stepping parameter $\tau \ll 1$

$$\partial_t \rho \simeq \frac{1}{\tau}(\rho_+ - \rho_-)$$

and deploy an explicit Euler scheme

$$\int_T \langle \partial_t \rho, \phi \rangle_{\mathfrak{g}} = \int_T u^k \langle \rho, \partial_k \phi \rangle_{\mathfrak{g}} - \int_{\partial T} n_k u^k \langle \hat{\rho}, \phi \rangle_{\mathfrak{g}} \quad \forall \phi \in L^2(M;\mathfrak{g}), T \subset \mathcal{S}(M) \tag{4.17}$$

$$\int_T \langle \frac{1}{\tau}(\rho_+ - \rho_-), \phi \rangle_{\mathfrak{g}} = \int_T u^k \langle \rho_-, \partial_k \phi \rangle_{\mathfrak{g}} - \int_{\partial T} n_k u^k \langle \hat{\rho}_-, \phi \rangle_{\mathfrak{g}} \quad \forall \phi \in L^2(M;\mathfrak{g}), T \subset \mathcal{S}(M) \tag{4.18}$$

$$\int_T \langle \rho_+, \phi \rangle_{\mathfrak{g}} = \int_T \langle \rho_-, \phi \rangle_{\mathfrak{g}} + \tau \left( \int_T u^k \langle \rho_-, \partial_k \phi \rangle_{\mathfrak{g}} - \int_{\partial T} n_k u^k \langle \hat{\rho}_-, \phi \rangle_{\mathfrak{g}} \right) \quad \forall \phi \in L^2(M;\mathfrak{g}), T \subset \mathcal{S}(M). \tag{4.19}$$

We note that the argument involving charge conservation per element directly carries over to this time-discretized case. An illustration of the FEM time stepping in equation 4.19 is given in figures 4.4 and 4.5.

## 4.6 Current Source Terms

We would like to complement the pure Yang-Mills action in 4.4 with source terms in the form of color currents. In the continuum this amounts to the addition of the term

$$\int_M \langle \mathcal{J}, \mathcal{A} \rangle$$

where the angled brackets combine the pairing of 1-forms and Lie algebra vectors. This expression can not be directly translated to the case involving distributional connections and we therefore need to construct comparable discrete terms.

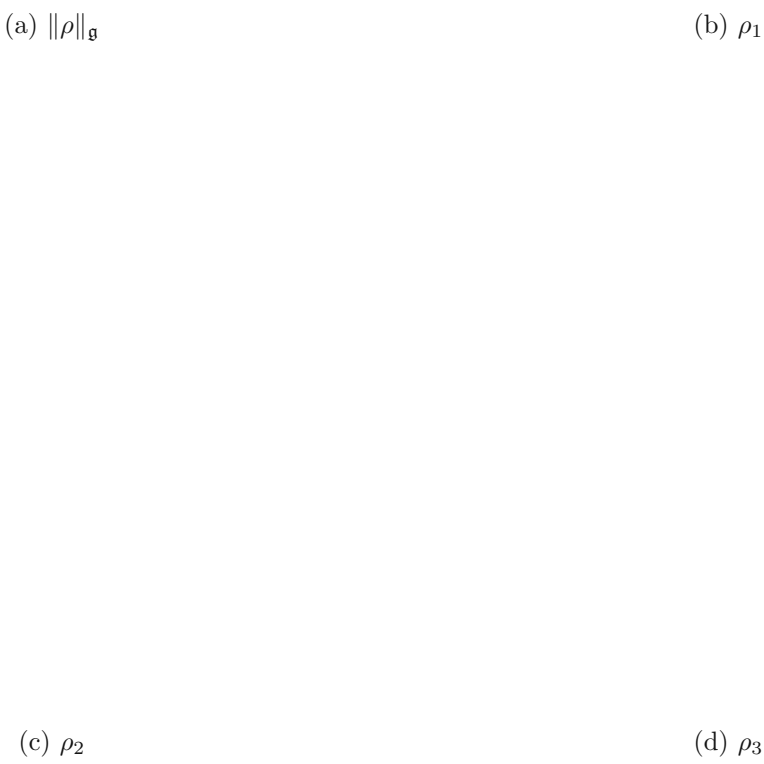

(a) $\|\rho\|_{\mathfrak{g}}$ (b) $\rho_1$

(c) $\rho_2$ (d) $\rho_3$

Figure 4.4: An illustration of the parallel transport for a gaussian charge distribution $\rho$ on a coarse mesh with a wind $u$ going clockwise. Blue and red correspond to vanishing and high values respectively. All links $U$ except for one are trivially set to the identity $\mathbb{1}$. This single link couples color components $\rho_1$ and $\rho_2$. It is visible that the overall norm $\|\rho\|_{\mathfrak{g}}$ as a distribution almost evolves as if being simply carried by the wind (with some numerical artifacts).

The discrete connection is represented by parallel transporters consisting of Lie group-valued functions $(U_{T_{n-1}})_{T_{n-1}\in\mathcal{S}_{n-1}}$ on codimension 1-simplices. They may be parametrized via similar Lie algebra-valued functions $(\mathcal{A}_{T_{n-1}})_{T_{n-1}\in\mathcal{S}_{n-1}}$ using the exponential map $U_{T_{n-1}} = \exp\{\mathcal{A}_{T_{n-1}}\}$. The values $\mathcal{A}_{T_{n-1}}$ can loosely be interpreted as gauge field components perpendicular to the element interface $T_{n-1} \in \mathcal{S}_{n-1}$. The simulation of color current $\mathcal{J}$ fluxes through these interfaces makes use of respective upwind values $\hat{\mathcal{J}}_{T_{n-1}}$. It therefore

(a) $\|\rho\|_{\mathfrak{g}}$ (b) $\rho_1$

(c) $\rho_2$ (d) $\rho_3$

Figure 4.5: An illustration of the parallel transport for a gaussian charge distribution $\rho$ on a coarse mesh with a wind $u$ going clockwise. Blue and red correspond to vanishing and high values respectively. All links $U$ except for the ones associated to one element are trivially set to the identity $\mathbb{1}$. However, these non-trivial links are generated by means of a gauge transformation on that particular element. This setting is therefore physically equivalent to a trivial connection. It is visible that the overall norm $\|\rho\|_{\mathfrak{g}}$ as a distribution evolves as if being simply carried by the wind. The exact color components themselves are gauge dependent.

is a natural idea to pair $\mathcal{A}_{T_{n-1}}$ with the normal flux of $\hat{\mathcal{J}}_{T_{n-1}} \cdot \hat{n} = \left(\hat{\mathcal{J}}_{T_{n-1}}\right)_{\hat{n}}$ at the element interface $T_{n-1}$.

$$\int_{T_{n-1}} \langle \left(\hat{\mathcal{J}}_{T_{n-1}}\right)_{\hat{n}}, \mathcal{A}_{T_{n-1}} \rangle_{\mathfrak{g}}$$

While it is slightly concerning, that $\mathcal{A}$ in this case does not follow a suitable transformation behaviour and that this coupling term is therefore not gauge symmetric, we note that this is also an issue in LGT and the continuum [5]. The entire dual Wilson action including these terms in three dimensions then takes on the form of

$$S_{W^*}^{(\mathrm{FEM})} = \sum_{E,E' \in \mathcal{S}_1} C_{EE'} \langle \ln W_E, \ln W_{E'} \rangle_{\mathfrak{g}} + \sum_{F \in \mathcal{S}_2} \int_F \langle \left( \hat{\mathcal{J}}_F \right)_{\hat{n}}, \mathcal{A}_F \rangle_{\mathfrak{g}}. \tag{4.20}$$

Applying mass-lumping and approximating the logarithm we settle upon the action

$$S_{W^*}^{(\mathrm{FEM})} = \sum_{E \in \mathcal{S}_1} C_{EE'} \langle \mathbb{1} - W_E, \mathbb{1} - W_E \rangle_{\mathfrak{g}} + \sum_{F \in \mathcal{S}_2} \int_F \langle \left( \hat{\mathcal{J}}_F \right)_{\hat{n}}, \mathcal{A}_F \rangle_{\mathfrak{g}}. \tag{4.21}$$

## 4.7 Discrete Yang-Mills Equations for Dual Wilson Action

Using a discrete connection comparable to that in Regge calculus with a modified Wilson action as in 4.21, the corresponding discrete Yang-Mills equations can be obtained by means of variation. In this section we discuss this for the mass-lumped approximation corresponding to equation 4.11 with current source terms described in section 4.6. Following the notation and calculation in section 6.6 of the appendix, we obtain the equations in 6.9

$$\sum_{B : U_I \in W_B} 2C_{BB} (-1)^{\sigma(W_B, U_I)} \operatorname{Re} \operatorname{Tr} \{ t_a W_B \} = \operatorname{Re} \operatorname{Tr} \left\{ t_a \int_I \left( \hat{\mathcal{J}} \right)_{\hat{n}} \right\}$$

where $W_B$ refers to the plaquette around a bone $B$, $C_{BB}$ stands for the respective weight and $I$ is an interface between elements where the parallel transporter $U_I$ resides.

As done before we would like to split these equations into spatial and temporal parts for time stepping simulations. For illustrational purposes, we now settle on a mesh with two spatial and one temporal dimension. In a time stepping simulation where the spatial mesh remains static, links $U$ can be classified as either spatial or temporal. Hence depending on whether $U_I$ belongs to a temporal or spatial interface $I$, we obtain two qualitatively different cases of equations.

### Variation with Respect to Temporal $U$ - Gauss Constraint

We write down the variation with respect to temporal parallel transporters $U_I$ belonging to an interface $I$ between the virtually identical cells $T^+, T^-$ in successive time steps. In temporal gauge the plaquettes $W_E$ around spatial edges of interest $E$ reduce to the product of new spatial $U_F^+$ and old spatial links $U_F^-$ where $F$ is the space-time face spanned by the edge $E$ as well as the temporal direction. In this variation with respect to temporal parallel transporters $U_T$ the orientation of the plaquettes will always start by looping forward in time and out of the element $T$. We therefore add an index $T$ as in $W_E^T$ to avoid orientation ambiguity.

$$W_E^T := \begin{cases} U_E^+ (U_E^-)^\dagger & \text{if } U_E \text{ points out of } T \\ (U_E^+)^\dagger U_E^- & \text{if } U_E \text{ points into } T \end{cases}$$

The thus obtained equation

$$\sum_{E : U_I \in W_E} 2C_{EE} \operatorname{Re} \operatorname{Tr} \{ t_a W_E^T \} = \operatorname{Re} \operatorname{Tr} \left\{ t_a \int_T \rho \right\} \tag{4.22}$$

is referred to as the Gauss constraint, as it represents the analogue to Gauss' law in electrodynamics: the sources of electric fields (or in this case temporal plaquettes $W_E^T$) are given by charges $\rho$. This is visualized in figure 4.6.

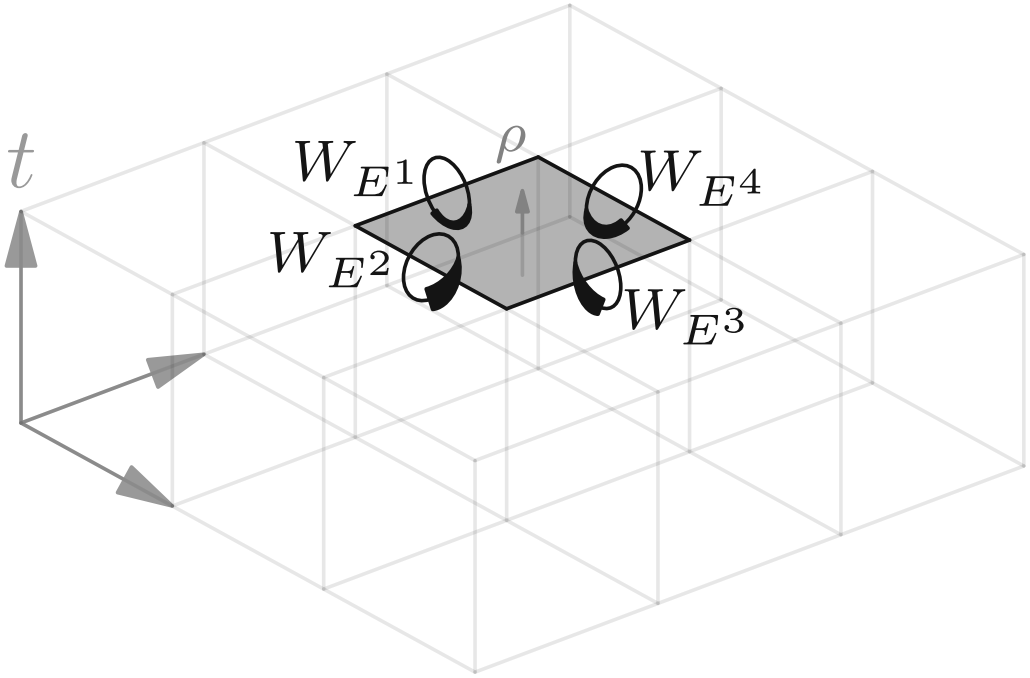


Figure 4.6: A section of a three dimensional lattice where the vertical direction represents time and the horizontal mesh corresponds to one time-slice. The Gauss constraint obtained in the variation with respect to a temporal parallel transporter $U_I$ that connects to the later time-slice involves all connected temporal plaquettes $(W_{E^k})_{k=1,2,3,4}$ as well as the charge $\rho$. This therefore is an equation involving parallel transporters from two successive time-slices.

### Variation with Respect to Spatial $U$ - Time Stepping Equation

Continuing with the variation with respect to spatial parallel transporters $U_I$, we can then rearrange the equations such that the new links in the next time-slice are expressed in terms of the old ones.

$$\sum_{E':U_F\in W_{E'}} C_{E'E'}(-1)^{\sigma(W_{E'},U_F)}\,\mathrm{Re\,Tr}\{t_a W_{E'}\} = \mathrm{Re\,Tr}\left\{t_a \int_F \left(\hat{j}\right)_{\hat{n}}\right\} \tag{4.23}$$

$$\sum_{E':U_F\in W_{E'}} C_{E'E'}(-1)^{\sigma(W_{E'},U_F)}(W_{E'})_a = \int_F \left(\hat{j}\right)_{\hat{n},a} \tag{4.24}$$

$$(W_{E^+})_a = \frac{1}{C_{E^+E^+}} \sum_{E'\in\{E^-,E^l,E^r\}} C_{E'E'}(-1)^{\sigma(W_{E'},U_F)}(W_{E'})_a + \int_F \left(\hat{j}\right)_{\hat{n},a} \tag{4.25}$$

$(-1)^{\sigma(W_{E^+},U_F)} = -1$ in this case leads to the cancellation of the global sign on the right side. These equations may be used in principle to perform time stepping simulations as illustrated in figure 4.7.

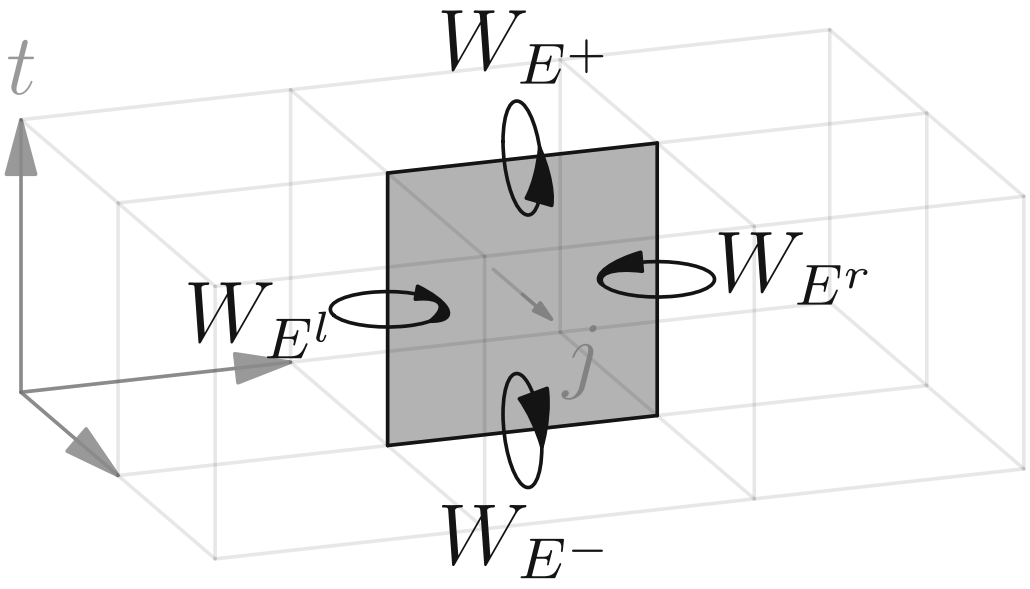


Figure 4.7: A section of a three dimensional lattice where the vertical direction represents time and the horizontal mesh corresponds to one time-slice. The discrete equations of motion obtained in the variation with respect to a spatial parallel transporter $U_I$ that connects two elements in one time-slice involves all connected plaquettes $W_{E^+}, W_{E^l}, W_{E^r}, W_{E^-}$ and the charge current $j$. They can be rearranged to express $W_{E^+}$ containing new link variables from the later time-slice in terms of old link variables in $W_{E^l}, W_{E^r}$ and $W_{E^-}$. In other words, they represent a time stepping procedure.

For more details in an $SU(2)$ implementation see section 6.6.1 in the appendix. In figure 4.8 we give an example for the energy densities obtained during a time stepping simulation using the dual LGT formulation.

## 4.8 Interpolation of Gauge Field $\mathcal{A}$

In order to approximate continuous gauge fields $\mathcal{A} \in \Lambda^1(M;\mathfrak{g})$ we require means to interpolate them using discrete parallel transporters $U \in G$. A link between the two is established by the parallel transport equation, which can be solved using the path ordered exponential 2.13

$$\begin{aligned} U(t) &= \mathcal{P}\left\{\exp\left\{\int_0^t \mathcal{A}(\dot\gamma(t'))\mathrm{d}t'\right\}\right\} \\ &:= \sum_{n=0}^{\infty}\int_0^1\int_0^{t'_n}\int_0^{t'_{n-1}}\cdots\int_0^{t'_2}\mathcal{A}(\dot\gamma(t'_n))\cdots\mathcal{A}(\dot\gamma(t'_1))\mathrm{d}t'_1\cdots\mathrm{d}t'_n \end{aligned}$$

along a given curve $\gamma$. In our discretization with a mesh, we seek parallel transporters $U_{TT'}$ that carry objects between different elements $T$ and $T'$. One choice therefore is to define $U_{TT'}$ as the path ordered exponential

$$U_{TT'} = \mathcal{P}\left\{\exp\left\{\int_{\gamma_{TT'}}\mathcal{A}\right\}\right\} = \mathcal{P}\left\{\exp\left\{\int_0^1\mathcal{A}(\dot\gamma_{TT'}(t))\mathrm{d}t\right\}\right\}$$

going between element barycenters as illustrated in figure 4.9. In practical terms, we will settle on substituting the path ordered exponential with a regular integral exponential

$$U_{TT'} = \mathcal{P}\left\{\exp\left\{\int_{\gamma_{TT'}}\mathcal{A}\right\}\right\} \simeq \exp\left\{\int_{\gamma_{TT'}}\mathcal{A}\right\} \tag{4.26}$$

which is easy to compute and serves as an approximation for small curve lengths and nearly constant $\mathcal{A}$.

(a) $\mathcal{H}_{\mathcal{B}}$ (b) $\mathcal{H}_{\mathcal{E}}$

Figure 4.8: Illustration of a simulation involving the dual LGT approach on a coarse two-dimensional lattice. Blue and red correspond to vanishing and high values respectively. Figures 4.8a and 4.8b visualize the magnetic and electric energy densities $\mathcal{H}_{\mathcal{B}}$ (associated to vertices) and $\mathcal{H}_{\mathcal{E}}$ (associated to dual edges), respectively, calculated from the distributional connection interpolated in finite element spaces. The initial conditions are given by a single non-trivial plaquette variable in the center of the domain.

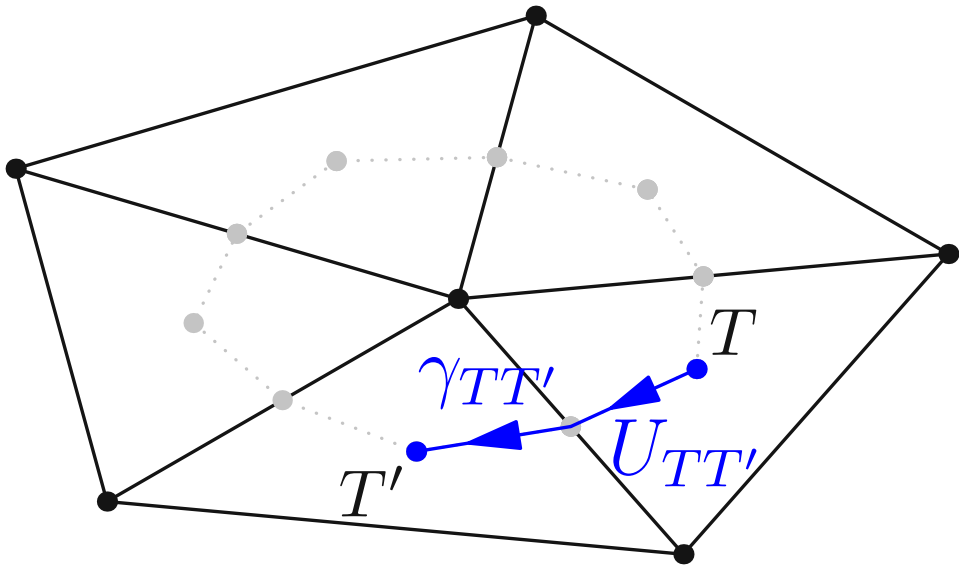


Figure 4.9: Visualization of a vertex patch in black and its barycentric dual lattice in grey. The blue curve $\gamma_{TT'}$ along the dual lattice connecting barycenters of elements $T$ and $T'$ is used to define the parallel transporter $U_{TT'}$ by means of the path ordered exponential.

## 4.9 Gauss Constraint

### Initial Conditions fulfilling Gauss constraint

In an electromagnetic time stepping simulation, the initial electric field $E := -\partial_t A$ that satisfies Gauss' law $\nabla \cdot E = \rho$ needs to be included in the initial conditions in addition to $A$ and $\rho$ itself. In direct analogy, we

seek here adequate initial conditions by prescribing spatial gauge links in the first and second time-slices as well as the initial spatial charge. However, these have to be compatible in terms of the Gauss constraint for each element $T \in \mathcal{S}$ in 4.22

$$\sum_{E \in \partial T} C_{EE} 2 \operatorname{Re} \operatorname{Tr}\{t_a W_E^T\} = \operatorname{Re} \operatorname{Tr}\left\{ t_a \int \rho^- \right\} \quad \forall T \in \mathcal{S}.$$

The set of links in two successive time-slices, obtained from the approximate interpolation of continuous gauge fields $\mathcal{A}$, as described in section 4.8, are not guaranteed to satisfy this equation. After fixing spatial gauge links $U_I^-$ and spatial charge density $\rho^-$ in the first time-slice we will try to construct gauge links $U_I^+$ in the next time-slice in accordance to equation 4.22 as close as possible to interpolated $\mathcal{A}$ fields in the next time-slice.

Just as in the case of the electromagnetic Gauss' law ($\nabla \cdot E = \rho$), the Gauss constraint has in general no unique solution. This can also be understood on a two-dimensional mesh: the number of elements (triangles) which represent $\rho$'s degrees of freedom are in general different from the number of interfaces (edges) which represent the plaquettes $W_E$ degrees of freedom, yielding a non-square system of equations. Guessing the correct initial conditions that satisfy the non-linear Gauss constraint for a given charge distribution is a challenge. Instead of specifying initial conditions directly, we will pursue an iterative approach in which we approximate them.

With fixed $U_E^-$ and $\rho$, we first specify some initial conditions for $U_E^+$ as a first guess via the interpolation procedure outlined in section 4.8. The iterative method should proceed in small steps to modify the links in the later time step $U_E^+$ to incrementally fix the Gauss constraint. We formulate this goal as a minimization problem of the function $L[U_E^+, U_E^-]$

$$L[U_E^+, U_E^-] = \sum_T \sum_a \left(G_a^T\right)^2 \tag{4.27}$$

$$G_a^T = \sum_{E \in \partial T} C_{EE} 2 \operatorname{Re} \operatorname{Tr}\{t_a W_E^T\} - \int_T \rho_a^- \tag{4.28}$$

which measures the quadratic error of the total Gauss constraint violation. In order to implement a Newton-type method, we evaluate the group derivative of this function $\delta_{\mathcal{A}_{E'}} L[W_E]$ with respect to a perturbation of the parallel transporter $U_{E'} = \exp\{\mathcal{A}_{E'}\}$ associated to a particular edge $E'$ in the appendix 6.7.2. Based on this, the $U_{E'}$ group element's update in the form of

$$U_{E'} \to e^{-\varepsilon \delta_{\mathcal{A}'_{E'}} L[W_E] \mathcal{A}'_{E'}} U_{E'}$$

with stepping parameter $\varepsilon \ll 1$ may be applied. In practice, the directions may be chosen by specifying generators $\mathcal{A}' \in (t_a)_{a=1,\dots,\dim \mathfrak{g}}$ performing a combined update of the form

$$U_{E'} \to e^{-\varepsilon \sum_{a=1}^{\dim \mathfrak{g}} \delta_{t_a} L[W_E] t_a} U_{E'}.$$

### Conservation of Gauss-constraint through time

As noted before, the Gauss constraint 4.22 represents the non-Abelian analogue of charge conservation of the mass-lumped dual Wilson action 4.11. In a time stepping simulation and a static mesh where initial conditions in the first time-slice satisfy this property, one can show that it is further fulfilled down the line in future time-slices. While it is in principle possible to demonstrate this algebraically in terms of expressions, it is more straight forward and insightful to manipulate loop expressions on the **dual mesh** (or in other words, the mesh present in standard lattice gauge theory) symbolically. In 2+1 dimensions this means that parallel transporters and (space-time-)currents are associated to mesh edges. The proof involving symbolic manipulations of plaquettes in the appendix 6.7.3 is independent of the exact spatial mesh geometry as well as individual plaquette weights $C_{EE}$.

## 4.10 Dual LGT-FEM Simulation - Proof of Concept

We now summarize and combine all the aspects introduced in section 4 to propose a proof-of-principle simulation method that exhibits both gauge symmetry in the LGT sense and discrete charge conservation in the form of the Gauss constraint. More specifically, we focus on the scenario of a moving particle wavefront in two spatial and one time dimension, whose direction and speed of propagation are fixed and which "drags" along the gauge field. We neglect any recoil forces the gauge field exerts on the particles, similar to [40] and [31]. The evolution of said particles can be then described using a wind vector field $u$ as well as parallel transport with regard to the continuously changing connection.

### Method Summary

- We fix a particular gauge group $G = SU(N)$ defined in section 6.3.1 which represents color symmetry gauge transformations of the Yang-Mills theory.
- We consider a two-dimensional spatial domain $M_S$ and look at the space-time manifold given by $M = I_t \times M_S$ where $I_t \subset \mathbb{R}$ is the time interval of interest. With a triangulation (mesh) of $M_S$ and a constant time stepping parameter $\tau \ll 1$ we generate a triangulation of the space-time manifold consisting of virtually identically meshed time-slices. The associated (generalized) simplicial complex is $\mathcal{S}(M)$.
- As in Regge Calculus described in section 2.11, we define the discrete distributional connection on codimension-1-simplices $F \in \mathcal{S}_2(M)$ (or faces in $2+1$ dimensions) as $SU(N)$-valued parallel transporters $(U_F)_{F\in\mathcal{S}_2(M)}$ connecting two elements. Each $U_F \in G$ will be parametrized by a Lie algebra element $\mathcal{A}_F \in \mathfrak{g}$ using the exponential map $U_F = \exp\{\mathcal{A}_F\}$. Each parallel transporter $U_F$ will be assumed to be sufficiently close to the identity $\mathbb{1} \in G$. We will be exclusively assuming temporal gauge, where all parallel transporters in the time direction are set to the identity $\mathbb{1} \in G$. Therefore the degrees of freedom are represented by all spatial links for each time-slice $t$ which we shall denote as $(U_F)_{F\in\mathcal{S}_2(M)_t}$.
- The direction of particle propagation will be given by a temporally static wind vector field $u \in \Lambda^1(M_S)$.
- We define the charge distribution $\rho \in L^2(M;\mathfrak{g})$ as a discontinuous Lie algebra-valued function. $\left(\left(\hat{\mathcal{J}}_F\right)_{\hat{n}}\right)_{F\in\mathcal{S}_2(M)}$ refers to the flux density $\left(\hat{\mathcal{J}}_F\right)_{\hat{n}} = \rho u^k n_k$ passing through the codimension-1-simplex $F$ connecting two elements.
- We approximate the Yang-Mills action in definition 44 with the dual Wilson action including charge current source terms defined in equation 4.21 with approximations involving mass-lumping and Taylor expansion of the logarithm $\ln W \simeq \mathbb{1} - W$.
- By variation with respect to temporal parallel transporters we obtain the Gauss constraint in equation 4.22 - the discrete analogue to Gauss' law.
- Variation with respect to spatial parallel transporters yields equations of motion 4.25 for the time-slice-wise distributional connection $(U_F)_{F\in\mathcal{S}_2(M)_t}$. These preserve the Gauss constraint over time.
- The time evolution of the charge density $\rho$ follows the charge conserving explicit Euler time-discretization of the DG-assisted parallel transport equation 4.19 discussed in section 4.5.

### Preparing the Simulation

The initial steps for setting up a simulation are:

### Continuous Initial Conditions

The initial conditions for the particle wavefront are given by an initial charge density $\rho(t=0) \in L^2(M_S;\mathfrak{g})$, a wind vector field $u \in \Lambda^1(M_S)$ as well as the initial gauge field $\mathcal{A}(t=0) \in \Lambda^1(M_S;\mathfrak{g})$ and its electric fields $\mathcal{E}(t=0) = -\partial_t \mathcal{A}(t=0) \in \Lambda^1(M_S;\mathfrak{g})$. These should satisfy the generalized Gauss law $\mathrm{div}_{\mathcal{A}}\mathcal{E} = \rho$ in the continuum.

### Interpolating Continuous Initial Conditions

The continuous charge $\rho(t=0) \in L^2(M_S;\mathfrak{g})$ may be interpolated using standard FEM into discrete $L^2$-spaces of higher order. The initial gauge field $\mathcal{A}(t=0) \in \Lambda^1(M_S;\mathfrak{g})$ on the other hand will be interpolated using (an approximation of) the path ordered exponential defined in equation 4.26 as described in section 4.8 to obtain a distributional connection $(U_F)_{F\in\mathcal{S}_2(M)_0}$. The same procedure can be applied for gauge field in the next time-slice using $\mathcal{A}(t=\tau) \simeq \mathcal{A}(t=0) + \tau\partial_t\mathcal{A}(t=0)$ to set the connection $(U_F)_{F\in\mathcal{S}_2(M)_\tau}$.

### Fixing the Gauss Constraint

As the Interpolation procedure is not guaranteed to yield variables that satisfy the Gauss constraint exactly, we manually perform corrections by using a gradient descent method described in section 4.9.

## Running the Simulation

The overall time-stepping procedure splits itself into two successive and repeating steps associated to updates of the charge distribution $\rho_t \in L^2(M_S;\mathfrak{g})$ and the distributional connection $(U_F)_{F\in\mathcal{S}_2(M)_t}$ at times $t \in I_t$.

### $\rho$ Time Step - DG-assisted Parallel Transport

Based on the present charge $\rho_{t-\tau}$ and distributional connection $(U_F)_{F\in\mathcal{S}_2(M)_{t-\tau}}$, it is updated towards $\rho_t$ by using 4.19 of section 4.5

$$\int_T \langle \rho_t, \phi\rangle_{\mathfrak{g}} \quad = \int_T \langle \rho_{t-\tau}, \phi\rangle_{\mathfrak{g}} + \tau \quad \int_T u^k \langle \rho_{t-\tau}, \partial_k\phi\rangle_{\mathfrak{g}} - \tau \int_{\partial T} n_k u^k \langle \hat{\rho}_{t-\tau}, \phi\rangle_{\mathfrak{g}} \quad \forall \phi \in L^2(M;\mathfrak{g}), T \subset \mathcal{S}(M)$$

where we note the modified up-winding scheme in equation 4.15 compatible with parallel transport

$$(\hat{\rho})_T = \begin{cases} \rho_T & u^k(n_T)_k \geq 0 \\ \mathrm{Ad}_{U_{T'T}}\rho_{T'} & u^k(n_T)_k < 0 \end{cases}. \tag{4.29}$$

### $U$ Time Step - Discrete Yang-Mills Equations of Motion

Based on the present charge $\rho_t$ and distributional connections of the two latest time-slices $(U_F)_{F\in\mathcal{S}_2(M)_{t-\tau}}$ and $(U_F)_{F\in\mathcal{S}_2(M)_t}$, update the connection towards $(U_F)_{F\in\mathcal{S}_2(M)_{t+\tau}}$ by reconstructing $U_{F^+}$ for a particular face $F^+ \in \mathcal{S}_2(M)_{t+\tau}$ from $W_{E^+}$ in equation 4.25 of section 4.7

$$(W_{E^+})_a = \frac{1}{C_{E^+E^+}} \sum_{E'\in\{E^-,E^l,E^r\}} C_{E'E'}(-1)^{\sigma(W_{E'},U_F)}(W_{E'})_a + \int_F \left(\hat{j}\right)_{\hat{n},a}$$

where $W_E$ are suitable plaquette variables associated to the edges $E$ of $F \in \mathcal{S}_2(M)_t$.

# 5 Conclusion, Summary and Outlook

In this work we evaluated, analyzed and constructed discretizations for non-Abelian gauge theories. Simulations involving Lie algebra-valued exterior finite elements in a standard FEM variational formulation as described in section 3.3 exhibited neither charge conservation nor gauge symmetry. In particular it was observed, that at any point where different color components come into contact, charge violations became visible. The application of gauge transformations also created such unwanted defects. These did not seem to scale linearly with the amplitude of the fields initial conditions. All in all, only one particular scenario involving the collision of two flux-tubes was studied. Further investigation may help to quantify the above mentioned violations more generally.

The transition from the exterior derivative d in electromagnetism to the gauge-covariant derivative $\mathrm{d}_{\mathcal{A}} = \mathrm{d} + [\mathcal{A}, \cdot]$ in definition 43 generates non-linear field terms such as $[\mathcal{A}, \mathcal{A}]$. The property of the exterior derivative $\mathrm{d} \circ \mathrm{d} = 0$ can be generalized to $\mathrm{d}_{\mathcal{A}} \circ \mathrm{d}_{\mathcal{A}} = [\mathcal{F} \wedge \cdot]$. The latter forms the basis for the non-Abelian continuity equation in definition 46. In section 3.2 we mentioned that a discretization using exterior finite elements does not preserve this property $\mathrm{d}_{\mathcal{A}} \circ \mathrm{d}_{\mathcal{A}} = [\mathcal{F} \wedge \cdot]$ due to non-linearities. Furthermore, no generalization of Stokes' theorem for Lie algebra-valued forms is presently known. Finding a chain of suitable discrete spaces that are compatible with the gauge-covariant derivative $\mathrm{d}_{\mathcal{A}} = \mathrm{d} + [\mathcal{A}, \cdot]$, hence becomes a challenge. This and the difficulties noted during section 4.1 in constructing Lie group-valued finite element functions, that are self-consistent with respect to the group multiplication, seem to limit the use of higher order FEM if symmetries are to be preserved.

In order to construct a charge conserving and gauge symmetric discretization in section 4 we took inspiration from the literature. We analyzed Regge calculus [47], the works of Christiansen and Halvorsen et al. [14] [27] and reinterpreted LGT [22] on a dual lattice. This enabled the formulation of a dual Wilson action in equation 4.20 where the gauge field was replaced by a distributional connection living on codimension-1-simplices - similar to Regge calculus. With the approximations of the logarithm and mass-lumping we derive discrete Yang-Mills equations 6.9 by means of variation in section 6.6 that are intrinsically gauge symmetric. In section 6.7.3 we demonstrated that these equations are charge conserving in a discrete sense: the time stepping equations 4.25 preserve the so-called "Gauss constraint" equation 4.22. Future work may be directed towards extending these ideas and proofs to the cases without mass-lumping (with coupling between distinct plaquettes) and the full logarithm. A numerical comparison between discretizations involving standard FEM, LGT and the dual LGT formulation mentioned here is yet to be done.

Even though, the order of the distributional connection could not be raised in some sense (only one constant parallel transporter per element interface), this formulation enabled the use of charges with arbitrarily high order as described in section 4.5. In particular, using a modified up-winding mechanism in combination with discontinuous $L^2$-function spaces, a parallel transport equation with local charge conservation per element was formulated in equation 4.16. The resulting continuous charges and currents may be integrated over codimension-1-simplices in order to couple them to the distributional connection as in section 4.6.

To summarize, we were able to formulate a simulation method in section 4.10 that uses elements from both LGT and FEM and has desired symmetries. A complete numerical implementation and further tests to compare how this method fares against standard LGT and FEM are aspects for future work.

# 6 Appendix

## 6.1 Differential Forms in Index Notation

### Wedge Product

The wedge product $\omega \wedge \phi$ of a $k$-form $\omega \in \Lambda^k(M)$ and $l$-form $\phi \in \Lambda^l(M)$ in definition 2.1 can be represented in coordinates via antisymmetrization

$$(\omega \wedge \phi)_{\mu_1 \dots \mu_{k+l}} = \frac{1}{k!l!} \delta^{\nu_1 \dots \nu_k \lambda_{k+1} \dots \lambda_{k+l}}_{\mu_1 \dots \mu_{k+l}} \omega_{\nu_1 \dots \nu_k} \phi_{\lambda_{k+1} \dots \lambda_{k+l}}$$

using the generalized Kronecker symbol defined as

$$\delta^{\mu_1 \mu_2 \dots \mu_k}_{\nu_1 \nu_2 \dots \nu_k} := \begin{vmatrix} \delta^{\mu_1}_{\nu_1} & \delta^{\mu_2}_{\nu_1} & \dots & \delta^{\mu_k}_{\nu_1} \\ \delta^{\mu_1}_{\nu_2} & \delta^{\mu_2}_{\nu_2} & \dots & \delta^{\mu_k}_{\nu_2} \\ \dots & \dots & \dots & \dots \\ \delta^{\mu_1}_{\nu_k} & \dots & \dots & \delta^{\mu_k}_{\nu_k} \end{vmatrix} \quad \delta^{\alpha}_{\beta} = \begin{cases} 1 & \alpha = \beta \\ 0 & \alpha \neq \beta \end{cases} . \tag{6.1}$$

It may sometimes be useful to write it down alternatively

$$\delta^{\mu_1 \mu_2 \dots \mu_k}_{\nu_1 \nu_2 \dots \nu_k} = \varepsilon^{\mu_1 \mu_2 \dots \mu_k} \varepsilon_{\nu_1 \nu_2 \dots \nu_k}$$

using the Levi Civita symbol $\varepsilon_{\mu_1 \mu_2 \dots \mu_k}$

$$\varepsilon_{\mu_1 \mu_2 \dots \mu_k} = \begin{cases} 1 & \mu_1 \mu_2 \dots \mu_k \text{ even} \\ -1 & \mu_1 \mu_2 \dots \mu_k \text{ odd} \\ 0 & \mu_1 \mu_2 \dots \mu_k \text{ else} \end{cases} \tag{6.2}$$

The lower and upper position of the indices are essential when dealing with components of tensors in spacetime.

### Inner Product

The inner product in definition 5 can be translated into index notation using a formula of the metric rewritten in terms of orthonormal basis $(E_{(\alpha)})_{\alpha=1,\dots,d} \subset TM$ and respective cobasis $(e_{(\alpha)})_{\alpha=1,\dots,d} \subset TM^*$

$$g^{-1} = \sum_{(\alpha)=1}^{d} E_{(\alpha)} E_{(\alpha)} \quad g = \sum_{(\alpha)=1}^{d} e_{(\alpha)} e_{(\alpha)}$$

Using components of the basis vectors $(E^{\mu}_{(\alpha)})_{\alpha=1,\dots,d}$ and forms $\omega_{\mu_1 \dots \mu_k}$, $\omega_{\nu_1 \dots \nu_k}$ we can rewrite the expression in a compact form

$$\begin{aligned} &\sum_{\alpha_1=1}^{d} \dots \sum_{\alpha_k=1}^{d} \omega(E_{(\alpha_1)}, \dots, E^{\mu}_{(\alpha_k)}) \phi(E_{(\alpha_1)}, \dots, E(\alpha_k)) = \\ &= \sum_{\alpha_1=1}^{d} \dots \sum_{\alpha_k=1}^{d} \frac{1}{k!} \omega_{\mu_1 \dots \mu_k} E^{\mu_1}_{(\alpha_1)} \dots E^{\mu_k}_{(\alpha_k)} \frac{1}{k!} \phi_{\nu_1 \dots \nu_k} E^{\nu_1}_{(\alpha_1)} \dots E^{\nu_k}_{(\alpha_k)} = \\ &= \frac{1}{(k!)^2} \omega_{\mu_1 \dots \mu_k} \phi_{\nu_1 \dots \nu_k} \left( \sum_{\alpha_1=1}^{d} E^{\mu_1}_{(\alpha_1)} E^{\nu_1}_{(\alpha_1)} \right) \dots \left( \sum_{\alpha_k=1}^{d} E^{\mu_k}_{(\alpha_k)} E^{\nu_k}_{(\alpha_k)} \right) = \\ &= \frac{1}{(k!)^2} \omega_{\mu_1 \dots \mu_k} \phi_{\nu_1 \dots \nu_k} g^{\mu_1 \nu_1} \dots g^{\mu_k \nu_k} = \frac{1}{(k!)^2} \omega_{\mu_1 \dots \mu_k} \phi^{\mu_1 \dots \mu_k}. \end{aligned}$$

### Hodge Star Operator

The Hodge star operator in definition 6 corresponding to the Riemannian metric's volume form in 2.1.1 can be evaluated in component index notation as

$$\int_M \langle \star\omega, \phi\rangle = \int_M \omega \wedge \phi$$
$$\int_M \langle \star\omega, \phi\rangle \mathrm{Vol} = \int_M \omega \wedge \phi$$
$$\langle \star\omega, \phi\rangle \mathrm{Vol} = \omega \wedge \phi$$
$$(\star\omega)_{\mu_1\dots\mu_{n-k}}\phi^{\mu_1\dots\mu_{n-k}}\frac{1}{\sqrt{|g|}}\varepsilon_{\nu_1\dots\nu_n} = \frac{1}{k!(n-k)!}\delta^{\alpha_1\dots\alpha_k\beta_1\dots\beta_{n-k}}_{\nu_1\dots\nu_n}\omega_{\alpha_1\dots\alpha_k}\phi_{\beta_1\dots\beta_{n-k}}$$
$$(\star\omega)_{\mu_1\dots\mu_{n-k}}\phi^{\mu_1\dots\mu_{n-k}}\frac{1}{\sqrt{|g|}}\varepsilon_{\nu_1\dots\nu_n} = \frac{1}{k!(n-k)!}\varepsilon^{\alpha_1\dots\alpha_k\beta_1\dots\beta_{n-k}}\varepsilon_{\nu_1\dots\nu_n}\omega_{\alpha_1\dots\alpha_k}\phi_{\beta_1\dots\beta_{n-k}}$$
$$(\star\omega)_{\mu_1\dots\mu_{n-k}}\phi^{\mu_1\dots\mu_{n-k}} = \frac{1}{k!(n-k)!}\sqrt{|g|}\varepsilon^{\alpha_1\dots\alpha_k\beta_1\dots\beta_{n-k}}\omega_{\alpha_1\dots\alpha_k}\phi_{\beta_1\dots\beta_{n-k}}$$
$$(\star\omega)_{\mu_1\dots\mu_{n-k}}\phi^{\mu_1\dots\mu_{n-k}} = \frac{1}{k!(n-k)!}\sqrt{|g|}\varepsilon^{\alpha_1\dots\alpha_k}{}_{\mu_1\dots\mu_{n-k}}\omega_{\alpha_1\dots\alpha_k}\phi^{\mu_1\dots\mu_{n-k}}$$

$$\Rightarrow \star\omega = \frac{1}{k!(n-k)!}\sqrt{|g|}\varepsilon^{\mu_1\dots\mu_k}{}_{\mu_{k+1}\dots\mu_n}\omega_{\mu_1\dots\mu_k}\mathrm{d}x^{\mu_{k+1}}\wedge\dots\wedge\mathrm{d}x^{\mu_n}$$

where $\varepsilon_{\mu_1\dots\mu_n}$ is the fully antisymmetric permutation Levi-Civita symbol 6.2.

## 6.2 Non-Abelian Gauge Theories in Index Notation

In order to translate objects in the context of non-Abelian gauge theories into index notation we decompose Lie algebra-valued forms using generators $\mathrm{d}x^\mu \otimes \tau_m$ consisting of differentials $(\mathrm{d}x^\mu)_{\mu=1,\dots,\dim M}$ and the Lie algebra basis $(\tau_k)_{k=1,\dots,\dim\mathfrak{g}}$.

$$\mathcal{J} = \mathcal{J}_\mu \mathrm{d}x^\mu = J^m_\mu \mathrm{d}x^\mu \otimes \tau_m$$
$$\mathcal{A} = \mathcal{A}_\mu \mathrm{d}x^\mu = A^m_\mu \mathrm{d}x^\mu \otimes \tau_m$$
$$\mathcal{F} = \frac{1}{2}\mathcal{F}_{\mu\nu}\mathrm{d}x^\mu\wedge\mathrm{d}x^\nu = \frac{1}{2}F^m_{\mu\nu}(\mathrm{d}x^\mu\wedge\mathrm{d}x^\nu)\otimes\tau_m$$

The components $F^a_{\mu\nu}$ can also be written down using $A^a_\mu$

$$\begin{aligned}
\mathcal{F} &= \mathrm{d}\mathcal{A} + \frac{1}{2}[\mathcal{A}\wedge\mathcal{A}] = \\
&= \frac{1}{2}\delta^{\mu\nu}_{\alpha\beta}\partial_\mu A^c_\nu(\mathrm{d}x^\alpha\wedge\mathrm{d}x^\beta)\otimes\tau_c + \frac{1}{2}[A^a_\alpha\mathrm{d}x^\alpha\otimes\tau_a\wedge A^b_\beta\mathrm{d}x^\beta\otimes\tau_b] = \\
&= \frac{1}{2}\delta^{\mu\nu}_{\alpha\beta}\partial_\mu A^c_\nu(\mathrm{d}x^\alpha\wedge\mathrm{d}x^\beta)\otimes\tau_c + \frac{1}{2}A^a_\alpha A^b_\beta\mathrm{d}x^\alpha\wedge\mathrm{d}x^\beta\otimes[\tau_a,\tau_b] = \\
&= \frac{1}{2}\delta^{\mu\nu}_{\alpha\beta}\partial_\mu A^c_\nu(\mathrm{d}x^\alpha\wedge\mathrm{d}x^\beta)\otimes\tau_c + \frac{1}{2}A^a_\alpha A^b_\beta\mathrm{d}x^\alpha\wedge\mathrm{d}x^\beta\otimes f_{abc}\tau_c = \\
&= \frac{1}{2}\left(\delta^{\mu\nu}_{\alpha\beta}\partial_\mu A^c_\nu + f_{abc}A^a_\alpha A^b_\beta\right)\mathrm{d}x^\mu\wedge\mathrm{d}x^\nu\otimes\tau_c = \frac{1}{2}F^c_{\mu\nu}\mathrm{d}x^\mu\wedge\mathrm{d}x^\nu\otimes\tau_c \\
&\Rightarrow F^c_{\mu\nu} = \delta^{\mu\nu}_{\alpha\beta}\partial_\mu A^c_\nu + f_{abc}A^a_\alpha A^b_\beta \\
&\Rightarrow \mathcal{F}_{\mu\nu} = \delta^{\mu\nu}_{\alpha\beta}\partial_\mu\mathcal{A}_\nu + [\mathcal{A}_\alpha,\mathcal{A}_\beta]
\end{aligned}$$

### Yang-Mills Action

The inner product $\langle \mathcal{F}, \mathcal{F} \rangle$ using the scalar product $\langle \cdot, \cdot \rangle_{\Lambda^2(M;\mathfrak{g})}$ is

$$\begin{aligned}\langle \mathcal{F}, \mathcal{F} \rangle &= \langle \frac{1}{2} F^a_{\mu\nu} (\mathrm{d}x^\mu \wedge \mathrm{d}x^\nu) \otimes \tau_a, \frac{1}{2} F^b_{\alpha\beta} (\mathrm{d}x^\alpha \wedge \mathrm{d}x^\beta) \otimes \tau_b \rangle = \\ &= \langle \frac{1}{2} F^a_{\mu\nu} (\mathrm{d}x^\mu \wedge \mathrm{d}x^\nu), \frac{1}{2} F^b_{\alpha\beta} (\mathrm{d}x^\alpha \wedge \mathrm{d}x^\beta) \rangle_{\Lambda^2(M)} \langle \tau_a, \tau_b \rangle_{\mathfrak{g}} = \\ &= \frac{1}{4} F^a_{\mu\nu} (F^b)^{\mu\nu} c_{ab}\end{aligned}$$

where $c_{ab}$ is the matrix representing the Lie algebra inner product $c_{ab} = \langle \tau_a, \tau_b \rangle_{\mathfrak{g}}$ in the basis $(\tau_k)_{k=1,\dots,\dim \mathfrak{g}}$.

### 6.2.1 Strong Yang-Mills Equations

We derive the set of strong Yang-Mills equations from the weak ones in definition 45 by means of partial integration (ad-invariance of the inner product resembles a product rule) and vanishing boundary terms.

$$\begin{aligned}\langle \mathcal{F}(\mathcal{A}), \mathrm{d}_{\mathcal{A}} \mathcal{A}' \rangle &= \frac{1}{4} \langle \mathcal{F}^{\alpha\beta}, \delta^{\mu\nu}_{\alpha\beta} \partial_\mu \mathcal{A}'_\nu + 2[\mathcal{A}_\alpha, \mathcal{A}'_\beta] \rangle_{\mathfrak{g}} = \\ &= \frac{1}{2} \langle \mathcal{F}^{\mu\nu}, \partial_\mu \mathcal{A}'_\nu \rangle_{\mathfrak{g}} + \frac{1}{2} \langle \mathcal{F}^{\mu\nu}, [\mathcal{A}_\mu, \mathcal{A}'_\nu] \rangle_{\mathfrak{g}} = \\ &= \frac{1}{2} \partial_\mu \langle \mathcal{F}^{\mu\nu}, \mathcal{A}'_\nu \rangle_{\mathfrak{g}} - \frac{1}{2} \langle \partial_\mu \mathcal{F}^{\mu\nu}, \mathcal{A}'_\nu \rangle_{\mathfrak{g}} + (-1)^{1\cdot 2+1} \frac{1}{2} \langle [\mathcal{A}_\mu, \mathcal{F}^{\mu\nu}], \mathcal{A}'_\nu \rangle_{\mathfrak{g}} = \\ &= \frac{1}{2} \partial_\mu \langle \mathcal{F}^{\mu\nu}, \mathcal{A}'_\nu \rangle_{\mathfrak{g}} - \frac{1}{2} \langle \partial_\mu \mathcal{F}^{\mu\nu}, \mathcal{A}'_\nu \rangle_{\mathfrak{g}} - \frac{1}{2} \langle [\mathcal{A}_\mu, \mathcal{F}^{\mu\nu}], \mathcal{A}'_\nu \rangle_{\mathfrak{g}} = \\ &= \frac{1}{2} \partial_\mu \langle \mathcal{F}^{\mu\nu}, \mathcal{A}'_\nu \rangle_{\mathfrak{g}} - \frac{1}{2} \langle \partial_\mu \mathcal{F}^{\mu\nu} + [\mathcal{A}_\mu, \mathcal{F}^{\mu\nu}], \mathcal{A}'_\nu \rangle_{\mathfrak{g}}\end{aligned}$$

Integrating these expressions and applying Stokes' theorem we obtain

$$\begin{aligned}\int_M 2\langle \mathcal{F}(\mathcal{A}), \mathrm{d}_{\mathcal{A}} \mathcal{A}' \rangle \mathrm{dVol} &= \int_M \partial_\mu \langle \mathcal{F}^{\mu\nu}, \mathcal{A}'_\nu \rangle_{\mathfrak{g}} \mathrm{dVol} - \int_M \langle \partial_\mu \mathcal{F}^{\mu\nu} + [\mathcal{A}_\mu, \mathcal{F}^{\mu\nu}], \mathcal{A}'_\nu \rangle_{\mathfrak{g}} \mathrm{dVol} = \\ &= \int_{\partial M} n_\mu \langle \mathcal{F}^{\mu\nu}, \mathcal{A}'_\nu \rangle_{\mathfrak{g}} \mathrm{dS} - \int_M \langle \partial_\mu \mathcal{F}^{\mu\nu} + [\mathcal{A}_\mu, \mathcal{F}^{\mu\nu}], \mathcal{A}'_\nu \rangle_{\mathfrak{g}} \mathrm{dVol}.\end{aligned}$$

$$\begin{aligned}&\int_M 2\langle \mathcal{F}(\mathcal{A}), \mathrm{d}_{\mathcal{A}} \mathcal{A}' \rangle + \langle \mathcal{J}, \mathcal{A}' \rangle \mathrm{dVol} = \\ &\int_{\partial M} n_\mu \langle \mathcal{F}^{\mu\nu}, \mathcal{A}'_\nu \rangle_{\mathfrak{g}} \mathrm{dS} - \int_M \langle \partial_\mu \mathcal{F}^{\mu\nu} + [\mathcal{A}_\mu, \mathcal{F}^{\mu\nu}], \mathcal{A}'_\nu \rangle_{\mathfrak{g}} \mathrm{dVol} + \langle \mathcal{J}, \mathcal{A}' \rangle \mathrm{dVol}.\end{aligned}$$

Assuming that boundary terms vanish and using the fundamental lemma of variational calculus we obtain the strong Yang-Mills equations formulated in components

$$\partial_\mu \mathcal{F}^{\mu\nu} + [\mathcal{A}_\mu, \mathcal{F}^{\mu\nu}] = \mathcal{J}^\nu$$

as they are often used in physics. The differential operator $\partial_\mu \mathcal{B}^\mu + [\mathcal{A}_\mu, \mathcal{B}^\mu]$ is often referred to as gauge-covariant divergence.

### 6.2.2 Temporal Splitting of Yang-Mills Equations

We split the weak Yang-Mills equations in 45

$$\int_M \langle 2\mathcal{F}(\mathcal{A}), \mathrm{d}_{\mathcal{A}} \mathcal{A}' \rangle + \langle \mathcal{J}, \mathcal{A}' \rangle \mathrm{dVol} = 0$$

into temporal and spatial parts in temporal gauge $\mathcal{A}_0 = 0$.

$$\begin{aligned}
\mathrm{d}_{\mathcal{A}}\mathcal{A}' &= \mathrm{d}\mathcal{A}' + [\mathcal{A} \wedge \mathcal{A}'] = \\
&= \frac{1}{2}\left(\delta^{\alpha\beta}_{\mu\nu}\partial_\alpha \mathcal{A}'_\beta + \delta^{\alpha\beta}_{\mu\nu}[\mathcal{A}_\alpha, \mathcal{A}'_\beta]\right) \mathrm{d}x^\mu \wedge \mathrm{d}x^\nu = \\
&= \frac{1}{2}\left(\partial_\mu \mathcal{A}'_\nu - \partial_\nu \mathcal{A}'_\mu + [\mathcal{A}_\mu, \mathcal{A}'_\nu] - [\mathcal{A}_\nu, \mathcal{A}'_\mu]\right) \mathrm{d}x^\mu \wedge \mathrm{d}x^\nu =
\end{aligned}$$

We may restrict this expression to indices $\mu = 0, \nu = n = 1, 2, 3$ due to antisymmetry.

$$\begin{aligned}
(\mathrm{d}_{\mathcal{A}}\mathcal{A}')_{0n} &= \partial_0 \mathcal{A}'_n - \partial_n \mathcal{A}'_0 + [\mathcal{A}_0, \mathcal{A}'_n] - [\mathcal{A}_n, \mathcal{A}'_0] = \\
&= \partial_0 \mathcal{A}'_n - \partial_n \mathcal{A}'_0 - [\mathcal{A}_n, \mathcal{A}'_0] =
\end{aligned}$$

$$\begin{aligned}
\langle \mathcal{F}(\mathcal{A}), \mathrm{d}_{\mathcal{A}}\mathcal{A}' \rangle &= \frac{1}{4}\langle \mathcal{F}^{\mu\nu}, \left(\mathrm{d}_{\mathcal{A}}\mathcal{A}'\right)_{\mu\nu} \rangle = \\
&= \frac{1}{2}\langle \mathcal{F}^{0n}, \left(\mathrm{d}_{\mathcal{A}}\mathcal{A}'\right)_{0n} \rangle + \frac{1}{4}\langle \mathcal{F}^{mn}, \left(\mathrm{d}_{\mathcal{A}}\mathcal{A}'\right)_{mn} \rangle = \\
&= \frac{1}{2}\langle \mathcal{F}^{0n}, \partial_0 \mathcal{A}'_n - \partial_n \mathcal{A}'_0 - [\mathcal{A}_n, \mathcal{A}'_0] \rangle + \frac{1}{4}\langle \mathcal{F}^{mn}, \left(\mathrm{d}_{\mathcal{A}}\mathcal{A}'\right)_{mn} \rangle = \\
&= -\frac{1}{2}\langle \mathcal{F}^{0n}, \partial_n \mathcal{A}'_0 + [\mathcal{A}_n, \mathcal{A}'_0] \rangle + \frac{1}{2}\langle \mathcal{F}^{0n}, \partial_0 \mathcal{A}'_n \rangle + \frac{1}{4}\langle \mathcal{F}^{mn}, \left(\mathrm{d}_{\mathcal{A}}\mathcal{A}'\right)_{mn} \rangle =
\end{aligned}$$

We include the source terms $\mathcal{J} = \mathcal{J}_\mu \mathrm{d}x^\mu$

$$\langle \mathcal{J}, \mathcal{A}' \rangle = \langle \mathcal{J}^\mu, \mathcal{A}'_\mu \rangle = \langle \mathcal{J}^0, \mathcal{A}'_0 \rangle + \langle \mathcal{J}^m, \mathcal{A}'_m \rangle$$

and split the weak Yang-Mills equations

$$\int_M 2\langle \mathcal{F}(\mathcal{A}), \mathrm{d}_{\mathcal{A}}\mathcal{A}' \rangle + \langle \mathcal{J}, \mathcal{A}' \rangle \mathrm{dVol} = 0$$

according to test functions $\mathcal{A}'_0$ and $(\mathcal{A}'_n)_{n=1,2,3}$

$$\begin{aligned}
&\int_M -\langle \mathcal{F}^{0n}, \partial_n \mathcal{A}'_0 + [\mathcal{A}_n, \mathcal{A}'_0] \rangle + \int_M \langle \mathcal{J}^0, \mathcal{A}'_0 \rangle = 0 \\
&\int_M \langle \mathcal{F}^{0n}, \partial_0 \mathcal{A}'_n \rangle + \int_M 2 \cdot \frac{1}{4}\langle \mathcal{F}^{mn}, (\mathrm{d}_{\mathcal{A}}\mathcal{A}')_{mn} \rangle + \int_M \langle \mathcal{J}^m, \mathcal{A}'_m \rangle = 0.
\end{aligned}$$

"Lowering" indices by using the metric

$$\begin{aligned}
&\int_M \langle \mathcal{F}_{0n}, \partial_n \mathcal{A}'_0 + [\mathcal{A}_n, \mathcal{A}'_0] \rangle + \int_M \langle \mathcal{J}^0, \mathcal{A}'_0 \rangle = 0 \\
&\int_M -\langle \mathcal{F}_{0n}, \partial_0 \mathcal{A}'_n \rangle + \int_M 2 \cdot \frac{1}{4}\langle \mathcal{F}_{mn}, (\mathrm{d}_{\mathcal{A}}\mathcal{A}')_{mn} \rangle + \int_M \langle \mathcal{J}^m, \mathcal{A}'_m \rangle = 0
\end{aligned}$$

and renaming

$$\begin{aligned}
\mathcal{E}_n &:= -\mathcal{F}_{0n} = -\partial_0 \mathcal{A} = -\partial_t \mathcal{A} \\
\mathcal{A}'_\mu &:= (\rho', \mathcal{E}'_x, \mathcal{E}'_y, \mathcal{E}'_z)_\mu \\
\mathcal{J}^\mu &:= (\rho, j_x, j_y, j_z)^\mu
\end{aligned}$$

$$-\int_M \langle \mathcal{E}_n, \partial_n \rho' + [\mathcal{A}_n, \rho'] \rangle + \int_M \langle \rho, \rho' \rangle = 0$$
$$\int_M \langle \mathcal{E}_n, \partial_0 \mathcal{E}'_n \rangle + \int_M 2 \cdot \frac{1}{4} \langle \mathcal{F}_{mn}, (\mathrm{d}_{\mathcal{A}} \mathcal{A}')_{mn} \rangle + \int_M \langle \mathcal{J}_m, \mathcal{E}'_m \rangle = 0$$

$$\int_M \langle \mathcal{E}_n, \mathrm{d}_{\mathcal{A}} \rho' \rangle = \int_M \langle \rho, \rho' \rangle$$
$$-\int_M \langle \mathcal{E}_n, \partial_0 \mathcal{E}'_n \rangle - \int_M 2 \cdot \frac{1}{4} \langle \mathcal{F}_{mn}, (\mathrm{d}_{\mathcal{A}} \mathcal{A}')_{mn} \rangle = \int_M \langle j_m, \mathcal{E}'_m \rangle$$

we can interpret these equations with derivative $\partial_0 = \partial_t$ and remaining spatial exterior covariant derivative $\mathrm{d}_{\mathcal{A}} \mathcal{E}'$

$$\begin{aligned}(\mathrm{d}_{\mathcal{A}} \mathcal{A}')_{mn} &= \sum_{\alpha,\beta=0}^{3} \delta^{\alpha\beta}_{mn} (\partial_\alpha \mathcal{A}'_\beta + \mathcal{A}_\alpha \mathcal{A}'_\beta) = \\ &= \sum_{a,b=1}^{3} \delta^{ab}_{mn} (\partial_a \mathcal{A}'_b + \mathcal{A}_a \mathcal{A}'_b) = \\ &= \sum_{a,b=1}^{3} \delta^{ab}_{mn} (\partial_a \mathcal{A}'_b + \mathcal{A}_a \mathcal{E}'_b) =: \mathrm{d}_{\mathcal{A}} \mathcal{E}'\end{aligned}$$

$$\int_M \langle \mathcal{E}, \mathrm{d}_{\mathcal{A}} \rho' \rangle = \int_M \langle \rho, \rho' \rangle$$
$$-\int_M \langle \mathcal{E}, \partial_t \mathcal{E}' \rangle - \int_M \langle 2\mathcal{F}, \mathrm{d}_{\mathcal{A}} \mathcal{E}' \rangle = \int_M \langle j, \mathcal{E}' \rangle.$$

## 6.3 Lie Groups

### 6.3.1 Special Unitary Group $SU(N)$

The Special Unitary Lie Group $SU(N)$ consisting of hermitean $\mathbb{C}^{N\times N}$ matrices with unit determinant

$$SU(N) := \{U \in \mathbb{C}^{N\times N} | UU^\dagger = U^\dagger U = \mathbb{1}, \det U = 1\}$$

plays a central role in gauge theories. The associated Lie algebra $su(N)$ is the vector space of anti-hermitean traceless $\mathbb{C}^{N\times N}$ matrices

$$su(N) := \{U \in \mathbb{C}^{N\times N} | U^\dagger = -U, \operatorname{Tr} U = 0\}$$

This can be seen by evaluating a tangent vector $\partial_t U(0)$ of a curve $t \mapsto U(t)$ going through the Lie groups identity $U(0) = \mathbb{1} \in G$

$$U : \mathbb{R} \to \mathbb{C}^{n\times n} \quad U^\dagger U = \mathbb{1}, U(0) = \mathbb{1}$$

$$\begin{aligned}\frac{d}{dt}(U^\dagger(t)U(t))|_{t=0} &= \left[\frac{d}{dt}U^\dagger(t)U(t) + U^\dagger(t)\frac{d}{dt}U(t)\right]|_{t=0} = \\ &= \frac{d}{dt}U^\dagger(0)U(0) + U^\dagger(0)\frac{d}{dt}U(0) = 0 \\ &= \frac{d}{dt}U^\dagger(0) + \frac{d}{dt}U(0) = 0 \\ &\Rightarrow \left[\frac{d}{dt}U(0)\right]^\dagger = -\frac{d}{dt}U(0)\end{aligned}$$

and the identity $\det \exp\{A\} = \exp \operatorname{Tr} A$.

$$1 = \det \exp A = \exp \operatorname{Tr} A \Rightarrow \operatorname{Tr} A = \ln 1 = 0$$

There also exists a canonical pairing on the Lie algebra in the form of the complex Frobenius scalar product

$$\langle \cdot, \cdot \rangle_{\mathfrak{g}} : \begin{cases} \mathfrak{g} \times \mathfrak{g} & \to & \mathbb{C} \\ (\sigma, \tau) & \mapsto & \langle \sigma, \tau \rangle_{\mathfrak{g}} = \mathrm{Tr}\{\sigma\tau^\dagger\} \end{cases}$$

which is symmetric

$$\begin{aligned} \langle \sigma, \tau \rangle_{\mathfrak{g}} &= \mathrm{Tr}\{\sigma\tau^\dagger\} = \\ &= \mathrm{Tr}\{\tau^\dagger\sigma\} = \\ &= \mathrm{Tr}\{-\tau(-\sigma^\dagger)\} = \\ &= (-1)^2\mathrm{Tr}\{\tau\sigma^\dagger\} = \\ &= \mathrm{Tr}\{\tau\sigma^\dagger\} = \langle \tau, \sigma \rangle \end{aligned}$$

and non-degenerate. It is Ad-invariant under the adjoint action $\mathrm{Ad}_g$ with elements $g \in SU(N)$ due to $g^\dagger = g^{-1}$.

$$\begin{aligned} \langle \mathrm{Ad}_g\sigma, \mathrm{Ad}_g\tau \rangle_{\mathfrak{g}} &= \langle g\sigma g^{-1}, g\tau g^{-1} \rangle_{\mathfrak{g}} = \\ &= \mathrm{Tr}\{g\sigma g^{-1}(g\tau g^{-1})^\dagger\} = \\ &= \mathrm{Tr}\{g\sigma g^{-1} g\tau^\dagger g^{-1}\} = \\ &= \mathrm{Tr}\{\sigma\tau^\dagger g^{-1} g\} = \\ &= \mathrm{Tr}\{\sigma\tau^\dagger\} = \langle \sigma, \tau \rangle_{\mathfrak{g}} \end{aligned}$$

as well ad-invariant under the ("infinitesimal") adjoint action $\mathrm{ad}_\nu = [\nu, \cdot]$ with $\nu \in su(N)$ due to $\nu^\dagger = -\nu$.

$$\begin{aligned} \langle \mathrm{ad}_\nu\sigma, \tau \rangle_{\mathfrak{g}} &= \langle [\nu, \sigma], \tau \rangle_{\mathfrak{g}} = \\ &= \mathrm{Tr}\{(\nu\sigma - \sigma\nu)\tau^\dagger\} = \\ &= \mathrm{Tr}\{\nu\sigma\tau^\dagger - \sigma\nu\tau^\dagger\} = \\ &= \mathrm{Tr}\{\nu\sigma\tau^\dagger\} - \mathrm{Tr}\{\sigma\nu\tau^\dagger\} = \\ &= \mathrm{Tr}\{\sigma\tau^\dagger\nu\} - \mathrm{Tr}\{\sigma\nu\tau^\dagger\} = \\ &= \mathrm{Tr}\{\sigma\tau^\dagger\nu - \sigma\nu\tau^\dagger\} = \\ &= \mathrm{Tr}\{\sigma(\tau^\dagger\nu - \nu\tau^\dagger)\} = \\ &= \mathrm{Tr}\{\sigma(\nu^\dagger\tau - \tau\nu^\dagger)^\dagger\} = \\ &= -\mathrm{Tr}\{\sigma(\nu\tau - \tau\nu)^\dagger\} = \\ &= -\mathrm{Tr}\{\sigma[\nu, \tau]^\dagger\} = -\langle \sigma, \mathrm{ad}_\nu\tau \rangle_{\mathfrak{g}} \end{aligned}$$

**Special Unitary Group** $SU(2)$

Further specializing to the case of $SU(2)$, a basis of the Lie Algebra $su(2)$ can be constructed with the help of the so-called Pauli matrices $(\sigma_k)_{k=1,2,3}$

$$\sigma_1 = \sigma_x = \begin{pmatrix} 0 & 1 \\ 1 & 0 \end{pmatrix} \quad \sigma_2 = \sigma_y = \begin{pmatrix} 0 & -i \\ i & 0 \end{pmatrix} \quad \sigma_3 = \sigma_z = \begin{pmatrix} 1 & 0 \\ 0 & -1 \end{pmatrix}$$

They satisfy commutator $[X, Y] := XY - YX$ and anticommutator $\{X, Y\} = XY + YX$ relations.

$$[\sigma_k, \sigma_l] = \sigma_k\sigma_l - \sigma_l\sigma_k = 2i\varepsilon_{klm}\sigma_m$$

$$\{\sigma_k, \sigma_l\} = \sigma_k\sigma_l + \sigma_l\sigma_k = 2\delta_{kl}\mathbb{1}$$

where $\varepsilon_{klm}$ is the 3-dimensional fully antisymmetric Levi Civita symbol 6.2

$$\varepsilon_{klm} = \begin{cases} 1 & klm \text{ even} \\ -1 & klm \text{ odd} \\ 0 & klm \text{ else} \end{cases}$$

and $\delta_{kl}$ the Kronecker symbol 6.1

$$\delta_{kl} = \begin{cases} 0 & k \neq l \\ 1 & k = l \end{cases}.$$

The Lie Algebra $su(2)$ of the Lie group $SU(2)$ can be then spanned by a linear combination of $(i\sigma_k)_{k=1,2,3}$. Using the basis $(\tau_k)_{k=1,2,3} = (\frac{1}{i}\sigma_k)_{k=1,2,3}$ instead allows an identification of $su(2)$ and $SU(2)$ elements with quaternions [1].

$$\begin{aligned}\sigma_k\sigma_l &= \frac{1}{2}([\sigma_k, \sigma_l] + \{\sigma_k, \sigma_l\}) = \\ &= \frac{1}{2}(2i\varepsilon_{klm}\sigma_m + 2\delta_{kl}\mathbb{1}) = \\ &= i\varepsilon_{klm}\sigma_m + \delta_{kl}\mathbb{1}\end{aligned}$$

$$\begin{aligned}&\frac{1}{i}\sigma_k\frac{1}{i}\sigma_l = \varepsilon_{klm}\frac{1}{i}\sigma_m - \delta_{kl}\mathbb{1} \\ &\tau_k\tau_l = \varepsilon_{klm}\tau_m - \delta_{kl}\mathbb{1} \\ &k = l : \tau_k\tau_k = -\mathbb{1} \\ &k \neq l : \tau_k\tau_l = \varepsilon_{klm}\tau_m\end{aligned}$$

Using the exponential map we explicitly construct Lie Group elements $U(\rho^k) = e^{i\vec{\rho}\cdot\vec{\sigma}}$ from a linear combination of the Lie Algebra $i\vec{\rho}\cdot\vec{\sigma} = i\rho\hat{n}\cdot\vec{\sigma}$

$$\vec{\rho}\cdot\vec{\sigma} = \sum_{k=1}^{3}\rho^k\sigma_k = \sum_{i=1}^{3}\rho n^i\sigma_i = \rho(n^x\sigma_x + n^y\sigma_y + n^z\sigma_z)$$

where $\rho = \sqrt{\vec{\rho}\cdot\vec{\rho}} \in \mathbb{R}$ and $\hat{n} = \vec{\rho}/\rho \in \mathbb{R}^3$ is a normalized three-dimensional vector.

$$\begin{aligned}(\hat{n}\cdot\vec{\sigma})^2 &= \left(\sum_{k=1}^{3}(n^k\sigma_k)\right)\left(\sum_{l=1}^{3}(n^l\sigma_l)\right) = \\ &= \sum_{k=1}^{3}\sum_{l=1}^{3}n^k\sigma_k n^l\sigma_l = \\ &= \sum_{k=1}^{3}\sum_{l=1}^{3}n^k n^l\sigma_k\sigma_l = \\ &= \sum_{k=1}^{3}\sum_{l=1}^{3}n^k n^l\frac{1}{2}([\sigma_k, \sigma_l] + \{\sigma_k, \sigma_l\}) = \\ &= \sum_{k=1}^{3}\sum_{l=1}^{3}n^k n^l\frac{1}{2}(2i\sum_{m=1}^{3}\varepsilon_{klm}\sigma_m + 2\delta_{kl}\mathbb{1}) = \\ &= \underbrace{\sum_{k=1}^{3}\sum_{l=1}^{3}n^k n^l i\sum_{m=1}^{3}\varepsilon_{klm}\,\sigma_m}_{=0} + \sum_{k=1}^{3}\sum_{l=1}^{3}n^k n^l\delta_{kl}\mathbb{1} = \\ &= \sum_{k=1}^{3}n^k n^k\mathbb{1} = \mathbb{1} \\ &\Rightarrow (\hat{n}\cdot\vec{\sigma})^{2r} = \mathbb{1} \quad (\hat{n}\cdot\vec{\sigma})^{2r+1} = \hat{n}\cdot\vec{\sigma} \quad \forall r \in \mathbb{N}\end{aligned}$$

$$
\begin{aligned}
U(\rho^k) = e^{i\vec{\rho}\cdot\vec{\sigma}} = e^{i\rho\hat{n}\cdot\vec{\sigma}} = \\
&= \sum_{k=1}^{\infty} \frac{(i\rho)^k}{k!}(\hat{n}\cdot\vec{\sigma})^k = \\
&= \sum_{r=1}^{\infty} \frac{(i\rho)^{2r}}{(2r)!}(\hat{n}\cdot\vec{\sigma})^{2r} + \sum_{r=1}^{\infty} \frac{(i\rho)^{2r-1}}{(2r-1)!}(\hat{n}\cdot\vec{\sigma})^{2r-1} = \\
&= \sum_{r=1}^{\infty} \frac{(i\rho)^{2r}}{(2r)!}\mathbb{1} + \sum_{r=1}^{\infty} \frac{(i\rho)^{2r-1}}{(2r-1)!}(\hat{n}\cdot\vec{\sigma}) = \\
&= \sum_{r=1}^{\infty}(-1)^r \frac{\rho^{2r}}{(2r)!}\mathbb{1} + i\sum_{r=1}^{\infty}(-1)^{2r-1} \frac{\rho^{2r-1}}{(2r-1)!}(\hat{n}\cdot\vec{\sigma}) = \\
&= \cos\rho\mathbb{1} + i\sin\rho(\hat{n}\cdot\vec{\sigma})
\end{aligned}
$$

### 6.3.2 Representations and Compatibility with Exponential Maps

We show how smooth Lie group representations $R : GH \to End(V) \simeq \mathbb{C}^{n\times n}$ as in definition 34 connect the abstract exponential map $\exp : \mathfrak{g} \to G$ to the more concrete matrix exponential $e^A$ for matrices in $A \in \mathbb{C}^{n\times n}$. The definition of the abstract exponential $\exp\{\sigma\} \in G$ of $\sigma \in \mathfrak{g}$ is given in terms of a curve $\gamma_\sigma$

$$
\sigma \in \mathfrak{g} \Rightarrow \exp\{\sigma\} := \gamma_\sigma(1) : \ \frac{\mathrm{d}}{\mathrm{d}t}|_{t_0}\gamma_\sigma(t) = \frac{\mathrm{d}}{\mathrm{d}t}|_{t=0}\left(\gamma_\sigma(t_0)\circ\sigma(t)\right) \quad \forall t_0 \in [0,1],\ \gamma_\sigma(0) = \mathbb{1}
$$

This directly implies for the mapped curve $R(\gamma_\sigma)$

$$
\begin{aligned}
\frac{\mathrm{d}}{\mathrm{d}t}|_{t_0}R(\gamma_\sigma(t)) &= R\left(\frac{\mathrm{d}}{\mathrm{d}t}|_{t_0}\gamma_\sigma(t)\right) = \\
&= R\left(\frac{\mathrm{d}}{\mathrm{d}t}|_{t=0}\left(\gamma_\sigma(t_0)\circ\sigma(t)\right)\right) = \\
&= \frac{\mathrm{d}}{\mathrm{d}t}|_{t=0}R\left(\gamma_\sigma(t_0)\circ\sigma(t)\right) = \\
&= \frac{\mathrm{d}}{\mathrm{d}t}|_{t=0}\left(R\left(\gamma_\sigma(t_0)\right)R\left(\sigma(t)\right)\right) = \\
&= R\left(\gamma_\sigma(t_0)\right)\frac{\mathrm{d}}{\mathrm{d}t}|_{t=0}R\left(\sigma(t)\right) = \\
&= R\left(\gamma_\sigma(t_0)\right)R_*\left(\sigma\right)
\end{aligned}
$$

where the push-forward $R_*$ induces a representation on the Lie algebra as mentioned in the remark 2.6.5.

$$
\Rightarrow R(\gamma_\sigma(t)) = e^{R_*(\sigma)t}
$$

and therefore

$$
\Rightarrow R(\exp\{\sigma\}) = e^{R_*(\sigma)}.
$$

### 6.3.3 Group Derivative of Representations

The group derivative in definition 61 of a representation $R : G \to GL(n,\mathbb{C})$ is

$$
\begin{aligned}
\delta_{\mathcal{A}'}R(g) &:= \frac{\mathrm{d}}{\mathrm{d}t}|_{t=0}R(\exp\{t\mathcal{A}'\}\circ g) = \\
&= \frac{\mathrm{d}}{\mathrm{d}t}|_{t=0}\left(R(\exp\{t\mathcal{A}'\})R(g)\right) = \\
&= \frac{\mathrm{d}}{\mathrm{d}t}|_{t=0}\left(e^{tR_*(\mathcal{A}')}R(g)\right) = \\
&= \frac{\mathrm{d}}{\mathrm{d}t}|_{t=0}e^{tR_*(\mathcal{A}')}R(g) = R_*(\mathcal{A}')R(g)
\end{aligned}
$$

where $R_* : \mathfrak{g} \to \mathbb{C}^{n\times n}$ stands for the push forward of $R$ which induces a linear representation of the Lie algebra $\mathfrak{g}$. Choosing a different function for the inverse $f(g) = R(g^{-1})$ we obtain the group derivative

$$\begin{aligned}\delta_{\mathcal{A}'} f(g) &:= \frac{\mathrm{d}}{\mathrm{d}t}|_{t=0} R((\exp\{t\mathcal{A}'\} \circ g)^{-1}) = \\ &= \frac{\mathrm{d}}{\mathrm{d}t}|_{t=0} R(g^{-1} \circ \exp\{-t\mathcal{A}'\}) = \\ &= \frac{\mathrm{d}}{\mathrm{d}t}|_{t=0} \left(R(g^{-1})R(\exp\{-t\mathcal{A}'\})\right) = \\ &= \frac{\mathrm{d}}{\mathrm{d}t}|_{t=0} \left(R(g^{-1})e^{-tR_*(\mathcal{A}')}\right) = \\ &= R(g^{-1})\frac{\mathrm{d}}{\mathrm{d}t}|_{t=0} e^{-tR_*(\mathcal{A}')} = -R(g^{-1})R_*(\mathcal{A}').\end{aligned}$$

## 6.4 Parallel Transport

### 6.4.1 Transformation of Parallel Transporter $U$

The transformation behaviour of $U(t) \in G$

$$U(t) \to g(\gamma(t))U(t)g^{-1}(\gamma(0))$$

directly follows from that of $\mathcal{A}$

$$\mathcal{A} \to g\mathcal{A}g^{-1} - \mathrm{d}gg^{-1}$$

due to the differential equation:

$$\begin{aligned}\frac{\mathrm{d}}{\mathrm{d}t}U(t) + \mathcal{A}(\dot\gamma(t))U(t) &= 0 \\ \frac{\mathrm{d}}{\mathrm{d}t}U(t)U^{-1}(t) &= -\mathcal{A}(\dot\gamma(t))\end{aligned}$$

$$\begin{aligned}&\frac{\mathrm{d}}{\mathrm{d}t}\left\{g(\gamma(t))U(t)g^{-1}(\gamma(0))\right\} g(\gamma(0))U^{-1}(t)g^{-1}(\gamma(t)) = \\ &= \frac{\mathrm{d}}{\mathrm{d}t}g(\gamma(t))\underbrace{U(t)g^{-1}(\gamma(0))g(\gamma(0))U^{-1}(t)}_{=\mathbb{1}}g^{-1}(\gamma(t)) + \\ &+ g(\gamma(t))\frac{\mathrm{d}}{\mathrm{d}t}U(t)\underbrace{g^{-1}(\gamma(0))g(\gamma(0))}_{=\mathbb{1}}U^{-1}(t)g^{-1}(\gamma(t)) = \\ &= \frac{\mathrm{d}}{\mathrm{d}t}g(\gamma(t))g^{-1}(\gamma(t)) + g(\gamma(t))\frac{\mathrm{d}}{\mathrm{d}t}U(t)U^{-1}(t)g^{-1}(\gamma(t)) = \\ &= \mathrm{d}g(\dot\gamma(t))g^{-1}(\gamma(t)) - g(\gamma(t))\mathcal{A}(\gamma(t))g^{-1}(\gamma(t)) = \\ &= -\left\{g(\gamma(t))\mathcal{A}(\gamma(t))g^{-1}(\gamma(t)) - \mathrm{d}g(\dot\gamma(t))g^{-1}(\gamma(t))\right\}\end{aligned}$$

### 6.4.2 Path-Ordered Exponential

*Proof.* (of definition 51) First we show that the expression converges. Because of $\mathcal{A} : TM \to C^\infty(M)$ and $\gamma \in C^\infty([0,1], M)$ on the compact set $[0,1]$ we have that each $\mathcal{A}(\dot\gamma(t'))$ is bounded $\|\mathcal{A}(\dot\gamma(t'))\|_{L^\infty} < C$ for all times $t' \in [0,1]$ (with the Frobenius matrix norm).

The measure of the index set, over which it is integrated, is by induction $t^n/n!$.

$$\int_0^{t_2'} \mathrm{d}t_1' = t_2' = \frac{(t_2')^1}{(2-1)!}$$
$$\int_0^{t_n'} \int_0^{t_{n-1}'} \cdots \int_0^{t_2'} \mathrm{d}t_1' \cdots \mathrm{d}t_{n-1}' = \frac{(t_n')^{n-1}}{(n-1)!}$$
$$\int_0^{t_{n+1}'} \int_0^{t_n'} \int_0^{t_{n-1}'} \cdots \int_0^{t_2'} \mathrm{d}t_1' \cdots \mathrm{d}t_{n-1}' \mathrm{d}t_n' = \int_0^{t_{n+1}'} \frac{(t_n')^{n-1}}{(n-1)!} \mathrm{d}t_n' = \frac{(t_{n+1}')^n}{n!}$$
$$\int_0^{t_{n+1}'=t} \int_0^{t_n'} \int_0^{t_{n-1}'} \cdots \int_0^{t_2'} \mathrm{d}t_1' \cdots \mathrm{d}t_n' = \frac{t^n}{n!}$$

Therefore we can estimate the path ordered exponential with the regular exponential function, which can be bounded uniformly for all $t \in [0,1]$.

$$\begin{aligned}
\|U(t)\| &= \left\| \mathcal{P} \left\{ \exp\left\{ \int_0^t \mathcal{A}(\dot\gamma(t)) \mathrm{d}t' \right\} \right\} \right\| \\
&:= \left\| \sum_{n=0}^{\infty} \int_0^t \int_0^{t_n'} \int_0^{t_{n-1}'} \cdots \int_0^{t_2'} \mathcal{A}(\dot\gamma(t_n')) \cdots \mathcal{A}(\dot\gamma(t_1')) \mathrm{d}t_1' \cdots \mathrm{d}t_n' \right\| \leq \\
&\leq \sum_{n=0}^{\infty} \left\| \int_0^t \int_0^{t_n'} \int_0^{t_{n-1}'} \cdots \int_0^{t_2'} \mathcal{A}(\dot\gamma(t_n')) \cdots \mathcal{A}(\dot\gamma(t_1')) \mathrm{d}t_1' \cdots \mathrm{d}t_n' \right\| \leq \\
&\leq \sum_{n=0}^{\infty} \frac{t^n}{n!} \|\mathcal{A}(\dot\gamma)\|_{L^\infty}^n = \exp\left\{ \|\mathcal{A}(\dot\gamma)\|_{L^\infty} t \right\} < C < \infty
\end{aligned}$$

Due to uniform convergence, we may swap the order of derivative and summation.

$$\begin{aligned}
&\frac{\mathrm{d}}{\mathrm{d}t} U(t) = \frac{\mathrm{d}}{\mathrm{d}t} \mathcal{P} \left\{ \exp\left\{ \int_0^t \mathcal{A}(\dot\gamma(t')) \mathrm{d}t' \right\} \right\} \\
&:= \frac{\mathrm{d}}{\mathrm{d}t} \sum_{n=0}^{\infty} \int_0^t \int_0^{t_n'} \int_0^{t_{n-1}'} \cdots \int_0^{t_2'} \mathcal{A}(\dot\gamma(t_n')) \cdots \mathcal{A}(\dot\gamma(t_1')) \mathrm{d}t_1' \cdots \mathrm{d}t_n' = \\
&= \sum_{n=0}^{\infty} \frac{\mathrm{d}}{\mathrm{d}t} \int_0^t \int_0^{t_n'} \int_0^{t_{n-1}'} \cdots \int_0^{t_2'} \mathcal{A}(\dot\gamma(t_n')) \cdots \mathcal{A}(\dot\gamma(t_1')) \mathrm{d}t_1' \cdots \mathrm{d}t_n' = \\
&= \sum_{n=1}^{\infty} \mathcal{A}(\dot\gamma(t)) \int_0^{t_n'} \int_0^{t_{n-1}'} \cdots \int_0^{t_2'} \mathcal{A}(\dot\gamma(t_n')) \cdots \mathcal{A}(\dot\gamma(t_1')) \mathrm{d}t_1' \cdots \mathrm{d}t_{n-1}' = \\
&= \sum_{n=0}^{\infty} \mathcal{A}(\dot\gamma(t)) \int_0^{t_n'} \int_0^{t_{n-1}'} \cdots \int_0^{t_2'} \mathcal{A}(\dot\gamma(t_n')) \cdots \mathcal{A}(\dot\gamma(t_1')) \mathrm{d}t_1' \cdots \mathrm{d}t_n' = \\
&= \mathcal{A}(\dot\gamma(t)) \sum_{n=0}^{\infty} \int_0^{t_n'} \int_0^{t_{n-1}'} \cdots \int_0^{t_2'} \mathcal{A}(\dot\gamma(t_n')) \cdots \mathcal{A}(\dot\gamma(t_1')) \mathrm{d}t_1' \cdots \mathrm{d}t_n' = \mathcal{A}(\dot\gamma(t)) U(t)
\end{aligned}$$

□

### Path-Ordered Exponential for Commuting $\mathcal{A}$s

In the case where individual $\mathcal{A}$'s commute the path ordered exponential reduces to the regular exponential. To see this we rewrite the $n$-th integral over the parameter variables $(t_k)_{k=1,\dots,n}$ via the set $\Delta_{12\dots n} = \{0 \leq t_1 \leq t_2 \leq \dots \leq t_n \leq t\}$

$$\begin{aligned}
&\int_0^t \int_0^{t_n'} \int_0^{t_{n-1}'} \cdots \int_0^{t_2'} \mathcal{A}(\dot\gamma(t_n')) \cdots \mathcal{A}(\dot\gamma(t_1')) \mathrm{d}t_1' \cdots \mathrm{d}t_n' = \\
&= \int_{\Delta_{12\dots n}} \prod_{k=n}^{1} \mathcal{A}(\dot\gamma(t_k')) \mathrm{d}^n t'
\end{aligned}$$

and note that the indices of the integration variables $(t_k)_{k=1,\dots,n}$ may be renamed, for example to a different permutation $\sigma = (\sigma(1), \dots, \sigma(n))$.

$$\int_{\Delta_{12\dots n}} \prod_{k=n}^{1} \mathcal{A}(\dot\gamma(t'_k))\mathrm{d}^n t' = \int_{\Delta_\sigma} \prod_{k=n}^{1} \mathcal{A}(\dot\gamma(t'_{\sigma(k)}))\mathrm{d}^n t'$$

It is now possible to show, that the union over all $n!$ sets $\Delta_\sigma$ is the $n$-dimensional hypercube $\bigcup_{\sigma\in\Pi(n)} \Delta_\sigma = [0,t]^n \subset \mathbb{R}^n$. Hence the integral can be recast into a new form by introducing the so-called time ordering operator $\mathcal{T}$ which takes care of the parameter ordering.

$$\begin{aligned}
&\int_0^t \int_0^{t'_n} \int_0^{t'_{n-1}} \cdots \int_0^{t'_2} \mathcal{A}(\dot\gamma(t'_n)) \cdots \mathcal{A}(\dot\gamma(t'_1))\mathrm{d}t'_1 \cdots \mathrm{d}t'_n = \\
&= \frac{1}{n!} \sum_{\sigma\in\Pi(n)} \int_{\Delta_\sigma} \prod_{k=n}^{1} \mathcal{A}(\dot\gamma(t'_{\sigma(k)}))\mathrm{d}^n t' = \frac{1}{n!} \int_{[0,t]^n} \mathcal{T}\left\{\mathcal{A}(\dot\gamma(t'_n)) \dots \mathcal{A}(\dot\gamma(t'_1))\right\} \mathrm{d}^n t'
\end{aligned}$$

Here it becomes clear, that commutativity of all $\mathcal{A}$ nullifies the effect of $\mathcal{T}$-ordering, as places can be swapped to ones liking. That together with the independence of integral boundaries in this expression enables the splitting of each parameter integral

$$\begin{aligned}
&\frac{1}{n!} \int_{[0,t]^n} \mathcal{T}\left\{\mathcal{A}(\dot\gamma(t'_n)) \dots \mathcal{A}(\dot\gamma(t'_1))\right\} \mathrm{d}^n t' = \\
&= \frac{1}{n!} \int_0^t \dots \int_0^t \mathcal{T}\left\{\mathcal{A}(\dot\gamma(t'_n)) \dots \mathcal{A}(\dot\gamma(t'_1))\right\} \mathrm{d}^n t' = \\
&= \frac{1}{n!} \int_0^t \dots \int_0^t \mathcal{A}(\dot\gamma(t'_n)) \dots \mathcal{A}(\dot\gamma(t'_1))\mathrm{d}^n t' = \\
&= \frac{1}{n!} \int_0^t \mathcal{A}(\dot\gamma(t'_n))\mathrm{d}t_n \dots \int_0^1 \mathcal{A}(\dot\gamma(t'_1))\mathrm{d}t_1 == \frac{1}{n!} \left(\int_0^t \mathcal{A}(\dot\gamma(t'_n))\mathrm{d}t'\right)^n
\end{aligned}$$

and summing up all integrals we obtain

$$\begin{aligned}
&\mathcal{P}\left\{\exp\left\{\int_0^t \mathcal{A}(\dot\gamma(t'))\mathrm{d}t'\right\}\right\} \\
&:= \sum_{n=0}^{\infty} \int_0^t \int_0^{t'_n} \int_0^{t'_{n-1}} \cdots \int_0^{t'_2} \mathcal{A}(\dot\gamma(t'_n)) \cdots \mathcal{A}(\dot\gamma(t'_1))\mathrm{d}t'_1 \cdots \mathrm{d}t'_n = \\
&= \sum_{n=0}^{\infty} \frac{1}{n!} \int_{[0,t]^n} \mathcal{T}\left\{\mathcal{A}(\dot\gamma(t'_n)) \dots \mathcal{A}(\dot\gamma(t'_1))\right\} \mathrm{d}^n t' = \\
&= \sum_{n=0}^{\infty} \frac{1}{n!} \left(\int_0^t \mathcal{A}(\dot\gamma(t'_n))\mathrm{d}t'\right)^n = \exp\{\int_0^t \mathcal{A}(\dot\gamma(t'_n))\mathrm{d}t'\}
\end{aligned}$$

This is for instance the case in Abelian gauge theories, such as Electromagnetism with the $U(1)$ group, or if $\mathcal{A}$ is constant along $\gamma$.

### 6.4.3 Parallel Transporter Around a Small Loop

We take a small closed loop consisting of four straight line segments around a parallelogram of dimension $\varepsilon^2$ with $\varepsilon << 1$ in space-time and expand its respective parallel transporter $U$ in terms of $\varepsilon$. Each line has a coordinate parametrization of the form $\gamma^\mu(t) = x^\mu + t\dot\gamma^\mu$ where $x^\mu$ represents the starting point, $t \in [0, \varepsilon]$ the parameter and $\dot\gamma^\mu$ the tangent vector. With the Taylor expansion of

$$\mathcal{A}_\nu(\gamma^\lambda(t)) = \mathcal{A}_\nu(x^\lambda + t\dot\gamma^\lambda) = \mathcal{A}_\nu(x^\lambda) + \partial_\mu \mathcal{A}_\nu(x^\lambda)\dot\gamma^\mu t + \mathcal{O}(t^2)$$

The parallel transporter up to $\mathcal{O}(\varepsilon^2)$ is then

$$\begin{aligned}
U[\gamma](\varepsilon) &= \mathcal{P}\left\{\exp\left\{\int_0^t \mathcal{A}(\dot\gamma(t))\mathrm{d}t'\right\}\right\} \\
&:= \sum_{n=0}^{\infty}\int_0^{\varepsilon}\int_0^{t'_n}\int_0^{t'_{n-1}}\cdots\int_0^{t'_2}\mathcal{A}(\dot\gamma(t'_n))\cdots\mathcal{A}(\dot\gamma(t'_1))\mathrm{d}t'_1\cdots\mathrm{d}t'_n \simeq \\
&\simeq \mathbb{1} + \int_0^{\varepsilon}\mathcal{A}_\nu(\gamma^\lambda(t'_1))\dot\gamma^\nu\mathrm{d}t'_1 + \int_0^{\varepsilon}\int_0^{t'_2}\mathcal{A}_\mu(\gamma^\lambda(t'_2))\mathcal{A}_\nu(\gamma^\lambda(t'_1))\dot\gamma^\mu\dot\gamma^\nu\mathrm{d}t'_1\mathrm{d}t'_2 + \mathcal{O}(\varepsilon^3) \simeq \\
&\simeq \mathbb{1} + \int_0^{\varepsilon}\mathcal{A}_\nu(x^\lambda)\dot\gamma^\nu + \partial_\mu\mathcal{A}_\nu(x^\lambda)\dot\gamma^\mu\dot\gamma^\nu t'_1\mathrm{d}t'_1 + \int_0^{\varepsilon}\int_0^{t'_2}\mathcal{A}_\mu(x^\lambda)\mathcal{A}_\nu(x^\lambda)\dot\gamma^\mu\dot\gamma^\nu\mathrm{d}t'_1\mathrm{d}t'_2 + \mathcal{O}(\varepsilon^3) = \\
&\simeq \mathbb{1} + \varepsilon\mathcal{A}_\nu(x^\lambda)\dot\gamma^\nu + \frac{\varepsilon^2}{2}\left(\partial_\mu\mathcal{A}_\nu(x^\lambda)\dot\gamma^\mu\dot\gamma^\nu + \mathcal{A}_\mu(x^\lambda)\mathcal{A}_\nu(x^\lambda)\dot\gamma^\mu\dot\gamma^\nu\right) + \mathcal{O}(\varepsilon^3).
\end{aligned}$$

The inverse parallel transporter associated to the curve $x^\mu+(\varepsilon-t)\dot\gamma^\mu$ but with the identical Taylor expansion of $\mathcal{A}_\nu$ as before (!) therefore delivers the same term with slightly different signs.

$$U^{-1}[\gamma](\varepsilon) \simeq \mathbb{1} - \varepsilon\mathcal{A}_\nu(x^\lambda)\dot\gamma^\nu + \frac{\varepsilon^2}{2}\left(-\partial_\mu\mathcal{A}_\nu(x^\lambda)\dot\gamma^\mu\dot\gamma^\nu + \mathcal{A}_\mu(x^\lambda)\mathcal{A}_\nu(x^\lambda)\dot\gamma^\mu\dot\gamma^\nu\right) + \mathcal{O}(\varepsilon^3).$$

Multiplying the parallel transporters of all four segments and keeping terms up to $\mathcal{O}(\varepsilon^2)$ we would obtain

$$U = \mathbb{1} + \varepsilon^2\left(\partial_\mu\mathcal{A}_\nu(x^\lambda) - \partial_\nu\mathcal{A}_\mu(x^\lambda) + [\mathcal{A}_\mu(x^\lambda),\mathcal{A}_\nu(x^\lambda)]\right)\dot\gamma^\mu_{(1)}\dot\gamma^\nu_{(2)} + \mathcal{O}(\varepsilon^3)$$

where the bracketed expression contains the components of the Yang-Mills field strength $\mathcal{F}_{\mu\nu}$. Thus,

$$U = \mathbb{1} + \varepsilon^2\mathcal{F}_{\mu\nu}\dot\gamma^\mu_{(1)}\dot\gamma^\nu_{(2)} + \mathcal{O}(\varepsilon^3). \tag{6.3}$$

## 6.5 Flux-tube Simulation Using Exterior Finite Elements

In this section we describe the intial conditions used in the simulation using standard exterior finite elements. We specify initial conditions for both fields $\mathcal{E}$ and $\mathcal{A}$ to model two colliding waves in three spatial dimensions. For simplicity we assume full symmetry in one spatial axis to enable an effective two-dimensional simulation. This means that the waves will propogate in cylinder like shapes which we will call flux-tubes. We will also apply gauge transformations to initial conditions, which will simplify it to so-called "vacuum gauge terms" as initially we have $\mathcal{A} = 0$.

### $z$-Symmetric Flux Tubes

We express everything in a coordinate system with labels $x^\mu = (x^0, x^1, x^2, x^3)^\mu = (t, x, y, z)^\mu$ where $t$ stands for time and the $z$-direction represents the symmetry axis. The initial conditions for one so-called flux-tube in polar coordinates

$$\begin{aligned}
\vec r &= (x, y) \\
\|\vec r\| &= \sqrt{r\cdot r} = \sqrt{x^2+y^2}, \phi = \arctan 2(y, x)
\end{aligned}$$

is given by starting values $\mathcal{A}$ and $\mathcal{E} = -\partial_t\mathcal{A}$ in temporal gauge.

$$\begin{aligned}
\mathcal{A}_k &= 0 \quad k = 1, 2, 3 \\
\mathcal{E}_k &= \delta_{kz}\mathcal{E}_0 e^{-\frac{\|\vec r\|^2}{2\sigma^2}}
\end{aligned}$$

where $\sigma \in \mathbb{R}^+$ represents the width of the distribution and $\mathcal{E}_0 \in \mathfrak{g}$ is the amplitude of the color field. These satisfy the previously mentioned Gauss constraint

$$\nabla_k\mathcal{E}^k = \partial_k\mathcal{E}^k + [\underbrace{\mathcal{A}_k}_{=0}, \mathcal{E}^k] = \partial_k\delta^k_z\mathcal{E}_0 e^{-\frac{\|\vec r\|^2}{2\sigma^2}} = \mathcal{E}_0\underbrace{\partial_z e^{-\frac{\|\vec r\|^2}{2\sigma^2}}}_{=0} = 0$$

A scenario in which non-linear terms show their effect would be two spatially separated flux-tubes centered around $\vec{p}_1 = (x_1, y_1)$ and $\vec{p}_2 = (x_2, y_2)$ with distinct color amplitudes $\mathcal{E}_1 \neq \mathcal{E}_2 \in \mathfrak{g}$ whose propagating waves are set for collision.

$$\begin{aligned}\mathcal{A}_k &= 0 \quad k = 1, 2, 3\\ \mathcal{E}_k &= \delta_{kz}\mathcal{E}_1 e^{-\frac{\|\vec{r}-\vec{p}_1\|^2}{2\sigma^2}} + \delta_{kz}\mathcal{E}_2 e^{-\frac{\|\vec{r}-\vec{p}_2\|^2}{2\sigma^2}} \quad k = 1, 2, 3\end{aligned}$$

Examinable Physical observables would be the longitudinal and transversal energies of electric and magnetic fields

$$H_{\mathcal{E},L} = \int_{M_S} \langle \mathcal{E}_z, \mathcal{E}_z \rangle_{\mathfrak{g}} \tag{6.4}$$

$$H_{\mathcal{B},L} = \int_{M_S} \langle \mathcal{B}_z, \mathcal{B}_z \rangle_{\mathfrak{g}} \tag{6.5}$$

$$H_{\mathcal{E},T} = \int_{M_S} \sum_{k=x,y} \langle \mathcal{E}_k, \mathcal{E}_k \rangle_{\mathfrak{g}} \tag{6.6}$$

$$H_{\mathcal{B},T} = \int_{M_S} \sum_{k=x,y} \langle \mathcal{B}_k, \mathcal{B}_k \rangle_{\mathfrak{g}} \tag{6.7}$$

### z-Splitting

The $z$-symmetry enables a reformulation to an effective $2+1$-dimensional space-time simulation where additional terms arise due to the $z$-components of fields. For this purpose we use index notation and split the $z$-components from the rest. We first look at the spatial exterior covariant derivative $\mathrm{d}_{\mathcal{A}}$ with connection 1-form $\mathcal{A} = \sum_{\mu=1}^{3} A_\mu^m \mathrm{d}x^\mu \otimes \tau_m$ acting on 0-forms $f \in \Lambda^0(M; \mathfrak{g})$, or in other words the gauge-covariant gradient.

$$\begin{aligned}\mathrm{d}_{\mathcal{A}} f &= \mathrm{d}f + [\mathcal{A}, g] = \\ &= \sum_{\mu=1}^{3} \partial_\mu f^m \mathrm{d}x^\mu \otimes \tau_m + [\sum_{\mu=1}^{3} A_\mu^n \mathrm{d}x^\mu \otimes \tau_n \wedge f^m \tau_m] = \\ &= \sum_{\mu=1}^{3} \left(\partial_\mu f^k + f_{nmk} A_\mu^n f^m\right) \mathrm{d}x^\mu \otimes \tau_k\end{aligned}$$

$$(\mathrm{d}_{\mathcal{A}} f)_\alpha^a = \partial_\alpha f_a + f_{mna} A_\alpha^m f_n = \begin{pmatrix} \partial_x f_a \\ \partial_y f_a \\ \partial_z f_a \end{pmatrix}_\alpha + f_{mna} \begin{pmatrix} A_x^m f_n \\ A_y^m f_n \\ A_z^m f_n \end{pmatrix}_\alpha$$

If there is no $z$-dependence in the expression then

$$(\mathrm{d}_{\mathcal{A}} f)_\alpha^a = \begin{pmatrix} \partial_x f_a + A_x^m f_n \\ \partial_y f_a + A_y^m f_n \\ A_z^m f_n \end{pmatrix}$$

where the $x$ and $y$ components can be regarded as the two-dimensional covariant derivative. We next look at the spatial exterior covariant derivative $\mathrm{d}_{\mathcal{A}}$ acting on 1-forms $f \in \Lambda^1(M; \mathfrak{g})$, or in other words the gauge-covariant curl. Here we skip a few similar steps and obtain

$$(\mathrm{d}_{\mathcal{A}} \mathcal{J})_\alpha^a = \sum_{\mu,\nu=1}^{3} \epsilon_{\alpha\mu\nu} \partial^\mu J_a^\nu + \epsilon_{\alpha\mu\nu} f_{amn} A_m^\mu J_n^\nu$$

We split parts in the second term into spatial dimensions $x, y, z$

$$\epsilon_{\alpha\mu\nu}A^\mu_m J^\nu_n = \begin{pmatrix}\epsilon_{x\mu\nu}A^\mu_m J^\nu_n\\ \epsilon_{y\mu\nu}A^\mu_m J^\nu_n\\ \epsilon_{z\mu\nu}A^\mu_m J^\nu_n\end{pmatrix}_\alpha = \begin{pmatrix}\epsilon_{xzy}A^z_m J^y_n + \epsilon_{xyz}A^y_m J^z_n\\ \epsilon_{yzx}A^z_m J^x_n + \epsilon_{yxz}A^x_m J^z_n\\ \epsilon_{z\mu\nu}A^\mu_m J^\nu_n\end{pmatrix}_\alpha = \begin{pmatrix}-A^z_m J^y_n + A^y_m J^z_n\\ A^z_m J^x_n - A^x_m J^z_n\\ \epsilon_{z\mu\nu}A^\mu_m J^\nu_n\end{pmatrix}_\alpha$$

to get

$$(\mathrm{d}_\mathcal{A}\mathcal{J})^a_\alpha = \begin{pmatrix}-\partial_z J^y_n + \partial_y J^z_a\\ \partial_z J^x_n - \partial_x J^z_a\\ \sum_{\mu,\nu=x,y}\epsilon_{z\mu\nu}\partial^\mu J^\nu_a\end{pmatrix}_\alpha + f_{amn}\begin{pmatrix}-A^z_m J^y_n + A^y_m J^z_n\\ A^z_m J^x_n - A^x_m J^z_n\\ \sum_{\mu,\nu=x,y}\epsilon_{z\mu\nu}A^\mu_m J^\nu_n\end{pmatrix}_\alpha$$

where the $z$-component can be interpreted as the covariant derivative in the $xy$-plane. Again, if there is no $z$-dependence we can simplify.

$$(\mathrm{d}_\mathcal{A}\mathcal{J})^a_\alpha = \begin{pmatrix}\partial_y J^z_a\\ -\partial_x J^z_a\\ \sum_{\mu,\nu=x,y}\epsilon_{z\mu\nu}\partial^\mu J^\nu_a\end{pmatrix}_\alpha + f_{amn}\begin{pmatrix}-A^z_m J^y_n + A^y_m J^z_n\\ A^z_m J^x_n - A^x_m J^z_n\\ \sum_{\mu,\nu=x,y}\epsilon_{z\mu\nu}A^\mu_m J^\nu_n\end{pmatrix}_\alpha$$

Similar terms arise when calculating and splitting the curvature components. But here the factor $1/2$ in front of the wedge bracket should be considered.

## Vacuum Gauge Terms

The gauge field $\mathcal{A} \in \Lambda^1(M;\mathfrak{g})$ transforms under gauge transformations $g \in C^\infty(M,G)$ as

$$\mathcal{A} \mapsto \mathrm{Ad}_g\mathcal{A} - \mathrm{d}gg^{-1} = g\mathcal{A}g^{-1} - \mathrm{d}gg^{-1}$$

Starting with a vanishing vacuum field $A = 0$, the first term will always remain 0 due to linearity of the adjoint map $\mathrm{Ad}_g 0 = 0$. The second term however $\mathrm{d}gg^{-1}$ can be in general distinct from $-\mathrm{d}gg^{-1} \neq 0$. Such fields are therefore called "pure gauge", as they do not vanish but are gauge equivalent to $\mathcal{A} = 0$. We evaluate such terms in the case of $su(2)$ using spatial coordinates $x^\mu$ and bases for the Lie algebra. Let $i\sigma(x) = i\phi(x)n^k(x)\sigma_k \in \mathfrak{g}$ be the Lie Algebra element with $\phi(x) \in \mathbb{R}$ and a normalized vector $(n_k)_{k=1,2,3} \in \mathbb{R}^3$ that represents the gauge transformation $g(x) \in G$ via the exponential map

$$g(x) = \exp(i\sigma(x)) = \cos(\phi(x))\mathbb{1} + i\sin(\phi(x))n^k(x)\sigma_k$$

$$g^{-1}(x) = \exp(-i\sigma(x)) = \cos(\phi(x))\mathbb{1} - i\sin(\phi(x))n^k(x)\sigma_k.$$

We evaluate derivatives of $g$

$$\begin{aligned}\partial_\mu g(x) &= \partial_\mu\left(\cos(\phi)\mathbb{1} + i\sin(\phi)n^k(x)\sigma_k\right) =\\ &= -\partial_\mu\phi\sin(\phi)\mathbb{1} + i\partial_\mu\phi\cos(\phi)n^k(x)\sigma_k + i\sin(\phi)\partial_\mu n^k(x)\sigma_k =\end{aligned}$$

to get an expression for the vacuum gauge term $\partial_\mu g g^{-1}$

$$\begin{aligned}&\partial_\mu g g^{-1} =\\ &= \left[-\partial_\mu\phi\sin(\phi)\mathbb{1} + i\partial_\mu\phi\cos(\phi)n^k(x)\sigma_k + i\sin(\phi)\partial_\mu n^k(x)\sigma_k\right]\left[\cos(\phi)\mathbb{1} - i\sin(\phi)n^l\sigma_l\right] =\\ &= -\partial_\mu\phi\sin(\phi)\cos(\phi)\mathbb{1} + \partial_\mu\phi\sin(\phi)\cos(\phi)\underbrace{(n^k\sigma_k)(n^l\sigma_l)}_{=n^k n_k=1} + \sin^2(\phi)\underbrace{(\partial_\mu n^k\sigma_k)(n^l\sigma_l)}_{\partial_\mu n^k n_k=0} +\\ &\quad + i\left(\partial_\mu\phi\sin^2(\phi)(n^k\sigma_k) + \partial_\mu\phi\cos^2(\phi)(n^k\sigma_k) + \sin(\phi)\cos(\phi)(\partial_\mu n^k\sigma_k)\right) =\\ &= i\left(\partial_\mu\phi n^k + \sin(\phi)\cos(\phi)\partial_\mu n^k\right)\sigma_k =\\ &= i\left(\partial_\mu\phi n^k + \frac{1}{2}\sin(2\phi)\partial_\mu n^k\right)\sigma_k\end{aligned}$$

The three dimensional vector $(\partial_\mu \phi n^k + \frac{1}{2}\sin(2\phi)\partial_\mu n^k)_{k=1,2,3} \in \mathbb{R}^3$ represents the Lie Algebra element of $\mathrm{d}gg^{-1}$ in the basis $(i\sigma_k)_{k=1,2,3}$. For numerical implementation we are interested in the Lie algebra basis where the Lie brackets coefficient representation (the structure constants) $f_{klm}$

$$[\tau_k, \tau_l] = f_{klm}\tau_m$$

are directly related to the cross product. In other words choose the basis $(\frac{1}{2i}\sigma_k)_{k=1,2,3}$ such that $f_{klm} = \varepsilon_{klm}$ where $\varepsilon$ stands for the 3-dimensional fully antisymmetric Levi Civita symbol.

$$\begin{aligned}
&[\sigma_k, \sigma_l] = 2i\varepsilon_{klm}\sigma_m \\
&\frac{1}{(2i)^2}[\sigma_k, \sigma_l] = \frac{1}{(2i)^2}2i\varepsilon_{klm}\sigma_m \\
&[\frac{1}{2i}\sigma_k, \frac{1}{2i}\sigma_l] = \varepsilon_{klm}\frac{1}{2i}\sigma_m
\end{aligned}$$

If $(\phi n_k)_{k=1,2,3} \in \mathbb{R}^3$ are the coefficients in the basis $(\frac{1}{2i}\sigma_k)_{k=1,2,3}$ then we can retrace the above steps with the modification $\phi \to -\frac{1}{2}\phi$.

$$\sigma(x) = \phi(x)n^k(x)\frac{1}{2i}\sigma_k = i\left(-\frac{1}{2}\phi(x)n^k(x)\right)\sigma_k$$

$$\begin{aligned}
g(x) = \exp(\sigma(x)) &= \cos\left(-\frac{1}{2}\phi(x)\right)\mathbb{1} + i\sin\left(-\frac{1}{2}\phi(x)\right)n^k(x)\sigma_k = \\
&= \cos\left(\frac{1}{2}\phi(x)\right)\mathbb{1} - i\sin\left(\frac{1}{2}\phi(x)\right)n^k(x)\sigma_k = \\
&= \cos\left(\frac{1}{2}\phi(x)\right)\mathbb{1} + \sin\left(\frac{1}{2}\phi(x)\right)n^k(x)\frac{1}{i}\sigma_k
\end{aligned}$$

$$\begin{aligned}
\partial_\mu g(x)g^{-1} = &= i\left(\partial_\mu(-\frac{1}{2}\phi)n^k + \frac{1}{2}\sin\left(2(-\frac{1}{2}\phi)\right)\partial_\mu n^k\right)\sigma_k = \\
&= i\left(-\frac{1}{2}\partial_\mu\phi n^k - \frac{1}{2}\sin(\phi)\partial_\mu n^k\right)\sigma_k = \\
&= -2\left(-\frac{1}{2}\partial_\mu\phi n^k - \frac{1}{2}\sin(\phi)\partial_\mu n^k\right)\frac{1}{2i}\sigma_k = \\
&= \left(\partial_\mu\phi n^k + \sin(\phi)\partial_\mu n^k\right)\frac{1}{2i}\sigma_k
\end{aligned}$$

## 6.6 Dual Wilson Action

Using a discrete connection comparable to that in Regge calculus, we first introduce some notation for parallel transporters $U$ and plaquette variables $W$

- All cells/simplices of maximal dimension are indexed by numbers.
- $U_{ij}$ is a parallel transporter passing from the $i$-th to the $j$-th cell parametrized via the exponential map $U_{ij} = \exp\{\mathcal{A}_{ij}\}$
- $U_I$ is the parallel transporter belonging to the oriented interface $I$ connecting two cells.
- $\mathcal{A}_I$ are the components of the parallel transporter $U_I = \exp\{\mathcal{A}_I\}$ belonging to the oriented interface $I$ connecting two cells.
- The inverse parallel transporter represents $U_{ji} = U_{ij}^\dagger$

- $U_{ijk}$ is a parallel transporter passing from the $i$-th to the $j$-th and finally the $k$-th cell, in that order.
- LGT multiplication convention: $U_{ijk} = U_{ij}U_{jk}$.
- $W_{ijk}$ is a loop of parallel transporters starting at the $i$-th cell and passing through the other cells in that order.
- $W_B$ is a loop of parallel transporters going around the bone $B$ (edges in 3D) that carries an orientation.

and use the mass-lumped dual Wilson action in 4.21

$$S = \sum_{B\in\mathcal{S}_{n-2}} C_{BB}\langle(\mathbb{1} - W_B)(\mathbb{1} - W_B)^\dagger\rangle_{\mathfrak{g}} + \sum_{F\in\mathcal{S}_{n-1}} \int_F \langle\left(\hat{\mathcal{J}}_F\right)_{\hat{n}}, \mathcal{A}_F\rangle_{\mathfrak{g}} \tag{6.8}$$

where $W_B$ represents the plaquette variable associated to the bone $B$ and $C_{BB}$ stand for respective weights.

## Variation

### Variation of the Approximate Mass-Lumped Gauge Field Part

To vary the gauge field part of 6.8 with respect to individual parallel transporters we apply the group derivative 61. Varying $U = \exp\{\mathcal{A}\} \in G$ in the fundamental representation with respect to a perturbation $\delta\mathcal{A} = \delta A^k \tau_k \in \mathfrak{g}$ with the Lie algebra basis $t_k = \frac{1}{i}\sigma_k$ we get

$$\delta U = \delta\mathcal{A}\exp\{\mathcal{A}\} = \delta A^k \tau_k U.$$

For the inverse $U^{-1} = U^\dagger$ we get

$$\delta(U^{-1}) = \delta(U^\dagger) = -\exp\{-A\}\delta A = -\delta A^k U^\dagger \tau_k.$$

We vary the term

$$\langle(\mathbb{1} - W_B)(\mathbb{1} - W_B)^\dagger\rangle_{\mathfrak{g}} = \mathrm{Re}\,\mathrm{Tr}\Big\{(\mathbb{1} - W_B)(\mathbb{1} - W_B)^\dagger\Big\}$$

that is present in the action and contains a particular plaquette $W_B$.

$$\begin{aligned}\delta\,\mathrm{Re}\,\mathrm{Tr}\Big\{(\mathbb{1} - W_B)(\mathbb{1} - W_B)^\dagger\Big\} &= \mathrm{Re}\,\mathrm{Tr}\Big\{\delta(\mathbb{1} - W_B)(\mathbb{1} - W_B)^\dagger\Big\} + \mathrm{Re}\,\mathrm{Tr}\Big\{(\mathbb{1} - W_B)\delta(\mathbb{1} - W_B)^\dagger\Big\} = \\ &= \mathrm{Re}\,\mathrm{Tr}\Big\{-\delta W_B(\mathbb{1} - W_B)^\dagger + (\mathbb{1} - W_B)\delta W_B^\dagger\Big\} = \\ &= \mathrm{Re}\,\mathrm{Tr}\Big\{-\delta W_B(\mathbb{1} - W_B)^\dagger + \mathrm{h.c.}\Big\}\end{aligned}$$

Taking an exemplary plaquette $W_B = W_{123} = U_{12}U_{23}U_{31}$ and varying it $\delta W_B$ with respect to the middle transporter $U_{23}$ we obtain

$$\delta W_B = \delta(U_{12}U_{23}U_{31}) = U_{12}\delta U_{23}U_{31} = U_{12}\delta A^k_{23}\tau_k U_{23}U_{31} = \delta A^k_{23} U_{12}\tau_k U_{23}U_{31}.$$

For the inverse loop $W_B^\dagger = W_{132} = U_{13}U_{32}U_{21}$

$$\delta(W_B^\dagger) = U_{13}\delta U_{32}U_{21} = U_{13}\delta(-A^k_{23})U_{32}t_k U_{21} = -\delta A^k_{23}U_{13}U_{32}\tau_k U_{21}$$

we note that care needs to be taken with regard to the ordering. Using cyclicity of the trace we rearrange the term that contains $W_{123}$

$$\begin{aligned}\mathrm{Re}\,\mathrm{Tr}\Big\{-\delta W_{123}(\mathbb{1} - W_{123})^\dagger\Big\} &= \mathrm{Re}\,\mathrm{Tr}\Big\{-\delta A^k_{23}U_{12}\tau_k U_{23}U_{31}(\mathbb{1} - U_{13}U_{32}U_{21})\Big\} = \\ &= -\delta A^k_{23}\,\mathrm{Re}\,\mathrm{Tr}\{U_{12}\tau_k U_{23}U_{31}\} + \delta A^k_{23}\,\mathrm{Re}\,\mathrm{Tr}\{U_{12}\tau_k U_{23}U_{31}U_{13}U_{32}U_{21})\} = \\ &= -\delta A^k_{23}\,\mathrm{Re}\,\mathrm{Tr}\{U_{12}\tau_k U_{23}U_{31}\} + \delta A^k_{23}\,\mathrm{Re}\,\mathrm{Tr}\{\tau_k\} = -\delta A^k_{23}\,\mathrm{Re}\,\mathrm{Tr}\{\tau_k W_{231}\}.\end{aligned}$$

Analogously for the loop $W_{321}$ that contains the inverse $U_{23}^{-1} = U_{32}$ we obtain

$$\begin{aligned}\operatorname{Re}\operatorname{Tr}\Big\{-\delta W_{321}(\mathbb{1}-W_{321})^\dagger\Big\} &= \operatorname{Re}\operatorname{Tr}\Big\{\delta A^k_{23} U_{32}\tau_k U_{21}U_{13}(\mathbb{1}-U_{31}U_{12}U_{23})\Big\} = \\ &= \delta A^k_{23}\operatorname{Re}\operatorname{Tr}\{U_{32}\tau_k U_{21}U_{13}\} + \delta A^k_{23}\operatorname{Re}\operatorname{Tr}\{U_{32}\tau_k U_{21}U_{13}U_{31}U_{12}U_{23})\} = \\ &= \delta A^k_{23}\operatorname{Re}\operatorname{Tr}\{U_{32}\tau_k U_{21}U_{13}\} + \delta A^k_{23}\operatorname{Re}\operatorname{Tr}\{\tau_k\} = \delta A^k_{23}\operatorname{Re}\operatorname{Tr}\{\tau_k W_{213}\}\end{aligned}$$

an opposite sign as well as a seemingly different ordering. But in all cases, the generator $t_k$ always precedes the parallel transporter $U_{kl}$ which starts at the same element $k$ as the one varied.

The variation of the gauge part with respect to a single link $U_I$ for an element-interface $I$ in total yields a term that contains all plaquettes $W_{B'}$ connected with $U_I$

$$\begin{aligned}\delta_{U_I} S &= \sum_{B':U_I\in W_{B'}} C_{B'B'}\delta_U \operatorname{Re}\operatorname{Tr}\Big\{(\mathbb{1}-W_{B'})(\mathbb{1}-W_{B'})^\dagger\Big\} = \\ &= \sum_{B':U_I\in W_{B'}} C_{B'B'}\operatorname{Re}\operatorname{Tr}\Big\{-\delta W_{B'}(\mathbb{1}-W_{B'})^\dagger + \text{h.c.}\Big\} = \\ &= \sum_{B':U_I\in W_{B'}} C_{B'B'} 2\operatorname{Re}\operatorname{Tr}\Big\{-\delta W_{B'}(\mathbb{1}-W_{B'})^\dagger\Big\} = \\ &\simeq \delta A^a_{U_I}\sum_{B':U_I\in W_{B'}} C_{B'B'}(-1)^{\sigma(B',U_I)} 2\operatorname{Re}\operatorname{Tr}\{t_a W_{B'}\}\end{aligned}$$

which contains expressions involving only loops $W_{B'}$ which contain this particular link $U_I$, as indicated by the sum. The order and sign $(-1)^{\sigma(W_{B'},U_I)}$ of $W_{B'}$ needs to be chosen carefully according to relative orientations: $W_{B'}$ and $U_I$ always start in the same element, a minus sign $\sigma(W_{B'},U_I) = -1$ is picked up when $W_{B'}$ uses the conjugate link $U_I^\dagger = U^{-1}$. We set the variation to 0 to obtain the discrete Yang-Mills equations in the absence of currents

$$\sum_{B':U_I\in W_{B'}} C_{B'B'}(-1)^{\sigma(W_{B'},U_I)} 2\operatorname{Re}\operatorname{Tr}\{t_a W_{B'}\} = 0 \quad \forall U_I.$$

### Variation of the Current Source Term

For the coupling term in 6.8 of the form $\langle\left(\hat{\mathcal{J}}\right)_{\hat{n}}, \mathcal{A}\rangle_{\mathfrak{g}}$ with $\mathcal{A} = \ln U$, the group derivative of definition 61 would require the evaluation of

$$\delta_{\mathcal{A}'}\mathcal{A} := \frac{\mathrm{d}}{\mathrm{d}t}|_{t=0} \ln\left(e^{t\delta\mathcal{A}}U\right)$$

with the matrix logarithm ln. This however yields an expression which (due to non-commutativity) is qualitatively similar to equation 2.17 and therefore can not be easily evaluated. For simplicity we evade this complication by linearly varying $\mathcal{A} = \ln W \in \mathfrak{g}$ in the Lie algebra $\mathfrak{g}$ directly, even though this is not fully consistent with the group derivative.

Linear Variation of the source term in 6.8 with respect to the Lie algebra components $\mathcal{A}$ yields

$$\int\langle\left(\hat{\mathcal{J}}\right)_{\hat{n}}, \mathcal{A}\rangle_{\mathfrak{g}} \xrightarrow{\delta\mathcal{A}} \int\langle\left(\hat{\mathcal{J}}\right)_{\hat{n}}, \delta\mathcal{A}\rangle_{\mathfrak{g}} = \langle\int\left(\hat{\mathcal{J}}\right)_{\hat{n}}, \delta\mathcal{A}\rangle_{\mathfrak{g}}.$$

We rewrite the expression

$$\begin{aligned}\langle\int\left(\hat{\mathcal{J}}\right)_{\hat{n}}, \delta\mathcal{A}\rangle_{\mathfrak{g}} &= \langle\delta\mathcal{A}, \int\left(\hat{\mathcal{J}}\right)_{\hat{n}}\rangle_{\mathfrak{g}} = \\ &= \langle\delta A^a\tau_a, \int\left(\hat{\mathcal{J}}\right)_{\hat{n}}\rangle_{\mathfrak{g}} = \\ &= \delta A^a\langle\tau_a, \int\left(\hat{\mathcal{J}}\right)_{\hat{n}}\rangle_{\mathfrak{g}} = \\ &= \delta A^a\operatorname{Re}\operatorname{Tr}\left\{\tau_a\int\left(\hat{\mathcal{J}}\right)^\dagger_{\hat{n}}\right\} = -\delta A^a\operatorname{Re}\operatorname{Tr}\left\{\tau_a\int\left(\hat{\mathcal{J}}\right)_{\hat{n}}\right\}\end{aligned}$$

and can complement the previous gauge field part in equation 6.9 to incorporate external color currents.

$$\sum_{B:U_I\in W_B} 2C_{BB}(-1)^{\sigma(W_B,U_I)}\operatorname{Re}\operatorname{Tr}\{t_a W_B\} - \operatorname{Re}\operatorname{Tr}\left\{\tau_a \int_I \left(\hat{\mathcal{J}}\right)_{\hat{n}}\right\} = 0$$

$$\sum_{B:U_I\in W_B} 2C_{BB}(-1)^{\sigma(W_B,U_I)}\operatorname{Re}\operatorname{Tr}\{t_a W_B\} = \operatorname{Re}\operatorname{Tr}\left\{\tau_a \int_I \left(\hat{\mathcal{J}}\right)_{\hat{n}}\right\} \tag{6.9}$$

Note that the upwind values $\hat{\mathcal{J}}$ implicitly contain parallel transporters depending upon the side on which the desired value resides. These equations are from a purely structural point of view similar to those obtainable from real time lattice gauge theory on a dual mesh. One noticeable difference is, that the continuous current $\mathcal{J}$ needs to be integrated per element face $F$.

### 6.6.1 Implementation for $SU(2)$

In the simulation we focus on the special case of $SU(2)$. Let $U = u_0\mathbb{1} + u_k\tau_k$. we have that $\operatorname{Re}\operatorname{Tr}\{\tau_k U\} = \operatorname{Re}\operatorname{Tr}\{\tau_k U\}$ picks out the vectorial part $u_k$

$$\begin{aligned}
\operatorname{Re}\operatorname{Tr}\{\tau_k U\} &= \operatorname{Re}\operatorname{Tr}\{\tau_a U\} = && (6.10)\\
&= \operatorname{Re}\operatorname{Tr}\{\tau_a u_\mu \tau_\mu\} = && (6.11)\\
&= \operatorname{Re}\operatorname{Tr}\left\{\frac{1}{i}\sigma_a u_\mu \frac{1}{i}\sigma_\mu\right\} = && (6.12)\\
&= \operatorname{Re}\operatorname{Tr}\{-u_\mu\sigma_a\sigma_\mu\} = && (6.13)\\
&= -u_\mu \operatorname{Re}\operatorname{Tr}\{\sigma_a\sigma_\mu\} = && (6.14)\\
&= -u_\mu \operatorname{Re}\operatorname{Tr}\{\delta_{a\mu}\mathbb{1}\} = && (6.15)\\
&= -u_\mu\delta_{a\mu}\operatorname{Re}\operatorname{Tr}\{\mathbb{1}\} = -2u_a && (6.16)
\end{aligned}$$

The rearranged discrete Yang Mills equations in 4.25 describe the evolution of $W_{E^+}$'s vectorial parts $(W_{E^+})_a$. This also uniquely fixes $(W_{E^+})_0$ near the identity using the formula

$$U = \sqrt{1 - u_l u_l}\mathbb{1} + u_k\tau_k.$$

If temporal gauge is chosen, then $W_{E^+} = U_{F^+}U_F^\dagger$. The updated spatial link in the next time-slice $U_{F^+}$ can be then reconstructed using the old link $U_F$ via

$$U_{F^+} = W_{E^+}U_F.$$

## 6.7 Charge Evolution

### 6.7.1 Global Charge - Not Conserved

We start with the weak non-Abelian transport equation reformulated in 4.14.

$$\int_M \langle\partial_t\rho,\phi\rangle_{\mathfrak{g}} + \int_{\partial M} n_k u^k\langle\rho,\phi\rangle_{\mathfrak{g}} - \int_M u^k\langle\rho,\partial_k\phi\rangle_{\mathfrak{g}} + \int_M u^k\langle[\mathcal{A}_k,\rho],\phi\rangle_{\mathfrak{g}} = 0$$

with a transporting wind $u^k$. We want to analyze under which circumstances we can expect global charge conservation. The interpretation of parallel transporting point particles using $SU(N)$ elements is a (complex) rotation in color space. Based on this idea one quantity one could analyze is the integral of the gauge-independent norm $\int_M \sqrt{\langle\rho(t),\rho(t)\rangle_{\mathfrak{g}}}$ per time-slice $t$

$$Q(t) = \int_M \sqrt{\langle\rho(t),\rho(t)\rangle_{\mathfrak{g}}}.$$

We formally evaluate an expression for the change of $Q$ over time

$$\begin{aligned}
\partial_t Q &= \partial_t \int_M \sqrt{\langle \rho, \rho \rangle_{\mathfrak{g}}} = \\
&= \int_M \partial_t \sqrt{\langle \rho, \rho \rangle_{\mathfrak{g}}} = \\
&= \int_M \frac{1}{\sqrt{\langle \rho, \rho \rangle_{\mathfrak{g}}}} \langle \partial_t \rho, \rho \rangle_{\mathfrak{g}} = \\
&= \int_M \langle \partial_t \rho, \frac{\rho}{\sqrt{\langle \rho, \rho \rangle_{\mathfrak{g}}}} \rangle_{\mathfrak{g}} = \\
&= \int_M u^k \langle \rho, \partial_k \left( \frac{\rho}{\sqrt{\langle \rho, \rho \rangle_{\mathfrak{g}}}} \right) \rangle_{\mathfrak{g}} - \int_{\partial M} n_k u^k \langle \rho, \frac{\rho}{\sqrt{\langle \rho, \rho \rangle_{\mathfrak{g}}}} \rangle_{\mathfrak{g}} - \int_M u^k \langle [\mathcal{A}_k, \rho], \frac{\rho}{\sqrt{\langle \rho, \rho \rangle_{\mathfrak{g}}}} \rangle_{\mathfrak{g}}
\end{aligned}$$

We alternatively rewrite $\rho$ using a decomposition $\rho = \|\rho\|_{\mathfrak{g}} e_\rho$ into a modulus $\|\rho\|_{\mathfrak{g}} = \sqrt{\langle \rho, \rho \rangle_{\mathfrak{g}}}$ and a normalized color direction field $e_\rho$ which satisfies $\langle e_\rho, e_\rho \rangle_{\mathfrak{g}} = 1$ (no implied summation over $\rho$, as it does not stand for an index in the sum conventional sense).

$$\begin{aligned}
\partial_t Q &= \int_M u^k \langle \|\rho\|_{\mathfrak{g}} e_\rho, \partial_k e_\rho \rangle_{\mathfrak{g}} - \int_{\partial M} n_k u^k \langle \|\rho\|_{\mathfrak{g}} e_\rho, e_\rho \rangle_{\mathfrak{g}} - \int_M u^k \langle [\mathcal{A}_k, \|\rho\|_{\mathfrak{g}} e_\rho], e_\rho \rangle_{\mathfrak{g}} = \\
&= \int_M u^k \|\rho\|_{\mathfrak{g}} \langle e_\rho, \partial_k e_\rho \rangle_{\mathfrak{g}} - \int_{\partial M} n_k u^k \|\rho\|_{\mathfrak{g}} - \int_M u^k \|\rho\|_{\mathfrak{g}} \langle [\mathcal{A}_k, e_\rho], e_\rho \rangle_{\mathfrak{g}} = \\
&= \int_M u^k \|\rho\|_{\mathfrak{g}} \frac{1}{2} \partial_k \underbrace{\langle e_\rho, e_\rho \rangle_{\mathfrak{g}}}_{=1} - \int_{\partial M} n_k u^k \|\rho\|_{\mathfrak{g}} - \int_M u^k \|\rho\|_{\mathfrak{g}} \underbrace{\langle [\mathcal{A}_k, e_\rho], e_\rho \rangle_{\mathfrak{g}}}_{=0} = - \int_{\partial M} n_k u^k \|\rho\|_{\mathfrak{g}}
\end{aligned}$$

The remaining term represents the current influx through the boundary $\partial M$. While this seems to be a satisfactory result, we need to note the restrictions imposed on $e_\rho$ during this manipulation. In particular, the formula $\partial_k \langle e_\rho, e_\rho \rangle_{\mathfrak{g}} = 0$ requires $e_\rho$ to be smooth, which could be difficult to achieve if regions with vanishing charges are present and $e_\rho$ may be discontinuous. Furthermore, the derivative of the square root $\sqrt{\langle \rho, \rho \rangle_{\mathfrak{g}}}$ could become problematic for vanishing values as well. Because of these complications further investigation is needed in order to understand global charge conservation in this context.

### 6.7.2 Group Derivative of the Gauss Constraint Error Function

We evaluate the group derivative $\delta_{\mathcal{A}_{E'}} L[W_E]$ of the error function in 4.28 with respect to a perturbation of the parallel transporter $U_{E'} = \exp\{\mathcal{A}_{E'}\}$ associated to a particular edge $E'$.

$$\begin{aligned}
\delta_{\mathcal{A}'_{E'}} L &= \delta_{\mathcal{A}'_{E'}} \sum_T \sum_a \left(G_a^T\right)^2 = \\
&= \sum_{T : E' \in \partial T} \sum_a \delta_{\mathcal{A}'_{E'}} \left[ \left(G_a^T\right)^2 \right] = \\
&= \sum_{T : E' \in \partial T} \sum_a 2 \delta_{\mathcal{A}'_{E'}} G_a^T G_a^T = \\
&= \sum_{T : E' \in \partial T} \sum_a \sum_{E \in \partial T} 4 C_{EE} \delta_{\mathcal{A}'_{E'}} \operatorname{Re} \operatorname{Tr}\{\tau_a W_E^T\} G_a^T = \\
&= \sum_{T : E' \in \partial T} \sum_a \sum_{E \in \partial T} 4 C_{EE} \operatorname{Re} \operatorname{Tr}\left\{\tau_a \delta_{\mathcal{A}'_{E'}} W_E^T\right\} G_a^T = \\
&= \sum_{T : E' \in \partial T} \sum_a 4 C_{E'E'} \operatorname{Re} \operatorname{Tr}\left\{\tau_a \delta_{\mathcal{A}'_{E'}} W_{E'}\right\} G_a^T =
\end{aligned}$$

The term $\delta_{\mathcal{A}'_{E'}} W^T_{E'}$ only remains for those loops $W^T_E$ which utilize $\mathcal{A}_{E'}$ in some manner, either in matching or opposing directions. This misalignment of respective orientations needs to be taken into account by including a relative sign as well as a different ordering between $\mathcal{A}_{E'}$ and links in $W^T_E$ in the variation as described in section 6.3.3.For matching directions of $\mathcal{A}_{E'}$ and $W^T_{E'} = U^+_{E'}(U^-_{E'})^\dagger$ we therefore have

$$\begin{aligned}\delta_{\mathcal{A}'_{E'}} W^T_{E'} &= \delta_{\mathcal{A}'_{E'}} U^+_{E'}(U^-_{E'})^\dagger \\ &= \mathcal{A}'_{E'} U^+_{E'}(U^-_{E'})^\dagger\end{aligned}$$

while for unmatching directions of $\mathcal{A}_{E'}$ and $W^T_E = (U^+_{E'})^\dagger U^-_{E'}$ we have

$$\begin{aligned}\delta_{\mathcal{A}'_{E'}} W^T_{E'} &= \delta_{\mathcal{A}'_{E'}} (U^+_{E'})^\dagger U^-_{E'} \\ &= -(U^+_{E'})^\dagger \mathcal{A}'_{E'} U^-_{E'}\end{aligned}$$

### 6.7.3 Conservation of Gauss Constraint

Given a spatially static mesh we symbolically prove, that the Gauss constraint is preserved through time if the associated equations of motion are applied. For this purpose, we will be using an exemplary mesh depicted in figure 6.1 with three time-slices labelled with symbols $-, 0, +$ and numbered vertices.

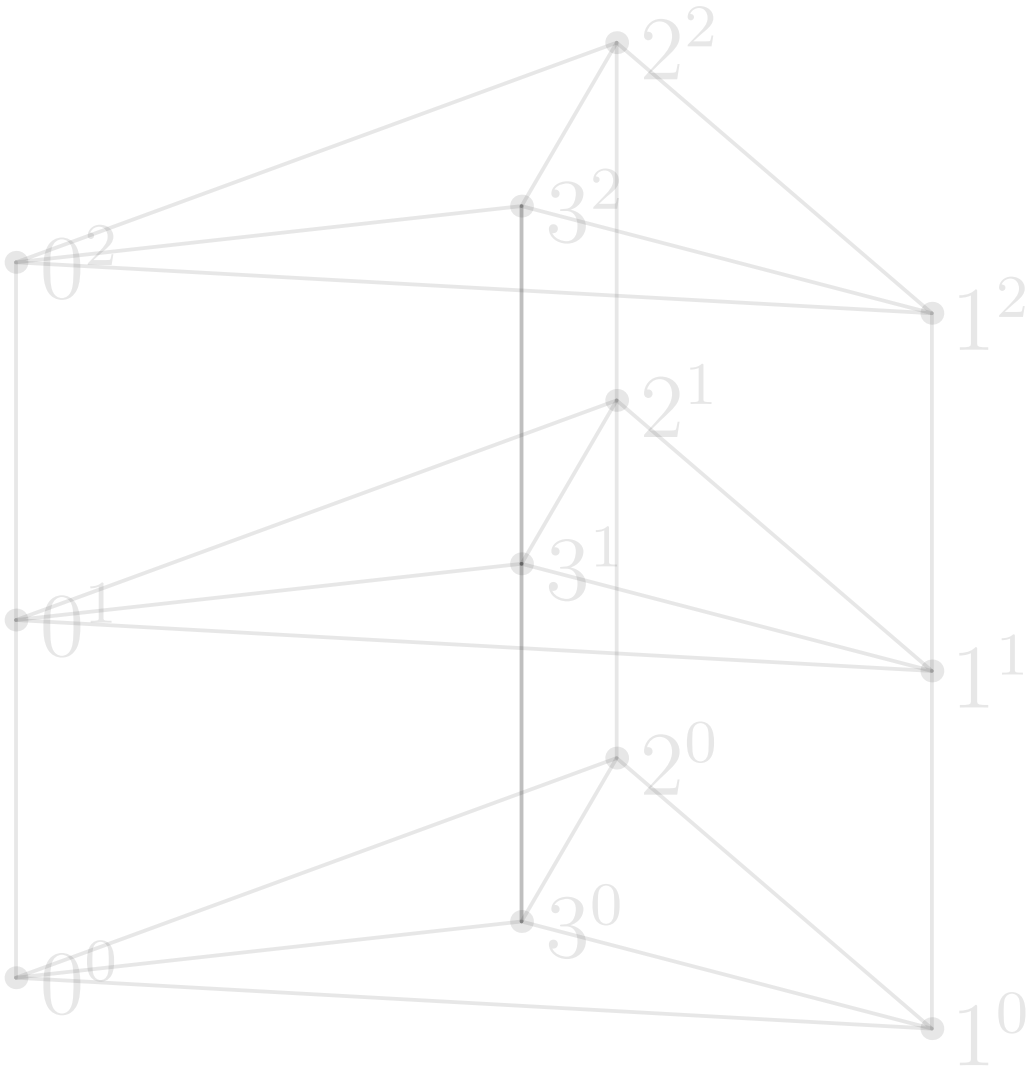


Figure 6.1: The exemplary lattice used to demonstrate the conservation of the Gauss constraint during time stepping simulations.

Let us assume that the Gauss constraint for the edge $E_{0^-0^0}$ connecting vertices $0^-$ and $0^0$ and the time stepping relation between all slices $-, 0, +$ as discussed in the previous section hold true. In this setting, we

visualize the term which arises when varying $W_{3^1 0^1 1^1 1^1}$-containing terms in the action with respect to a parallel transporter $U_{3^1 0^1}$ as indicated in figure 6.2 using an oriented loop with a dashed line. We symbolically add

$$2C_{013}\,\mathrm{Re}\,\mathrm{Tr}\{t_a W_{3^1 0^1 1^1 1^1}\} = 2\,\mathrm{Re}\,\mathrm{Tr}\{t_a U_{3^1 0^1} U_{0^1 1^1} U_{1^1 3^1}\} =$$

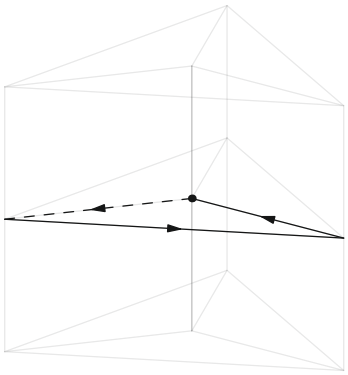

Figure 6.2: Symbolic illustration of the variation of a plaquette with respect to a parallel transporter

the terms of loops present in the variation 6.9 by combining the corresponding images as illustrated in the figure 6.3. We will include the weights $C$ here as well and will see that their exact values do not play a role here. The formula 6.16 implies that the sum of a pair of similar loops which start at the same point but are

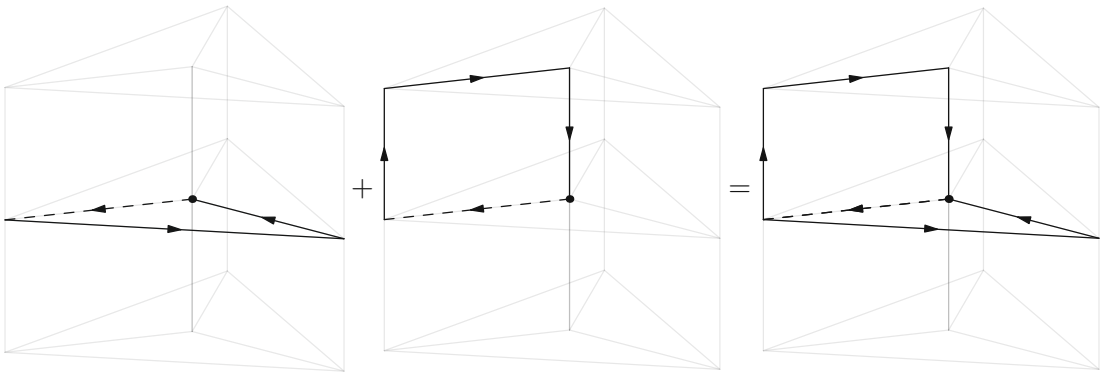

Figure 6.3: Symbolic addition of loop terms in the variation

reversely oriented to each other vanishes. This is because the respective parallel transporters $W$ and $W^\dagger$ are inverses of each other and respective $SU(2)$ coefficients satisfy $(W^\dagger)_a = -(W)_a$.

$$\mathrm{Re}\,\mathrm{Tr}\{t_a W\} + \mathrm{Re}\,\mathrm{Tr}\left\{t_a W^\dagger\right\} = -2(W)_a - 2(W^\dagger)_a = -2(W)_a + 2(W)_a = 0$$

As an example take the expression with opposing loops $W_{3^1 0^1 1^1 1^1}$ and $W_{3^1 1^1 0^1 1^1}$

$$2C_{013}\,\mathrm{Re}\,\mathrm{Tr}\{t_a W_{3^1 0^1 1^1 1^1}\} + 2C_{013}\,\mathrm{Re}\,\mathrm{Tr}\{t_a W_{3^1 1^1 0^1 1^1}\} = 0$$

which we pictorially represent via the equation in figure 6.4.

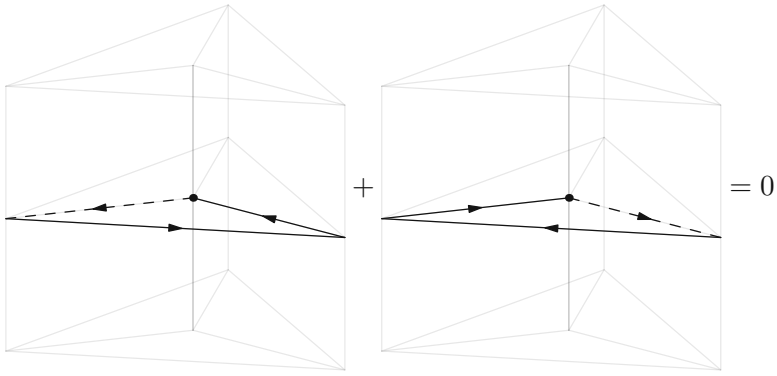


Figure 6.4: Symbolic illustration of how two loop terms cancel each other out.

With this notation we can draw the Gauss constraint involving the later time-slices in figure 6.5 where the drawing on the right side represents the charge $\rho$ associated to the respective temporal edge, or in terms of the space-time formalism, the temporal component of the space-time current.

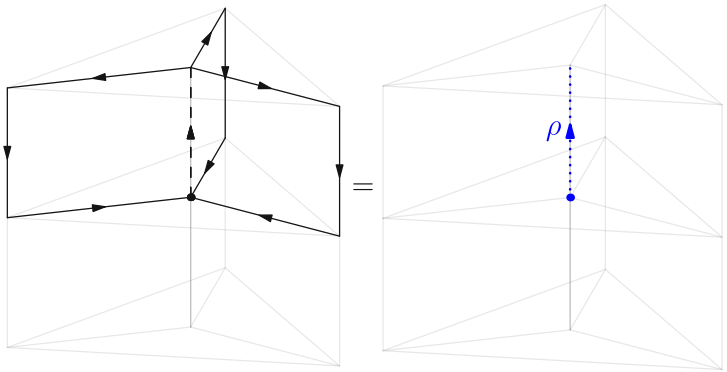


Figure 6.5: Symbolical representation of the Gauss constraint in the later time-slice

While we may draw a virtually identical diagram for the Gauss constraint involving earlier time-slices, it is instructive to use an equivalent equation which can be obtained by variation of temporal links in the negative time direction as symbollically illustrated in figure 6.6.

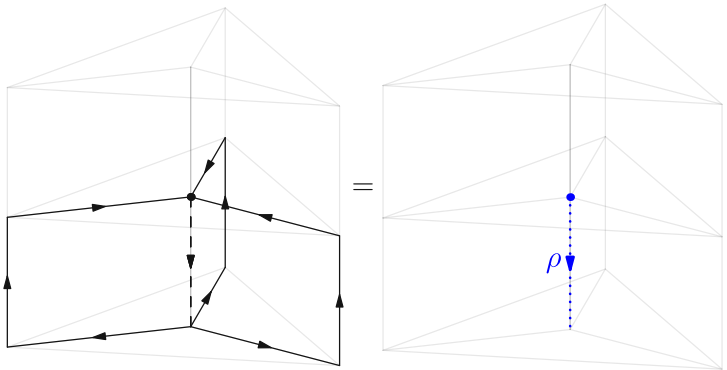


Figure 6.6: Symbolical representation of the Gauss constraint in the previous time-slice

This way all loop terms start at the same point, in this case $3^1$, and may be directly compared. The equations of motion for a single link can be analogously represented by figure 6.7 where the right side stands

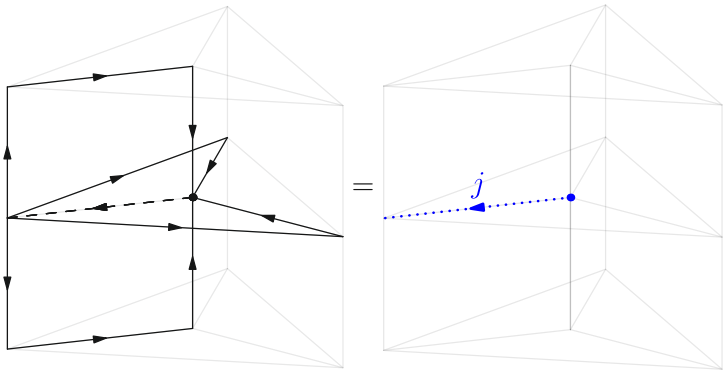


Figure 6.7: Symbolical representation of the equations of motion for a single link.

for the temporal current associated to the spatial edge. With this notation at hand we combine equations in figures 6.8, 6.9, 6.10, 6.11

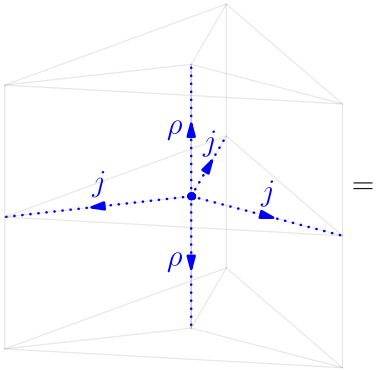


Figure 6.8: Symbolical summation of the charge current divergence at a (dual) vertex.

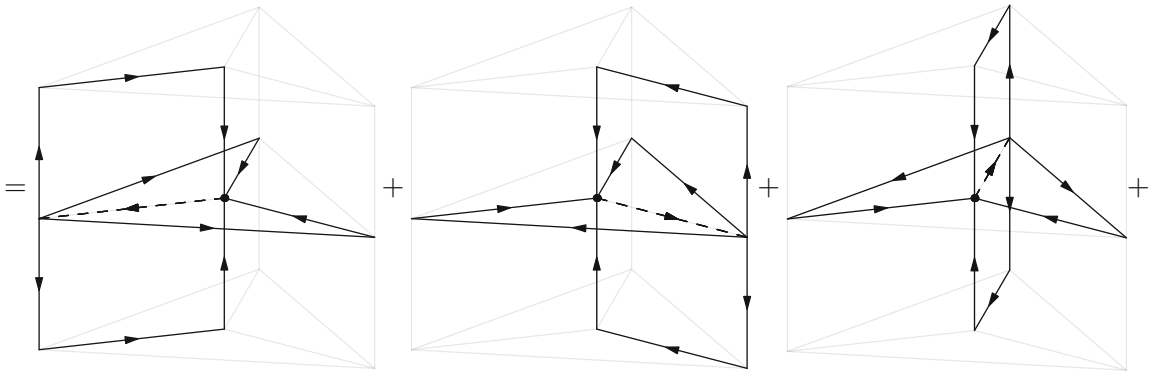


Figure 6.9: Symbolical summation of the equations of motion for each dashed edge.

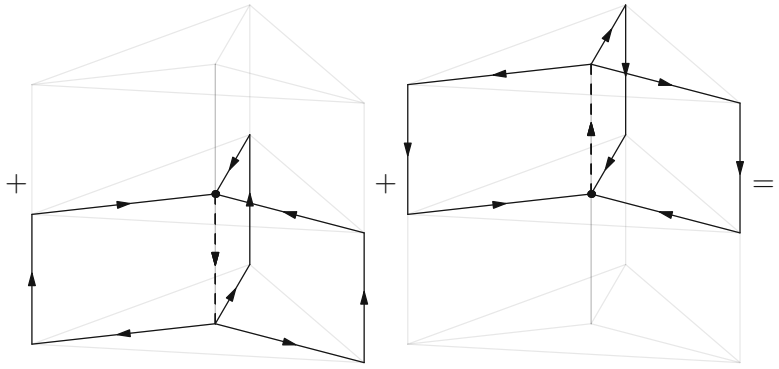

Figure 6.10: Symbolical summation of the Gauss constraint for both time-slices.

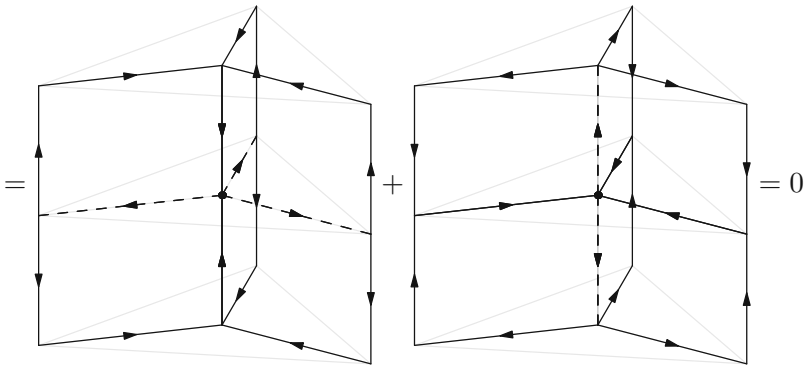

Figure 6.11: This leads to cancellation of all terms.

and notice, that all loops cancel out. Under the assumptions (Gauss constraint for the earlier time-slices and and equations of motion for each direction illustrated in figures 6.6 and 6.7) we infer that the Gauss constraint involving later time-slices of figure 6.5 holds if the symbolic equation in figure 6.12 representing

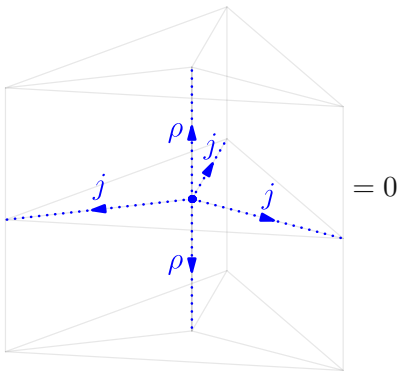


Figure 6.12: Symbolic continuity equation

the discrete non-Abelian continuity equation holds. As a consequence we also have that in the absence of any currents and charges the Gauss constraint is per default preserved in future time steps.

# Bibliography


[1] Simon L Altmann. *Rotations, quaternions, and double groups*. Courier Corporation, 2005.

[2] Douglas Arnold, Richard Falk, and Ragnar Winther. Finite element exterior calculus: from hodge theory to numerical stability. *Bulletin of the American mathematical society*, 47(2):281–354, 2010.

[3] Douglas N Arnold. *Finite element exterior calculus*. SIAM, 2018.

[4] Douglas N Arnold, Richard S Falk, and Ragnar Winther. Finite element exterior calculus, homological techniques, and applications. *Acta numerica*, 15:1–155, 2006.

[5] Henryk Arodź. On gauge invariant external sources in yang-mills theory. *Acta Physica Polonica. B*, 12(5), 1981.

[6] Seth K Asante, Bianca Dittrich, and Hal M Haggard. The degrees of freedom of area regge calculus: dynamics, non-metricity, and broken diffeomorphisms. *Classical and Quantum Gravity*, 35(13):135009, 2018.

[7] Thomas W Baumgarte and Stuart L Shapiro. *Numerical relativity: solving Einstein's equations on the computer*. Cambridge University Press, 2010.

[8] Yakov Berchenko-Kogan and Ari Stern. Charge-conserving hybrid methods for the yang–mills equations. *The SMAI Journal of computational mathematics*, 7:97–119, 2021.

[9] Carles Bona, Carlos Palenzuela-Luque, and Carles Bona-Casas. *Elements of numerical relativity and relativistic hydrodynamics: from Einstein's equations to astrophysical simulations*, volume 783. Springer, 2009.

[10] Katherine A Brading. Which symmetry? noether, weyl, and conservation of electric charge. *Studies in History and Philosophy of Science Part B: Studies in History and Philosophy of Modern Physics*, 33(1):3–22, 2002.

[11] Boguslaw Broda. Non-abelian stokes theorem in action. *arXiv preprint math-ph/0012035*, 2000.

[12] Moshe Carmeli. *Group theory and general relativity: representations of the Lorentz group and their applications to the gravitational field*. World Scientific, 2000.

[13] Michele Caselle, Alessandro D'Adda, and Lorenzo Magnea. Regge calculus as a local theory of the poincaré group. *Physics Letters B*, 232(4):457–461, 1989.

[14] Snorre H Christiansen and Tore G Halvorsen. A simplicial gauge theory. *Journal of mathematical physics*, 53(3), 2012.

[15] Snorre H Christiansen and Ragnar Winther. On constraint preservation in numerical simulations of yang–mills equations. *SIAM Journal on Scientific Computing*, 28(1):75–101, 2006.

[16] Bernardo Cockburn, George E Karniadakis, and Chi-Wang Shu. The development of discontinuous galerkin methods. In *Discontinuous Galerkin methods: theory, computation and applications*, pages 3–50. Springer, 2000.

[17] Keenan Crane. Discrete differential geometry: An applied introduction. *Notices of the AMS, Communication*, 1153, 2018.

[18] Alvaro De Rújula, Howard Georgi, and SL Glashow. Hadron masses in a gauge theory. *Physical Review D*, 12(1):147, 1975.

[19] Mathieu Desbrun, Eva Kanso, and Yiying Tong. Discrete differential forms for computational modeling. In *ACM SIGGRAPH 2006 Courses*, pages 39–54. 2006.

[20] Jérôme Droniou, Todd A Oliynyk, and Jia Jia Qian. A polyhedral discrete de rham numerical scheme for the yang–mills equations. *Journal of Computational Physics*, 478:111955, 2023.

[21] Aida X El-Khadra, Andreas S Kronfeld, and Paul B Mackenzie. Massive fermions in lattice gauge theory. *Physical Review D*, 55(7):3933, 1997.

[22] Christof Gattringer and Christian Lang. *Quantum chromodynamics on the lattice: an introductory presentation*, volume 788. Springer Science & Business Media, 2009.

[23] Evan S Gawlik and Michael Neunteufel. Finite element approximation of the einstein tensor. *arXiv preprint arXiv:2310.18802*, 2023.

[24] Jay Gopalakrishnan, Michael Neunteufel, Joachim Schöberl, and Max Wardetzky. Analysis of curvature approximations via covariant curl and incompatibility for regge metrics. *arXiv preprint arXiv:2206.09343*, 2022.

[25] Jeff Greensite. The confinement problem in lattice gauge theory. *Progress in Particle and Nuclear Physics*, 51(1):1–83, 2003.

[26] Walter Greiner, Stefan Schramm, and Eckart Stein. *Quantum chromodynamics*. Springer Science & Business Media, 2013.

[27] Tore Gunnar Halvorsen and Torquil Macdonald Sørensen. Simplicial gauge theory on spacetime. *Numerische Mathematik*, 125:733–760, 2013.

[28] John W Harris and Berndt Müller. The search for the quark-gluon plasma. *Annual Review of Nuclear and Particle Science*, 46(1):71–107, 1996.

[29] Ralf Hiptmair. Finite elements in computational electromagnetism. *Acta Numerica*, 11:237–339, 2002.

[30] Thomas JR Hughes. *The finite element method: linear static and dynamic finite element analysis*. Courier Corporation, 2012.

[31] Andreas Ipp and David Müller. Broken boost invariance in the glasma via finite nuclei thickness. *Physics Letters B*, 771:74–79, 2017.

[32] John David Jackson and Lev Borisovich Okun. Historical roots of gauge invariance. *Reviews of modern physics*, 73(3):663, 2001.

[33] John B Kogut. The lattice gauge theory approach to quantum chromodynamics. *Reviews of Modern Physics*, 55(3):775, 1983.

[34] Ivan Kolár, Peter W Michor, and Jan Slovák. *Natural operations in differential geometry*. Springer Science & Business Media, 2013.

[35] Jeffrey M Lee, Bennett Chow, Sun-Chin Chu, David Glickenstein, Christine Guenther, James Isenberg, Tom Ivey, Dan Knopf, Peng Lu, Feng Luo, et al. Manifolds and differential geometry. *Topology*, 643:658, 2009.

[36] Roland W Lewis, Perumal Nithiarasu, and Kankanhalli N Seetharamu. *Fundamentals of the finite element method for heat and fluid flow*. John Wiley & Sons, 2004.

[37] Larry McLerran. The physics of the quark-gluon plasma. *Reviews of Modern Physics*, 58(4):1021, 1986.

[38] Mark Meyer, Mathieu Desbrun, Peter Schröder, and Alan H Barr. Discrete differential-geometry operators for triangulated 2-manifolds. In *Visualization and mathematics III*, pages 35–57. Springer, 2003.

[39] Warner A Miller. The hilbert action in regge calculus. *Classical and Quantum Gravity*, 14(12):L199, 1997.

[40] David Mueller, Andreas Ipp, and Daniil Gelfand. Colored particle-in-cell simulations for heavy-ion collisions. 2016.

[41] Mikio Nakahara. *Geometry, topology and physics*. CRC press, 2003.

[42] Emmy Noether. Invariant variation problems. *Transport theory and statistical physics*, 1(3):186–207, 1971.

[43] Anastasis C Polycarpou. *Introduction to the finite element method in electromagnetics*. Springer Nature, 2022.

[44] Eduard Prugovečki and Eduard Prugovečki. The fibre bundle framework for classical general relativity. *Quantum Geometry: A Framework for Quantum General Relativity*, pages 30–65, 1992.

[45] Vincent Quenneville-Belair. A new approach to finite element simulations of general relativity. 2015.

[46] Claudia Ratti. Lattice qcd and heavy ion collisions: a review of recent progress. *Reports on Progress in Physics*, 81(8):084301, 2018.

[47] Tullio Regge. General relativity without coordinates. *Il Nuovo Cimento (1955-1965)*, 19(3):558–571, 1961.

[48] Oliver Sander. Geodesic finite elements of higher order. *IMA Journal of Numerical Analysis*, 36(1):238–266, 2016.

[49] Joachim Schöberl. C++ 11 implementation of finite elements in ngsolve. *Institute for analysis and scientific computing, Vienna University of Technology*, 30, 2014.

[50] Rea Simon Schuller Frederic. *Lectures on the Geometric Anatomy of Theoretical Physics*. 2013.

[51] Dale M Snider. An incompressible three-dimensional multiphase particle-in-cell model for dense particle flows. *Journal of computational physics*, 170(2):523–549, 2001.

[52] Stephen Bruce Sontz. *Principal Bundles: The Classical Case*. Springer, 2015.

[53] Barna Szabó and Ivo Babuška. Finite element analysis: Method, verification and validation. 2021.

[54] Wu-Ki Tung. *Group theory in physics*, volume 1. World Scientific, 1985.

[55] Robert M Wald. *General relativity*. University of Chicago press, 2010.

[56] Olek C Zienkiewicz and Robert L Taylor. *The finite element method for solid and structural mechanics*. Elsevier, 2005.